

**PEAK TO AVERAGE POWER RATIO REDUCTION IN
ORTHOGONAL FREQUENCY DIVISION MULTIPLEXED
SYSTEMS**

BY

ALOK JOSHI

**A THESIS SUBMITTED IN FULFILLMENT OF THE REQUIREMENTS FOR
THE DEGREE OF DOCTOR OF PHILOSOPHY**

IN

ELECTRONICS AND COMMUNICATION ENGINEERING

UNDER THE SUPERVISION OF

Dr. DAVINDER SINGH SAINI



**JAYPEE UNIVERSITY OF INFORMATION TECHNOLOGY
WAKNAGHAT, H.P, INDIA**

Enrollment No. 096004

December 2014

**PEAK TO AVERAGE POWER RATIO REDUCTION IN
ORTHOGONAL FREQUENCY DIVISION
MULTIPLEXED SYSTEMS**

By

ALOK JOSHI

**A THESIS SUBMITTED IN FULFILLMENT OF THE REQUIREMENTS FOR
THE DEGREE OF DOCTOR OF PHILOSOPHY**

IN

ELECTRONICS AND COMMUNICATION ENGINEERING



**JAYPEE UNIVERSITY OF INFORMATION TECHNOLOGY
WAKNAGHAT**

DECEMBER 2014

DECLARATION BY THE SCHOLAR

I hereby declare that the work reported in the Ph.D. thesis entitled **“Peak To Average Power Ratio Reduction in Orthogonal Frequency Division Multiplexed Systems”** submitted at **Jaypee University of Information Technology, Waknaghat, Solan, India**, is an authentic record of my work carried out under the supervision of **Dr. Davinder Singh Saini**. I have not submitted this work elsewhere for any other degree or diploma.

(Signature)

Alok Joshi

Department of Electronics & Communication Engineering

Jaypee Institute of Information Technology, Noida ,India

December 2014

CERTIFICATE

This is to certify that the work reported in the Ph.D. thesis entitled “**Peak To Average Power Ratio Reduction in Orthogonal Frequency Division Multiplexed Systems**”, which is being submitted by **Alok Joshi** in fulfillment for the award of degree of Doctor of Philosophy in Electronics and Communication Engineering Department at Jaypee University of Information Technology, is the record of candidate’s own work carried out by him under my supervision. This work has not been submitted partially or wholly to any other University or Institute for the award of this or any other degree or diploma.

(Signature of Supervisor)

Dr. Davinder Singh Saini

Associate Professor

Department of Electronics & Communication Engineering

Jaypee University of Information Technology , Waknaghat , Solan, H.P (India)

ACKNOWLEDGMENT

In completion of the research work shaped up during past few years, obstacles are bound to come in its way and needless to say that help from various sources poured in. I would like to mention few names, without whom this work would not have been reached to a significant stage. First of all, I would like to sincerely thank my research supervisor Dr. D. S. Saini from core of my heart who has continued to be a source of inspiration and driving force since the work is conceived. His constant contribution and engagement in sharing the new ideas cannot be described in words. I would also like to thank my DPMC members Prof. T.S. Lamba, Prof. S.V. Bhoosan, Prof. Ghanshyam Singh, Prof. Ashok Gupta and Dr. Pradeep Kumar , each of them gave significant suggestions in improving the quality of the research work. Next I would like to thank Prof. S.K. Kak for proving a world class research environment at JUIT. Finally, I would like to thank Brig. (Retd.) Balbir Singh for his timely help and advice.

(ALOK JOSHI)

TABLE OF CONTENTS

LIST OF FIGURES	i-iii
LIST OF TABLES	iv
LIST OF ABBREVIATIONS	v-viii
LIST OF SYMBOLS	ix-xi
ABSTRACT	xii-xiii
CHAPTER 1	1-7
INTRODUCTION	1
1.1 PROBLEM STATEMENT	3
1.2 THESIS ORGANIZATION	4
1.3 SIGNIFICANCE OF THE STUDY	6
1.4 CONTRIBUTION	7
CHAPTER 2	8-20
ORTHOGONAL FREQUENCY DIVISION MULTIPLEXED SYSTEM	8
2.1 ORTHOGONALITY AND OFDM SYSTEM	9
2.2 OFDM TRANSMITTER AND RECEIVER	10
2.2.1 GUARD INTERVAL AND CYCLIC PREFIX	11
2.2.2 OFDM SPECTRUM AND ADJACENT CHANNEL INTERFERENCE	13
2.2.3 IEEE 802.11A STANDARD	16

2.2.4	LONG TERM EVOLUTION	17
2.2.5	ISSUES ASSOCIATED WITH OFDM	19
(A)	LARGE DYNAMIC RANGE AND HIGH PEAK TO AVERAGE POWER RATIO	19
(B)	BIT ERROR RATE PERFORMANCE IN FADING ENVIRONMENTS	20
(C)	SYNCHRONIZATION	20
CHAPTER 3		21-56
	PEAK TO AVERAGE POWER RATIO PROBLEM IN OFDM	21
3.1	MEASURING PAPR	24
3.2	PAPR REDUCTION SCHEMES	28
3.2.1	CLIPPING AND ITS MODIFICATIONS	28
3.2.2	COMPANDING	31
3.2.3	WINDOWING METHOD	33
3.2.4	CODING METHOD	34
3.2.5	MULTIPLE SIGNAL REPRESENTATION TECHNIQUES	37
(A)	SELECTIVE MAPPING SCHEME (SLM)	37
(B)	PARTIAL TRANSMIT SEQUENCE (PTS)	41
(C)	INTERLEAVING TECHNIQUE	47

3.2.6 CONSTELLATION MODIFICATION METHODS	48
(A) TONE RESERVATION TECHNIQUE	49
(B) TONE INJECTION	52
(C) ACTIVE CONSTELLATION EXTENSION	55
CHAPTER 4	57-73
PARTIAL TRANSMIT SEQUENCE TECHNIQUE WITH LOW COMPUTATIONAL COMPLEXITY	57
4.1 PROPOSED LOW COMPLEXITY PTS SCHEME	65
4.2 PERFORMANCE OF PROPOSED SCHEME AND ITS COMPARISON WITH EXISTING SCHEMES	72
CHAPTER 5	74-83
PARTIAL TRANSMIT SEQUENCE TECHNIQUE WITHOUT NEED OF SIDE INFORMATION	74
5.1 PROPOSED PTS SCHEME WITHOUT SI	79
5.2 PERFORMANCE OF PROPOSED SCHEME WITHOUT SI	81
5.3 COMPARISON WITH EXISTING PTS SCHEMES WITHOUT SI	82
CHAPTER 6	84-110
PERFORMANCE ANALYSIS OF OFDM SYSTEMS IN FADING CHANNELS WITH CHANNEL CODING SCHEMES	84
6.1 FADING CHANNELS	86

6.1.1 RAYLEIGH DISTRIBUTION	86
6.1.2 Rician DISTRIBUTION	87
6.1.3 NAKAGAMI-M DISTRIBUTION	87
6.2 CONCATENATED CHANNEL CODES	88
6.2.1 SERIAL CONCATENATION	88
(A) REED SOLOMON CODES IMPLEMENTATION	89
(B) CONVOLUTION CODE IMPLEMENTATION	92
6.2.2 PARALLEL CONCATENATION	93
(A) TURBO CODE IMPLEMENTATION	93
(B) TURBO CODE DECODING	95
6.3 SIMULATION RESULTS	99
6.3.1 PERFORMANCE ANALYSIS FOR RS-CC CODED OFDM SYSTEM	99
6.3.2 PERFORMANCE ANALYSIS FOR TURBO CODED OFDM SYSTEM	106
CHAPTER 7	111-118
MODIFIED SLM, PTS AND DHT PRECODED OFDM SYSTEM FOR PAPR REDUCTION	111
7.1 DISCRETE HARTLEY TRANSFORM PRECODED OFDM SYSTEM	112
7.2 MODIFIED SLM, PTS AND DHT PRECODED OFDM SYSTEM	113

7.3 PAPR PERFORMANCE EVALUATION OF THE MODIFIED SLM, PTS AND DHT PRECODED SYSTEM	113
CHAPTER 8	119-121
CONCLUSION AND FUTURE WORK	119
8.1 CONCLUSION	119
8.2 FUTURE WORK	121
REFERENCES	122-137
AUTHOR'S PUBLICATIONS	138-139

LIST OF FIGURES

Figure No.	Caption	Page No.
Fig. 2.1 (a)	A single carrier system	8
Fig. 2.1 (b)	A multicarrier system	
Fig. 2.2	Effect of using orthogonal subcarriers on spectral efficiency	9
Fig. 2.3	Basic building blocks of an OFDM system	11
Fig. 2.4	OFDM symbol with GI	11
Fig. 2.5	ICI due to multipath	12
Fig. 2.6	Cyclic prefix in GI	12
Fig. 2.7	OFDM symbol with cyclic prefix	13
Fig. 2.8	OFDM spectrum of orthogonal sub carriers	14
Fig. 2.9	OFDM power spectrum for $N=64$	14
Fig. 2.10	Raised cosine shaped OFDM pulses	15
Fig. 2.11	PSD of OFDM using RC pulse shaping	16
Fig. 2.12 (a)	OFDMA	18
Fig. 2.12 (b)	SC-FDMA	
Fig. 2.13	LTE frame structure	18
Fig. 3.1	Envelope of an OFDM signal	22
Fig. 3.2	Input output characteristics of a HPA	23
Fig. 3.3	Relation between PDF, CDF and CCDF	24
Fig. 3.4	CCDF curve for 16-QAM OFDM with $N=64$	26
Fig. 3.5	CCDF curves for BPSK and M-QAM ($M=2, 4, 6$) using $N=512$	27
Fig. 3.6	CCDF curves for 16-QAM OFDM using $N=64, 128, 256, 1024$	28
Fig. 3.7	CCDF of OFDM after clipping at $CR=0.8$ and 1.0	30
Fig. 3.8	CCDF comparison of clipped and clipped-filtered OFDM	30
Fig. 3.9	μ -law companded 16-QAM OFDM signal	32
Fig. 3.10	Probability distribution function for companded and un-companded OFDM	33
Fig. 3.11	Selective mapping scheme (SLM)	37

Fig. 3.12	CCDF for SLM technique with $M=8, 10$	38
Fig. 3.13	Block diagram of PTS technique	43
Fig. 3.14	CCDF comparison of OFDM with and without PTS	44
Fig. 3.15	Adjacent partitioning	45
Fig. 3.16	Interleaved partitioning	46
Fig. 3.17	Pseudo random partitioning	46
Fig. 3.18	Interleaved OFDM technique	47
Fig. 3.19	Block interleaver	48
Fig. 3.20	Block diagram for TR scheme	50
Fig. 3.21	TR scheme for PAPR reduction in OFDM	50
Fig. 3.22	Typical building blocks of TI scheme	53
Fig. 3.23	Extended constellation in QPSK	54
Fig. 3.24	ACE for QPSK mapping	55
Fig. 5.1	Mapping of symbols due to rotation by eight phase weights	79
Fig. 5.2	Octagon representing remapping of quaternary points	80
Fig. 5.3	PAPR comparison of OM-PTS and C-PTS for sub-blocks sizes $V= 4, 5, 6, 7, 8$	82
Fig. 6.1	Multipath propagation in wireless channels	84
Fig. 6.2	Serial concatenation	89
Fig. 6.3	1/2 Convolution code encoder	92
Fig. 6.4	2/3 Convolution code encoder	93
Fig. 6.5	Parallel concatenation	94
Fig. 6.6	Turbo encoder	94
Fig. 6.7	RSC encoders used for turbo code generation	94
Fig. 6.8	Decoding scheme	95
Fig. 6.9	Trellis transition	96
Fig. 6.10	Calculating α	97
Fig. 6.11	Calculating β	98
Fig.6.12	BER comparison of un-coded and RS-CC coded-OFDM system	100

Fig. 6.13	BER comparison of RS-1/2 & 2/3 CC coded OFDM in Rayleigh channel	101
Fig. 6.14	BER comparison of RS-1/2 & 2/3 CC coded OFDM in Rician channel	102
Fig. 6.15	BER comparison of RS-1/2 & 2/3 CC coded OFDM in Nakagami channel	104
Fig. 6.16	BER comparison of RS-CC coded OFDM in various channels	105
Fig. 6.17	BER comparison of turbo coded OFDM in Rayleigh channel	106
Fig. 6.18	BER comparison of turbo coded OFDM in Rician channel	107
Fig. 6.19	BER comparison of turbo coded OFDM in Nakagami channel	108
Fig. 6.20	BER comparison of serial and parallel concatenation code for PSK	109
Fig. 7.1	Precoded OFDM transmitter	111
Fig. 7.2	Precoded OFDM receiver	111
Fig. 7.3	DHT Precoded -OFDM System	113
Fig. 7.4	Clipping filtering scheme	113
Fig. 7.5	PAPR comparison of DHT-precoded, SLM and their modified versions using 16-QAM	114
Fig. 7.6	PAPR comparison of PTS and its modified versions using 16-QAM for V=2, 4, 6	115
Fig. 7.7	CCDF curves for SLM, PTS, DHT precoded and their modified version for 16-QAM	115
Fig. 7.8	PAPR comparison of DHT-precoded, SLM and their modified versions using 64-QAM	116
Fig. 7.9	PAPR comparison of PTS and its modified versions using 64-QAM for V=2, 4, 6	117
Fig. 7.10	CCDF curves for SLM, PTS, DHT precoded and their modified version for 64-QAM	117

LIST OF TABLES

TABLE No.	CAPTION	PAGE No.
Table 2.1	OFDM time based parameters in IEEE 802.11a	17
Table 3.1	PEP values for OFDM with 4-subcarriers	35
Table 3.2	Phase factor combinations for $W=2$ and $V=4$	43
Table 4.1	Phase factors for $V=2$ and $W=4$	61
Table 4.2	Phase factors for $V=3$ and $W=4$	61
Table 4.3	CCRR of proposed scheme	72
Table 5.1	Octagonal mapping at transmitter	81
Table 5.2	De-mapping at receiver	81
Table 5.3	PAPR values and their comparison	82
Table 6.1	RS Code parameters	89
Table 6.2	Elements in $GF(2^3)$	91
Table 6.3	E_b/N_0 Vs BER values for RS-CC coded and un-coded OFDM	100
Table 6.4	E_b/N_0 Vs BER values for RS-CC coded OFDM in Rayleigh channel	101
Table 6.5	E_b/N_0 Vs BER values for RS-CC coded OFDM in Rician channel	103
Table 6.6	E_b/N_0 Vs BER values for RS-CC coded OFDM in Nakagami channel	104
Table 6.7	E_b/N_0 Vs BER values for turbo-coded OFDM in Rayleigh channel	107
Table 6.8	E_b/N_0 Vs BER values for turbo-coded OFDM in Nakagami and Rician channels	108
Table 7.1	PAPR in (dB) for SLM, PTS and DHT precoded schemes	118

LIST OF ABBREVIATIONS

2-G	2 nd Generation
3-G	Third generation systems
3GPP	Third generation partnership project
4-G	Fourth generation
AAC-TR	Adaptive amplitude clipping tone reservation algorithm
ABC	Artificial bee colony
ACE	Active constellation extension
ACGS	Adaptive clipping-noise guided sign- selection
ACI	Adjacent channel interference
ADC	Analog to digital converter
ADSL	Asymmetric digital subscriber line
AWGN	Additive white Gaussian noise channel
BCH	Bose Chaudhuri Hochquenghem
BCJR	Bahl, Cocke, Jelinek and Raviv
BER	Bit error rate
CB-ACE	Clipping based ACE
CCDF	Cumulative distribution function
CCRR	Computational complexity reduction ratio
CDF	Cumulative distribution function
CE	Cross entropy
CF	Crest factor
CGS	Clipping-noise guided sign- selection
CM	Cubic meter
CM	Conversion matrices

COFDM	Coded orthogonal frequency division multiplexing
C-PTS	Conventional partial transmit sequence
CR	Clipping ratio
DAB	Digital audio broadcast
DBC	Digital video broadcast
DEC	Decoder
DFT	Discrete Fourier transforms
DHT	Discrete Hartley transform
EDGE	Evolved data for GSM evolution
EXT	Extrinsic information
FEC	Forward error correction
FFT	Fast Fourier transform
FIR BPF	Finite impulse response band pass filter
GF	Galois fields
GI	Guard interval
GPRS	General packet radio services
GSM	Global system for mobile communications
HDSL	High speed digital subscriber line
HPA	High power amplifier
HSDPA	High speed downlink packet access
HSUPA	High speed uplink packet access
IBO	Input back-off
ICI	Inter carrier interference
IFFT	Inverse fast Fourier transforms
ISI	Inter carrier interference

KL	Kullback Leibler
LDPC	Low density parity check
LLR	Log-likelihood ratio
LTE	Long term evolution
MAP	Maximum a posteriori
MIMO	Multiple input multiple output
ML	Maximum likelihood
OBO	Output back-off
OFDM	Orthogonal frequency division multiplexing
OFDMA	Orthogonal frequency division multiple access
OM-PTS	Octagonal mapping based PTS scheme
OQAM-OFDM	Offset quadrature amplitude modulation based orthogonal frequency-division multiplexing
P/S	Parallel to serial converter
PAPR	Peak to average power ratio
PDF	Probability distribution function
PEP	Peak envelop power
PHY	Physical layer
PPC	Parabolic peak cancellation
PRC	Peak reduction carriers
PRT	Peak reduction tones
PTS	Partial transmit sequence
RC	Raised cosine
RSC	Recursive systematic convolution
RS-CC	Reed Solomon- Convolution code
S/P	Serial to parallel converter

SA	Simulated annealing
SC-FDMA	Single carrier frequency division multiple access
SI	Side information
SLM	Selective mapping
STBC	Space time block coded
TI	Tone injection
TR	Tone reservation
TS	Tabu search
UMTS	Universal mobile telecommunication systems
UWB	Ultra wide band
WiMAX	Worldwide interoperability of microwave access
WLAN	Wireless local area network
WMAN	Wireless metropolitan network

LIST OF SYMBOLS

B_{SC}	Bandwidth for the single carrier (SC) system
T_s	Symbol period for single carrier (SC) system
N	Narrow sub-channels/ subcarriers
σ_τ	Room mean square delay spread
$X_{l,k}$	Symbol carried by k^{th} subcarrier in l^{th} OFDM symbol
$T_{sym=N.T_s}$	Symbol period for OFDM
$e^{j2\pi f_k t}$	k^{th} subcarrier with frequency f_k
T_g	Guard interval
δ^f	Frequency offset
$I_m(\delta)$	Inter carrier interference
β	Roll-off factor
$\max[x(t)]^2$	Peak signal power
$E\{[x(t)]^2\}$	Average signal power
$x(t)_{bandpass}$	Bandpass OFDM signal
$x_I(t)$	In-phase component
$x_Q(t)$	Quadrature-phase component
$f_{Z_n}(z)$	Probability distribution function for variable z
$F(z) = P(Z < z)$	Cumulative distribution function
K	Clipping level
$\theta(t)$	Phase of OFDM signal
μ	Parameter for compression
$W[n]$	White Gaussian noise component

$N_q[n]$	Quantization noise
L	Oversampling factor
$I_0(\cdot)$	0 th order modified Bessel function of first kind
H	Window length
B	Attenuation factor
E_b/N_0	Bit energy to noise power ratio
M	No. of phase factors in SLM
b^m	Phase factor multiplied in SLM
\tilde{x}	Lowest PAPR signal transmitted
X	Data block in frequency domain
D' or $ \cdot $	Euclidian distance
H_n	Frequency response of the channel
r_n	Received signal
V	Sub-blocks in PTS
W	Phase weights
b_v	Phase factor multiplied in PTS
C	Set of PAPR reduction subcarriers
$O(\cdot)$	Order of complexity
$\lceil \cdot \rceil$	Ceiling function
$\ \cdot \ _H$	Hamming weight
$sign(\cdot)$	Sign of the variable inside bracket
CCRR ^x	CCRR multiplication
CCRR ⁺	CCRR addition
$Y_{i,v}$	i^{th} subcarrier in the v^{th} sub-block

Y^*	Conjugate of Y
\hat{H}_n	Estimated channel response
\hat{b}_v	Estimated phase sequence
χ^P	Set of pilot tones
B_c	Coherence bandwidth
$\bar{\tau}$	Mean delay spread
$\overline{\tau^2}$	The mean square value
f_d	Doppler spread
T_C	Coherence time
$\Gamma(\cdot)$	Gamma function
r	Code rate
t	Number of errors
$g(x)$	Generator polynomial
$e(x)$	Error vector
D_H	Hamming distance
Λ	log-likelihood ratio
P	Precoder matrix
H_n^k	DHT precoder matrix element

Abstract

High data rate transmission over wireless channel is a tedious task due to various channel impairments such as fading, inter symbol interference (ISI) especially when single carrier modulation is used. Orthogonal frequency division multiplexing (OFDM) is a multi-carrier transmission scheme where high data rate is split in narrowband low rate streams and transmitted in a parallel fashion using orthogonal subcarriers. Due to its immunity towards fading and ISI, OFDM is widely used in high data rate application such as digital audio broadcast (DAV), Digital video broadcast (DVB), wireless local area network (WLAN), wireless metropolitan area network (WMAN), high speed digital subscriber line (HDSL), asymmetric digital subscriber line (ADSL) and 4-G mobile technologies such as long term evolution (LTE) and worldwide interoperability of microwave access (WiMAX).

Apart from its advantages, OFDM too suffers from few drawbacks such as peak to average power ratio (PAPR) and poor bit error rate (BER) performance in severe fading channels, which are of major concern. OFDM is a multicarrier scheme, where subcarriers are independently modulated and the resultant signal has large envelope fluctuations or dynamic range. When such signal passes through high power amplifier (HPA) circuits, nonlinearity of HPA generates harmonics leading to in-band and out-of-band signal distortion. Large dynamic range signal requires more complex and costly HPA circuits. To avoid this problem, back-off is generally used but reducing the input power to make HPA work in linear region reduces the efficiency of HPA. There are various techniques available for PAPR reduction, some of them reduce PAPR at the cost of creating distortion and other techniques which are distortionless have some issues such as high complexity, side information etc.

Out of all the available distortionless PAPR reduction schemes, partial transmit sequence (PTS) is a widely used technique. In PTS, data is divided into sub-blocks and each one of them is multiplied with a phase sequence then PAPR is calculated for the combined signal, in similar manner a set of alternate OFDM signals are generated using different permutations from a set of phase sequences. Finally the candidate signal (PTS) with least PAPR is selected for transmission. PTS technique suffers from three problems, first: large number of the phase sequences need to be analyzed to find the candidate signal with least PAPR, second: high computational complexity as each candidate's generation requires some complex multiplications and addition which is very high for larger set of block size and phase weights and third: after finding the optimum set of phase sequence which generates lowest PAPR PTS, the information regarding the phase sequence need to be transmitted to the receiver for

correct detection of the OFDM signal. This side information (SI) requires additional bandwidth.

We have proposed a low complexity PTS scheme where candidates are generated from one another by exploiting correlation among them. Scheme offers significant reduction in computational complexity without decreasing the number of candidates and at the same time PAPR performance of the proposed scheme is same as conventional PTS scheme.

To avoid side information an octagonal mapping scheme is proposed where a simple look up table can find the used phase sequence at the transmitter. The scheme uses a larger set of eight phase weights.

To tackle the low BER problem in severe fading environments, channel coding schemes could be used in conjunction with OFDM system. Concatenated codes, which are combination of more than one coding methods perform better than stand-alone schemes. Coded orthogonal frequency division multiplexed (COFDM) systems using serial and parallel concatenation are simulated for Rayleigh, Rician and Nakagami fading channels. Detailed BER comparisons are done using Reed Solomon-Convolution code (RS-CC) as serial concatenation and Turbo codes as parallel concatenation channel coding scheme.

A post clipping-filtering scheme for PAPR reduction is also discussed for selective mapping (SLM), PTS and discrete Hartley transform (DHT) precoded systems. The proposed scheme significantly reduces PAPR in the above mentioned systems. Filtering and channel coding together reduces the distortion created by clipping.

INTRODUCTION

In last few years there is a sheer increase in the demand of high data rate at user end over wireless channels, due to development of high end multimedia applications. This demand has pushed the engineers to move to higher generation wireless and mobile systems especially for data transfer i.e. from 2G systems (global system for mobile communications- GSM-10 Kbps digitized voice), general packet radio services (GPRS- data rate up to 50 Kbps) and evolved data for GSM evolution (EDGE-200Kbps) to 3G systems (universal mobile telecommunication systems-UMTS-384 Kbps) like high speed uplink/downlink packet access (HSUPA/HSDPA) targeting 5-30 Mbps download.

In single carrier modulation (SCM) based multiple access schemes to achieve high data rate, the symbol duration is decreased and corresponding band width requirement is increased. In SCM, delay spread caused by the dispersive nature of the channel becomes significant when compared to symbol duration. The spread in symbol duration causes overlapping of pulses at the receiver resulting in inter symbol interference (ISI). In frequency domain, high bandwidth requirement also cause frequency selective fading which degrades signal quality. To eradicate the affect of ISI, we need complex equalizers to be used at the receiver, which certainly affects the overall cost of the system.

To achieve high data rate at low bandwidth requirement, concept of multicarrier transmission is used. Multicarrier transmission is first published in [1], where the concept of parallel transmission was introduced. This work was further explored in [2], where a parallel transmission scheme for amplitude modulation system was proposed. In the proposed scheme overlapping of carrier was allowed to increase data rate. The author has used quadrature carriers in adjacent channels, channels were spaced at $R/2$ for a bit rate of R , each using similar roll-off for spectral shaping. Authors gave the concept of Fourier transform communication system where Fourier transform of the data is taken and transmitted [3]. At the receiver discrete Fourier transformer is utilized to avoid the use of sinusoid generators and coherent detectors. The concept of work published in [3] was further utilized and a multi carrier transmission technique using discrete Fourier transforms (DFT) was proposed, giving birth to orthogonal frequency division multiplexed systems [4]. OFDM was first utilized for mobile communication [5], where author used DFT based narrowband multiplexed system and analyzed the effect of Rayleigh fading on the signal and proposed a pilot based correction method to reduce the distortion caused by the fading. The OFDM was investigated by

researchers extensively [6-7] showing that OFDM is best candidate to achieve high data rate in fading environments. A detailed survey of all the development in this regard is given in [4-5].

In OFDM systems the high data rate signal is sent over a parallel set of narrow band channels, narrow enough that effect of frequency selective fading is very limited and the time duration of symbol is sufficiently large that effect of delay spread or time dispersion is reduced significantly. Due to high spectral efficiency, OFDM emerged as a strong candidate for use in various wireless and mobile applications such as digital audio broadcast (DAB), digital video broadcast (DVB), High speed digital subscriber lines (HDSL) and asymmetrical digital subscriber lines (ADSL). OFDM is also being used for IEEE standard such as IEEE 802.11a, g, n, ac and HIPERLAN/2 for wireless LAN. It is also used in wireless personal area network ultra-wideband (UWB) IEEE 802.15.3a implementation. The mobile broadband wireless access standard IEEE 802.20 also uses OFDM.

In 4G systems OFDM is being used for long term evolution (LTE) and worldwide interoperability of microwave access (WiMAX) technologies using IEEE 802.16 standard to enable high speed mobile communication.

Despite the superiority of OFDM in high speed applications over wireless medium, there are certain issues related to OFDM which hampers its performance such as high peak to average power ratio (PAPR), requirement of precise synchronization between transmitter - receiver and low bit error rate performance in fading environments.

Being a multicarrier system, modulation by data symbols may lead to constructive or destructive superposition of these carriers, this lead to large peaks and fluctuations in OFDM envelope. When such a large dynamic signal passes through high power amplifier circuit employed onboard, it drives the circuit in to the saturation region. Nonlinear characteristics of HPA in saturation region cause spectral regrowth leading to in and out-of- band distortion. To avoid it, HPA made to work in linear region using back-off i.e. reducing the input whenever it goes beyond the linear region. Back-off decreases the efficiency of the amplifier. Large dynamic range not only increase the cost and complexity of HPA circuitry but also affect analog to digital convertor and digital to analog convertor employed at receiver and transmitter respectively.

To reduce PAPR various schemes are presented in literature such as *clipping* technique [18-25], where clipping is done around the peaks but the PAPR reduction is achieved at the

cost of increased distortion and BER. The modification include clipping with filtering [19-21]. *Companding* [26-27] technique where signal is compressed such that high peaks remain unaltered but lower peaks are increased so that average power of signal increases resulting in lower peak to average power ratio, but there is a increase in overall transmission power. *Windowing* [28-30] is another method for PAPR reduction, where signal is multiplied with a pre-determined window to suppress side lobes for avoiding high PAPR.

Coding technique [31-38] uses forward error correction codes such as Reed Muller, Block coding and Golay complementary sequences for PAPR reduction but technique is limited to small number of sub-carriers due to complexity issues and limited PAPR reduction capability.

Probabilistic *scrambling* techniques where changes in OFDM signal are made leading to modifications in constellation in such a way that PAPR of resultant signal decreases, these techniques are tone reservation (TR) [79-89], tone injection (TI) [78-79, 90-93] and active constellation extension (ACE) [94-100]. In TR technique, peak reductions carriers are added to the OFDM block for reducing PAPR of resultant signal. In TI technique, constellation size is increased such that each point could be mapped on to multiple points in a new constellation, choosing correct set of constellation points may result in to lower PAPR. Both of the schemes require higher transmission power due to increased constellation size and limited for lower constellation sizes. In ACE, few points on the boundary are modified such that BER is not affected, but larger constellation leads to higher transmission power however transmission power requirement is less than the TI and TR schemes.

In *multiple signaling* techniques, the input data block is scrambled and sequence with lowest PAPR is transmitted, such techniques are selective mapping (SLM) [50-66], partial transmit sequence (PTS) [67-72] and interleaved OFDM [73-78]. These techniques suffer from need of side information, optimization and computational complexity problem. However extensive solutions are proposed to address these problems.

Among all schemes mentioned above for PAPR reduction, PTS technique is proven to be most promising as reduction in PAPR is achieved without any signal distortion.

As far as the poor BER in fading environments are concerned channel coding schemes are employed with OFDM.

1.1 Problem Statement

In PTS technique, input data is subdivided in a number of disjointed set of sub-blocks and multiplied by set of weighted phase sequences to create multiple sequence which can be

transmitted (partial transmit sequence). PAPR is evaluated for each of these sequences and the one with least PAPR is selected for transmission. But this scheme poses two serious problems:

1. Finding the optimum phase sequence combination is a challenging and complex problem especially when number of sub blocks and subcarrier are higher, because an exhaustive search is done over all combination of permissible phase factors to find least PAPR PTS, these results in to increased computational complexity.
2. At receiver to recover the signal some side information (SI) about phase weighting sequences are required, this side information puts additional burden on channel bandwidth.

Aim of our study is to primarily take up the issues associated with PTS mentioned above and device modified PTS scheme which can be implemented at lower computational complexity without the need of side information. Study also take up the issues of poor BER in fading environments and channel coding schemes are implemented to improve it. In a modified PTS, SLM and DHT precoding method is also proposed where post clipping with filtering is used for further PAPR improvement.

1.2 Thesis Organization

The thesis incorporates OFDM principle, PAPR problem and existing reduction techniques, proposed low complexity partial transmit sequence without SI and performance analysis of OFDM system using channel codes in fading channels. The chapter wise details are as follows:

Chapter 2: Orthogonal Frequency Division Multiplexed System

Chapter gives basic insight in to OFDM systems. The basic mathematical analysis of OFDM generation and detection is explained. Concept of single carrier and multicarrier transmission with their comparison is discussed. ISI and ICI problems and their causes are stated. Use of guard band and implementation of cyclic prefix is presented. Chapter also discusses application of OFDM and issues associated with its performance.

Chapter 3: Peak to Average Power Ratio Problem in OFDM

Chapter takes up the issues of PAPR in OFDM system. Cause of PAPR and HPA characteristics is discussed. A detailed mathematical analysis of PAPR calculation using

complementary cumulative distribution function (CCDF) is discussed. Chapter presents various PAPR reduction techniques available in literature, including both with distortion and without distortion techniques. Chapter includes detailed literature review related to these techniques. Clipping, clipping-filtering, compression and windowing techniques along with their limitations are discussed in PAPR reduction techniques with distortion along with suitable MATLAB simulations. In distortion less techniques channel coding schemes, multiple signaling and probabilistic scrambling techniques are presented. In multiple signal representation techniques selective mapping, partial transmit sequence and interleaved OFDM are explained with their MATLAB simulations. Computational complexity, need of side information and phase sequence optimization problem associate with these techniques are also discussed. Chapter also incorporates various literatures available to take up above mentioned issues. In probabilistic scrambling techniques tone reservation, tone injection and active constellation techniques with their limitations are explained. Chapter describes why PTS is the most sought technique.

Chapter 4: Partial Transmit Sequence Technique with Low Computational Complexity

Chapter discusses the computational complexity of PTS scheme. Chapter includes a proposed modified PTS scheme with low computational complexity. Computational complexity is measured in form of computational complexity reduction ratio (CCRR) for complex addition and multiplication. Scheme utilizes the high correlation among the PTS candidates leading to generation of candidates from one another. Scheme compares the complexity of the proposed scheme with existing ones, and proves its superiority. Scheme also shows that there is no degradation in PAPR reduction performance.

Chapter 5: Partial Transmit Sequence Technique without Need of Side Information

Chapter describes the need of side information in PTS and its drawbacks. Chapter discusses various schemes proposed in literature for avoiding side information in PTS. An octagonal mapping based PTS scheme is proposed for transmitting PTS without side information. Proposed scheme is also compared with the existing ones.

Chapter 6: Performance Analysis of OFDM Systems in Fading Channels with Channel Coding Schemes

This chapter takes up the issue of low bit error rate of OFDM system in fading environments. Chapter discusses time dispersive and time varying nature of wireless channels. Concept of coherence bandwidth, delay spread, coherence time and Doppler spread is explained. Brief

discussion about flat, frequency selective, slow and fast fading is also included. Basics of Rayleigh, Rician and Nakagami- m fading are covered in the chapter. Chapter demonstrates the use of channel coding schemes for BER improvement of the OFDM system. In this chapter, serial concatenated and parallel concatenated codes are discussed. Chapter includes mathematical discussion about Reed-Solomon, 1/2 and 2/3 convolution codes. In parallel concatenated scheme turbo codes are discussed. A detailed discussion about Turbo decoding using maximum a posteriori (MAP), log-MAP and max-log-MAP is given in the chapter. In the end of the chapter BER curves for OFDM system with BPSK, QPSK, 16-QAM and 64-QAM for RS-1/2 CC and RS-2/3 coded OFDM systems are given. BER curves are drawn using MATLAB for additive white Gaussian noise channel (AWGN), Rayleigh, Rician and Nakagami ($m=3$) channels. Similar BER curves are simulated in MATLAB for turbo codes also. For all the above simulations corresponding E_b/N_0 values are tabulated against their respective BER.

Chapter 7: Modified SLM, PTS and DHT Precoded OFDM System for PAPR Reduction

Chapter discusses a post clipping and filtering method for PAPR reduction in SLM, PTS and DHT precoding systems. Chapter discusses DHT precoded system and MATLAB simulations are carried out for 16-QAM and 64-QAM OFDM systems. CCDF are compared for SLM, PTS and DHT precoded systems and their modified versions. Results show significant reduction in PAPR using post clipping and filtering.

Chapter 8: Conclusion, present and future work

Chapter sums up the entire thesis work and its contribution towards solving the issues associated with PTS and BER improvement in fading environment. It also mentions the work currently being done to deal with these issues. Chapter finally includes the future work which could be done to address above mentioned issues.

1.3 Significance of the Study

For providing high speed data connectivity over wireless channels 4th generation systems are currently in development and deployment stage worldwide. OFDM is the technique which is being used for the transmission purpose in 4G, however high peak to average power ratio hinders its superior performance. To avoid high PAPR OFDM signal, partial transmit sequence emerged as the most sought choice. Partial transmit sequence suffers from high computational complexity and need of side information, which affect implementation and

bandwidth efficiency of the system. Apart from this OFDM performance is degraded in fading environment; suitable channel coding schemes can improve the BER.

Our study addresses all the above mentioned issues, so it is quite relevant to present scenario.

1.4 Contribution

The contribution of the work presented in thesis can be listed as follows:

- A detailed description about OFDM system and its various building blocks, advantages and major drawbacks is given. (chapter-2)
- An extensive review of literature on available PAPR reduction techniques (with and without distortion) and proposed modifications is presented along with MATLAB simulations. (chapter-3)
- Partial transmit sequence and its major problem areas are discussed, the research work available to address these issues is also presented. (chapter-4)
- A low complexity PTS scheme is proposed, where computations are reduced by significant amount, however PAPR performance is at par with conventional PTS scheme. (chapter-4)
- A PTS scheme without side information is proposed, where need of side information is avoided, using octagonal mapping scheme. (chapter-5)
- Bit error rate performance of the OFDM system is analyzed with serial and parallel concatenation in various fading environments. For serial concatenation Reed-Solomon codes with convolution codes is used and for parallel concatenation turbo codes are used. Fading channels considered are Rayleigh, Rician and Nakagami. (chapter-6)
- For more PAPR reduction in a modified SLM, PTS and DHT precoded system is discussed where post clipping and filtering is used. PAPR reduction with the proposed modification is significant. (chapter-7)
- Conclusion drawn from the study and future scope. (chapter-8)

ORTHOGONAL FREQUENCY DIVISION MULTIPLEXED SYSTEM

This chapter gives a brief insight on orthogonal frequency division multiplexed (OFDM) system and issues related to it.

Due to dispersive nature of the channel single carrier (SC) systems suffer from inter symbol interference (ISI) especially at higher data rates. In wireless channel, due to high bandwidth requirement SC systems suffer from frequency selective fading. To compensate for this problem complex and expensive equalizers are required. On the other hand, multicarrier transmission techniques such as orthogonal frequency division multiplexed system [8-12], where a high-rate serial data stream is split up into a set of low data rate streams carried by modulated subcarriers and transmitted in parallel fashion. Thus the bandwidth of the each sub-channel carrying a subcarrier becomes small as compared to the coherence bandwidth of the channel and experiences flat fading, which require very simple equalization. This implies that the symbol time period is made long compared to the r.m.s delay spread of the time-dispersive channel, this is shown in Fig. 2.1.

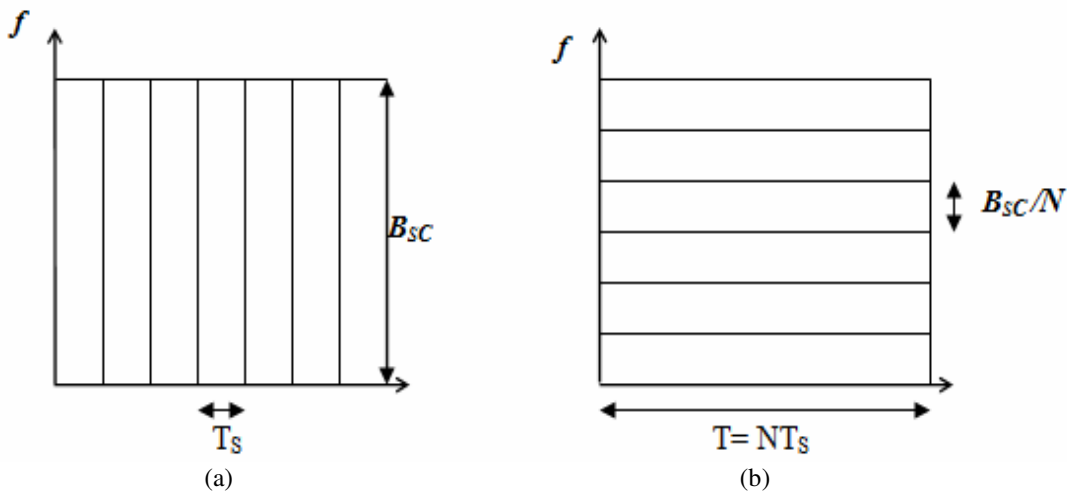


Fig. 2.1 (a) A single carrier system (b) A multicarrier system

In wireless communication systems if symbol period is at least 10 times of the r.m.s delay spread there will be no serious dispersion and no distortion due to ISI. If B_{SC} is the bandwidth for the single carrier system with symbol period T_s , whereas in multicarrier system the channel is split in to N narrow sub-channels each with bandwidth B_{SC}/N and symbol period $T = NT_s$.

If coherence bandwidth is B_C and delay spread is σ_τ , then:

$B_{SC} > B_C$ *Causing frequency selective fading and need complex equalizers*

$\frac{B_{SC}}{N} < B_C$ *Flat fading and simple equalization*

At the same time, symbol period $T = N.T_S > 10.\sigma_\tau$ ensures no ISI, thus making multicarrier system a suitable choice for high speed transmission in wireless channels.

2.1 Orthogonality and OFDM System

By selecting a special set of subcarrier frequencies which are orthogonal to each other, high spectral efficiency can be achieved as spectrum of single carrier system can be overlapped without any interference among them. Fig. 2.2 shows that in frequency division multiplexed systems guard band between the successive channel is provided to avoid interference whereas there is no such need in case of orthogonal carriers.

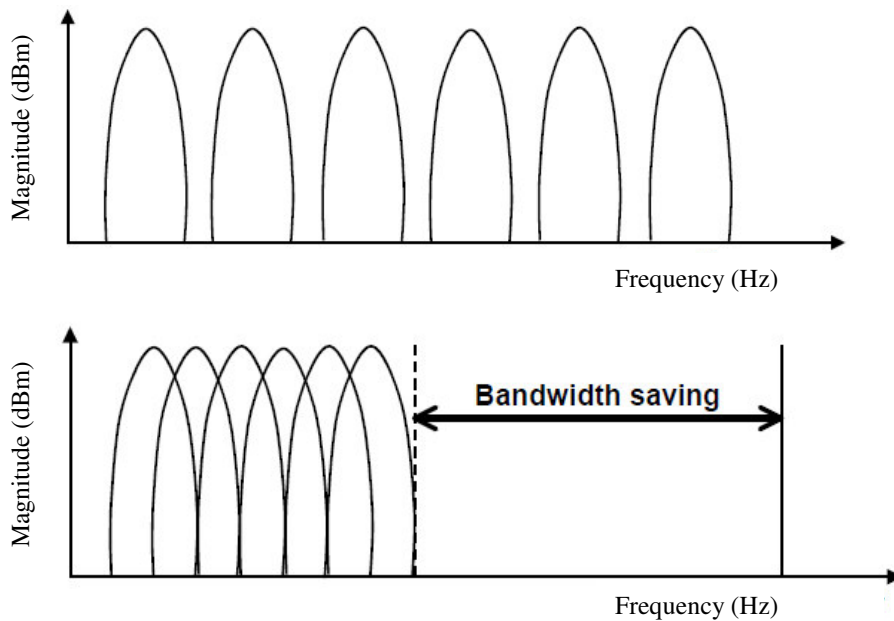


Fig 2.2 Effect of using orthogonal subcarriers on spectral efficiency

Fig. 2.2 shows, how bandwidth could be saved by using orthogonal frequencies. Lets say subcarriers are represented as $e^{j2\pi f_k t}$, $f_k = \frac{k}{T_{sym}}$ where $k=0, 1 \dots N-1$ and $T_{sym}=N.T_s$.

The orthogonality of two subcarriers can be defined as [9]:

$$\frac{1}{T_{sym}} \int_0^{T_{sym}} x_k(t) \cdot x_i^*(t) dt = \frac{1}{T_{sym}} \int_0^{T_{sym}} e^{\frac{j2\pi(k-i)t}{T_{sym}}} dt \quad (2.1)$$

$$= \begin{cases} 1 & \text{if } i = k \\ 0 & \text{otherwise} \end{cases} \quad \text{where } i, k \text{ are integers}$$

Similarly in discrete domain,

$$= \frac{1}{N} \sum_0^{N-1} e^{\frac{j2\pi(k-i)n}{N}} \quad \text{where } t = n \cdot T_s \quad (2.2)$$

$$= \begin{cases} 1 & \text{if } i = k \\ 0 & \text{otherwise} \end{cases} \quad \text{where } i, k \text{ are integers}$$

Thus OFDM signal with N subcarriers in continuous time domain can be represented as:

$$x(t) = \sum_{l=-\infty}^{\infty} \sum_{k=0}^{N-1} X_{l,k} \cdot e^{j2\pi f_k (t-lT_{sym})} \quad (2.3)$$

Where $X_{l,k}$ represents symbol carried by k^{th} subcarrier in l^{th} OFDM symbol. Eq. (2.3) is the equation of an IFFT operation.

Similarly in discrete time domain using sampling time $t = n \cdot T_s$ the OFDM signal can be given as:

$$x(n) = \sum_{k=0}^{N-1} X_{l,k} \cdot e^{j2\pi kn/N} \quad (2.4)$$

2.2 OFDM Transmitter and Receiver

The basic building block of an OFDM system is shown [9-10] in Fig.2.3. Inverse fast Fourier transforms (IFFT), fast Fourier transform (FFT) are used for generation and detection of OFDM signal respectively. Input to the IFFT block is N -point constellation created by a suitable mapping scheme such as M-QAM. These symbols are fed to IFFT block in parallel fashion using a serial to parallel converter (S/P). After inserting guard interval and cyclic prefix addition signal is sent serially using parallel to serial converter (P/S) to analog to digital converter (ADC) block. After

up conversion of signal frequency, signal is transmitted through radio channel. At receiver, opposite process that of the transmitter take place.

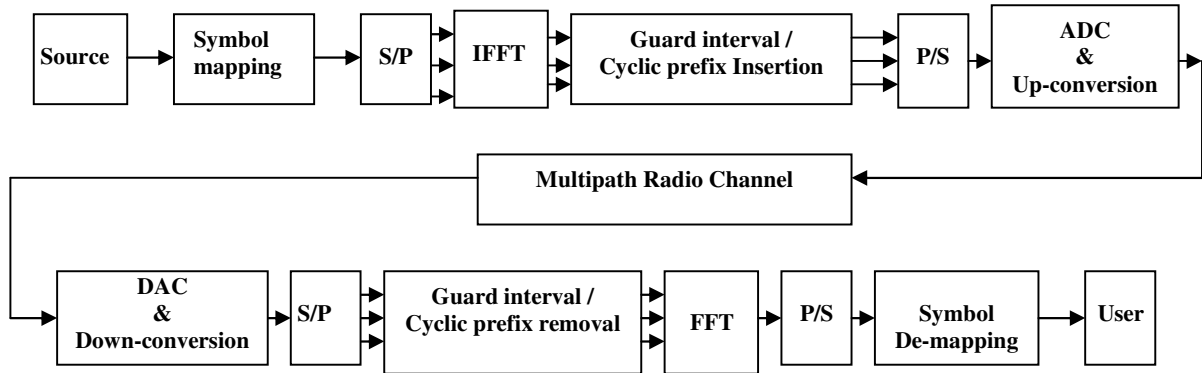


Fig. 2.3 Basic building blocks of an OFDM system

2.2.1 Guard Interval and Cyclic Prefix

Extending symbol duration T_S by N times the OFDM system is made robust against multipath delay spread. However ISI can be still be harmful in severe fading environments resulting in loss of orthogonality between signal and its delayed version. To avoid ISI, a guard interval (GI) is inserted in the symbol, the ISI effect of an OFDM symbol on the next symbol is confined within the guard interval which allows enough time for multipath signals from the previous symbol to die away before the information from the current symbol is gathered. The guard interval is usually chosen a value greater than delay spread.

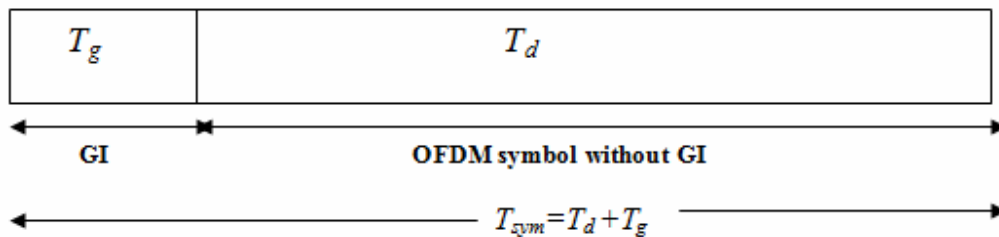


Fig.2.4 OFDM symbol with GI

The guard interval [9-12] is chosen such that:

$$T_g > T_{\text{delay-spread}} \quad (2.5)$$

However, due to insertion of guard interval another problem called inter carrier interference (ICI) may be created in the OFDM system. ICI [8, 11] is introduced due to the loss of the orthogonality of subcarriers. The loss of orthogonality may be due to the frequency offset, loss of synchronization or severe dispersion. Inserting GI [9], there is no integer number of cycle difference between subcarriers within the FFT interval, so they lose orthogonality. The loss of orthogonality in the delayed versions of subcarriers is shown in Fig.2.5.

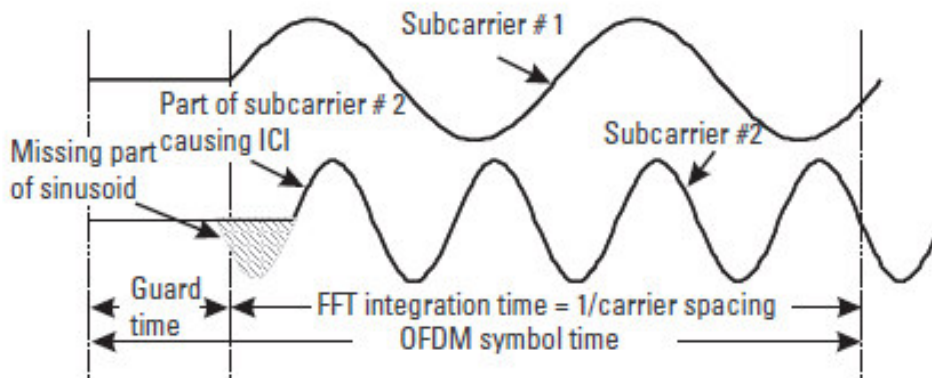


Fig. 2.5 ICI due to multipath

To eliminate ICI, the OFDM symbol is cyclically extended in the guard interval, called cyclic prefix as shown in Fig.2.6.

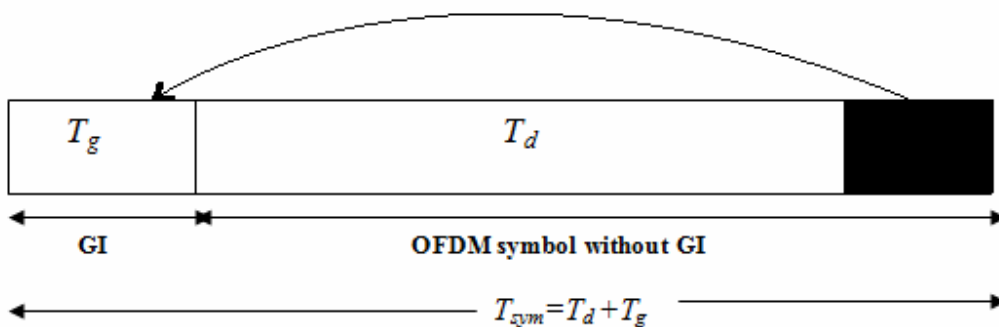


Fig. 2.6 Cyclic prefix in GI

This ensures that delayed replicas of the OFDM symbol always have an integer number of cycles within the FFT interval, as long as the delay spread is smaller than the guard interval (Fig.2.7).

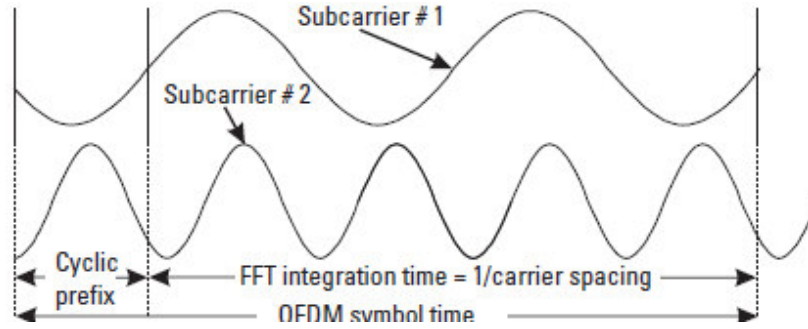


Fig. 2.7 OFDM symbol with cyclic prefix

If the frequencies for two successive subcarriers are:

$$\begin{aligned}
 k^{\text{th}} \text{ subcarrier} \quad \phi_k(t) &= e^{j2\pi kt/T} \\
 k+l^{\text{th}} \text{ subcarrier} \quad \phi_{k+l}(t) &= e^{j2\pi(k+l)t/T}
 \end{aligned} \tag{2.6}$$

If there is a frequency offset of δ in transmit and receive carrier frequencies i.e

$$\text{At receiver the received } k+l^{\text{th}} \text{ tone is} \quad \phi_k^\delta(t) = e^{j2\pi(k+l+\delta)t/T}$$

Then the interference between k^{th} and $k+l^{\text{th}}$ sub-channel is given by

$$I_l(\delta) = \int_0^T e^{j2\pi kt/T} \cdot e^{-(j2\pi(l+k+\delta)t/T)} dt = \frac{T(1 - e^{-j2\pi\delta})}{j2\pi(l+\delta)} = \frac{T|\sin(\pi\delta)|}{\pi|l+\delta|} \tag{2.7}$$

As the continuity of each delayed subcarrier has ensured by the cyclic prefix, its orthogonality with all other subcarriers is maintained over period T_d , such that:

$$\frac{1}{T_d} \int_0^{T_d} e^{j2\pi f_k(t-t_0)} \cdot e^{j2\pi f_i(t-t_0)} dt = 0; \text{ for } i \neq k, \tag{2.8}$$

Where the OFDM symbol arrives at a delay of t_0 , however using GI the data rate of OFDM is reduced by a factor of $\frac{T_d}{T_{\text{sym}}}$.

2.2.2 OFDM Spectrum and Adjacent Channel Interference

In OFDM symbols, each of the modulated subcarrier can be seen as a sinusoid multiplied with a rectangular pulse of duration equal to OFDM symbol duration T_d . In frequency domain the spectrum will be a *sinc* function with band width of $2/T_d$. So overall spectrum consists of many

shifted *sinc* functions. However, when these are sum up to derive the power spectrum, *sinc* function side lobes contribute to a large amount of out of band power leading to adjacent channel interference (ACI). The spectrum of sub-carrier is shown in Fig.2.8. The power spectrum of OFDM signal is simulated using MATLAB and plotted in terms of power spectral density (PSD) for $N=64$ and 16-QAM with side lobes is shown in Fig.2.9.

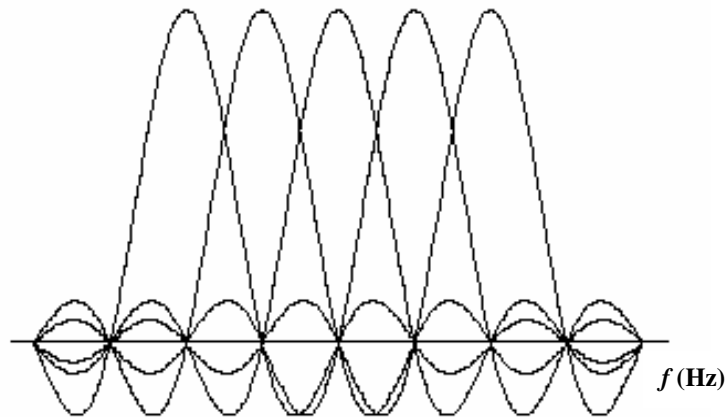


Fig. 2.8 OFDM spectrum of orthogonal sub carriers

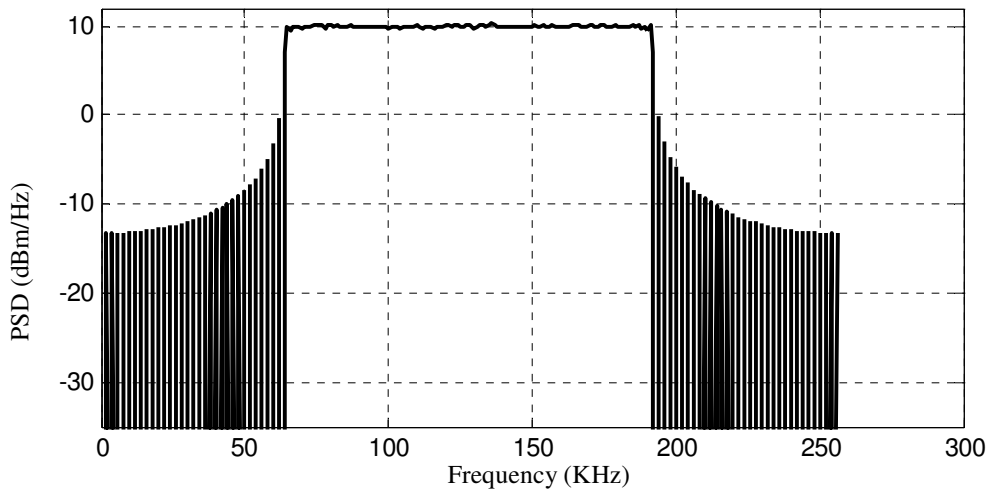


Fig.2.9 OFDM power spectrum for $N=64$

Side lobes are responsible for ACI and a band pass filter can be used to remove it, but it would require significant computation and highly complex circuit. Windowing technique to reshape the time domain rectangular pulse is one of the best solutions. Raised cosine (RC) window with various roll-off factors (β) is an ideal choice for shaping the OFDM pulse; this

allows reduction of side lobe power and out of band radiation in OFDM. Using Raised cosine window in guard band or extended guard band will not harm the data contained in the OFDM symbol. In practice, the guard band is further extended after insertion of CP for allowing roll-off of the rectangular pulse.

The raised cosine window function $w(t)$ is given as following [8-11]:

$$w(t) = \begin{cases} 0.5 \left(1 + \cos \left\{ \pi \left(1 + \frac{t}{\beta T_{sym}} \right) \right\} \right) & 0 \leq t \leq \beta T_{sym} \\ 1 & \beta T_{sym} \leq t \leq T_{sym} \\ 0.5 \left(1 + \cos \left\{ \pi \left(\frac{t - T_{sym}}{\beta T_{sym}} \right) \right\} \right) & T_{sym} \leq t \leq (1 + \beta) T_{sym} \end{cases} \quad (2.9)$$

In Fig. 2.10, the time domain OFDM pulse using raised cosine shaped pulse is shown.

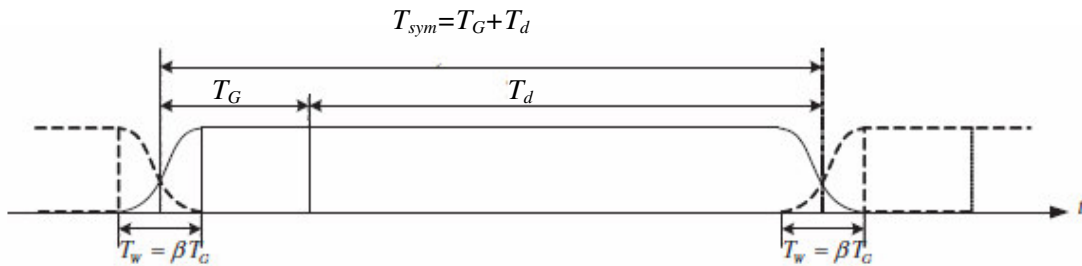


Fig. 2.10 Raised cosine shaped OFDM pulses

In Fig. 2.11, the effect of using time domain pulse shaping could be seen in power spectral density (PSD) curve, where effect of side lobes is significantly reduced at higher values of roll-off factor β .

Using virtual subcarrier is another method for reduction of ACI, where a set of unused carriers are used at both the ends of the OFDM transmission band of frequencies. However it affects the bandwidth efficiency, efficiency get reduced as number of unused carrier grows in number, but this method does not require additional computations. Virtual carrier method can be combined with raised cosine windowing to reduce the side lobe power or ACI.

2.2.3 IEEE 802.11a Standard

IEEE 802.11 [13] is a set of standards carrying out wireless local area network (WLAN) computer communication in the 2.4, 3.6 and 5 GHz frequency bands.

The IEEE 802.11a standard specifies an OFDM physical layer (PHY) that splits an information signal across 52 separate sub-carriers. Four of the sub-carriers are pilot subcarriers, the remaining 48 subcarriers provide separate wireless pathways for sending the information in a parallel fashion. The resulting sub-carrier frequency spacing is 0.3125 MHz (for 20 MHz bandwidth, with 64 possible sub-carrier frequency slots). The basic parameters for OFDM systems as per IEEE 802.11a standard are given in Table 2.1.

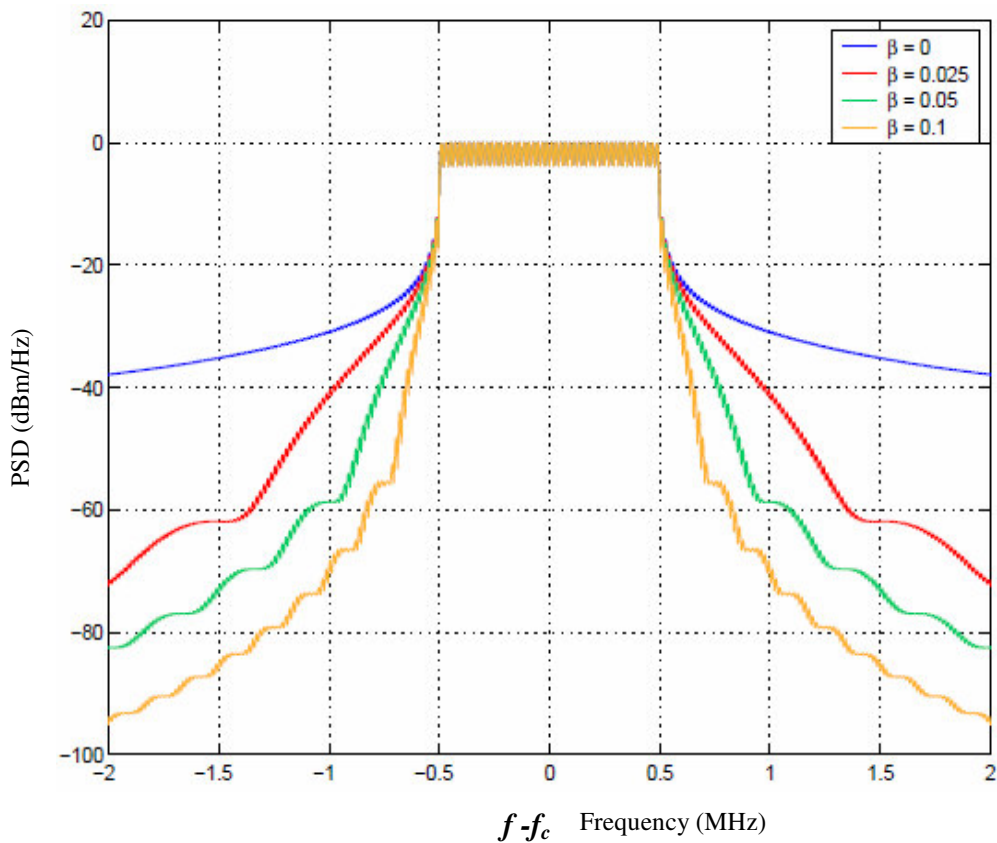


Fig. 2.11 Power spectral density of OFDM using RC pulse shaping

Table 2.1 OFDM time based parameters in IEEE 802.11a

Parameter	Value
FFT size	64
Number of digital sub-carriers	52
FFT Sampling frequency	20MHz
Sub-carrier spacing	312.5 KHz
Used subcarrier index	{-26 to -1, +1 to +26}
Guard interval , T_G	0.8 μ s
Data symbol duration, T_d	3.2 μ s
Total Symbol duration, T_{sym}	4 μ s
Mapping schemes	BPSK,QPSK,16-QAM, 64-QAM

2.2.4 Long Term Evolution

Long term evolution (LTE) is a 3.9 G technology which is commonly referred as 4G. LTE uses OFDM in downlink and single carrier FDMA in uplink. LTE was designed to provide a data rate of 100-300 Mbps in downlink and 50-75 Mbps in uplink over a bandwidth of 20 MHz. LTE supports both time division duplex (TDD) and frequency division duplex (FDD) in uplink and downlink. LTE uses multilayer transmission i.e. MIMO, allowing nodes to transmit several data streams on same carrier frequency. LTE also provide backward compatibility to existing 2G (GSM) and 3G (UMTS) systems.

2G system uses base transceiver (BTS) and base station controller (BSC) in base station sub systems (BSS), 3G uses nodes and radio network controllers (RNC) in UMTS terrestrial radio access network (UTRAN) however LTE uses only evolved nodes (e-Node) in evolved- UMTS terrestrial radio access network (e-UTRAN) at user interface. All the evolved nodes are directly connected to each other and there is no need of controller like BSC and RNC. This result in low latency since e-node can be directly connected to serving gateway for data access.

In downlink using OFDMA offers high spectral efficiency whereas in uplink SC-FDMA offers low peak to average power ratio resulting in improved battery performance. SC-FDMA is a

pre-coded version of OFDM, where data symbols are spread over more than one subcarrier in place of each subcarrier carrying different data symbol.

Fig. 2.12 shows the difference between OFDMA and SC-FDMA, in OFDMA each subcarrier of 15 KHz carries one unique data symbol and all the subcarriers are transmitted in parallel, in SC-FDMA each data symbol is carried in a bandwidth of 60 KHz by a single carrier.

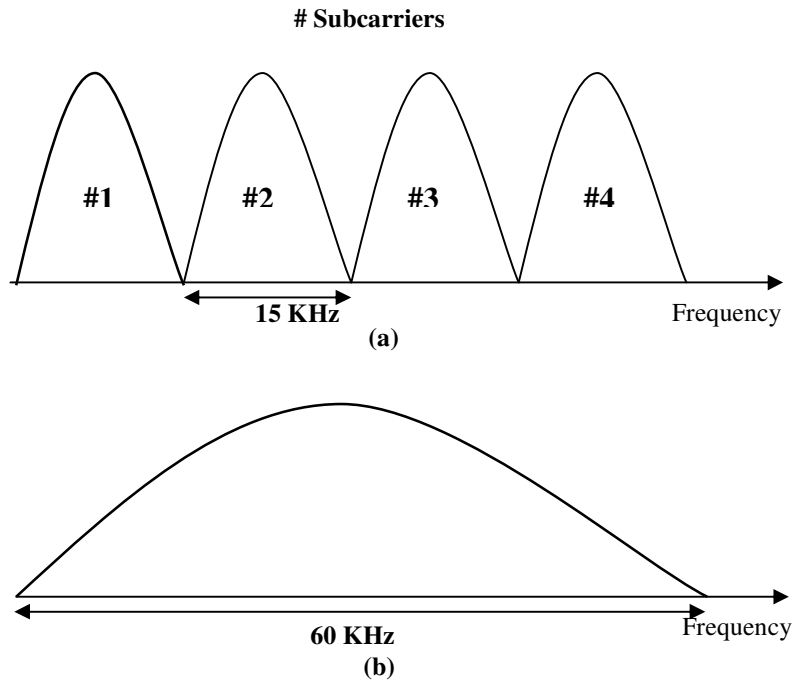


Fig. 2.12 (a) OFDMA (b) SC-FDMA

LTE offers flexible bandwidths from 1.4 MHz to 20 MHz, depending on the availability of spectrum. The frame structure for uplink and downlink in LTE is shown in Fig. 2.13, the frame duration is 10 ms. Frame comprises of 10 subframes and each subframe consists of two slots of 0.5 ms each. One slot of 0.5 ms carries 7-OFDM symbols and each OFDM symbol carries 12 subcarriers spaced at 15 KHz. Each slot is called a resource block and subframe is called a resource block pair.

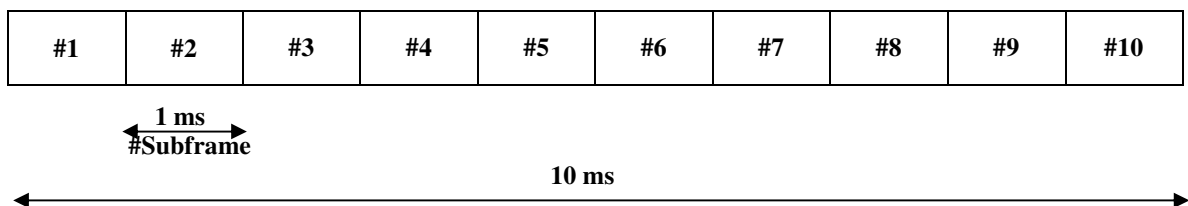


Fig. 2.13 LTE frame structure

Different number of resource blocks can be allocated to user depending upon the spectrum availability and requirement, e.g.

No. of resource blocks = 6

No. of subcarriers = $6 \times 12 = 72$

Occupied B.W = $72 \times 15 \text{ KHz} = 1.08 \text{ MHz}$

Transmission B.W = Occupied B.W + Guard Band = $1.08 + 0.32 = 1.4 \text{ MHz}$

Similarly for resource blocks 15, 25, 50, 75 and 100 the resultant transmission bandwidth would be 3, 5, 10, 15 and 20 MHz.

2.2.5 Issues Associated with OFDM

OFDM is bandwidth efficient technique which provides high amount of data rate and its immunity towards inter symbol interference and frequency selective fading makes it more attractive for the application such as digital audio broadcast (DAB), digital video broadcast (DVB), HIPERLAN/2, EUREKA 147/ADSL, MMAC standards. OFDM is also a preferred choice for downlink in 4G system such as long term evolution (LTE) and worldwide interoperability for microwave access (WiMAX) standards. OFDM is also deployed in MediaFlo, digital subscriber Line (DSL) applications. But at the same time, there are few demerits which hamper its performance. Few of the demerits are as follows:

A) Large Dynamic Range and High Peak to Average Power Ratio

Since OFDM comprises of a large number of independent subcarrier, the combined signal may have large variation in amplitudes. At the same time, if a number of subcarriers align in phase the peak power will have high value as compared to the average power. When such high PAPR OFDM signal face nonlinearity, it results in spectral re-growth and intermodulation. This leads to in-band and out of band distortion. This problem is more pronounced especially where high power amplifier (HPA) circuits are used such as in satellite downlink, HPA has nonlinear characteristic at high input power. Nonlinearity of HPA can be modelled as equation 2.10:

$$V_o(t) = f(v_i(t)) = a_1 v_i(t) + a_2 v_i^2(t) \cdots \cdots + a_N v_i^N(t) = \sum_{n=1}^N a_n v_i^n(t) \quad 2.10$$

For a dual tone signal given by

$$v_i(t) = \cos(\omega_1 t) + \cos(\omega_2 t) \quad 2.11$$

The output of amplifier would be

$$v_o(t) = a_1[\cos(\omega_1 t) + \cos(\omega_2 t)] + a_2[\cos(\omega_1 t) + \cos(\omega_2 t)]^2 + a_3[\cos(\omega_1 t) + \cos(\omega_2 t)]^3 + a_4[\cos(\omega_1 t) + \cos(\omega_2 t)]^4 \dots\dots \quad 2.12$$

This output contains frequency components at $\omega_1, 2.\omega_1, 3.\omega_1, \omega_2, 3.\omega_2$ and other harmonics of higher order along with intermodulation products terms like $\omega_1 \pm \omega_2, 2.\omega_1 \pm \omega_2, \omega_1 \pm 2.\omega_2, 2.\omega_1 \pm 2.\omega_2, \omega_1 \pm 3.\omega_2, 3.\omega_1 \pm \omega_2$. Harmonics and intermodulation products are mainly responsible for distortion caused by nonlinearity.

So reduction of PAPR is a major issue as it will also affect the cost and complexity of the circuit.

B) Bit Error Rate Performance in Fading Environments

OFDM suffers from poor bit error rate especially when the channel is severely faded due to multipath, such as in urban radio environment. In such case, the channel coding is one of the options to improve BER.

C) Synchronization

OFDM requires tight synchronization between transmitter and receiver. Slight synchronization error may lead to shift in carrier frequency which may further affect orthogonality of the subcarriers resulting in ICI.

Our work is primarily focused on the issue of high PAPR and its reduction. We have also taken up the issue of poor BER performance in fading environments and use of channel codes for improving BER.

PEAK TO AVERAGE POWER RATIO PROBLEM IN OFDM

This chapter provides a detailed discussion on peak to average power ratio (PAPR) [8-12, 14-17] problem in OFDM system and its implications. This chapter also includes discussion about various techniques available in literature for PAPR reduction and their performance.

In Multicarrier transmission the subcarriers are independent of each other. In time domain such composite signal has large dynamic range as subcarriers may align to produce constructive or destructive superposition. Constructive superposition will results in signal with high value of envelope peaks whereas destructive superposition may fade signal completely. Such large variation in signal power is measured in terms of peak to average power ratio. If data symbols modulate individual carrier in a manner that all of them align in same phase, in such case if number of carriers are N , then peak power would be N times the average value. The peak power would be the power of sinusoid signal with amplitude equal to maximum envelope value.

The variation in signal envelope can also be defined as crest factor (CF) [9] which is defined as:

$$CF = \frac{\text{peak value}}{\text{r.m.s value}} \tag{3.1}$$

Whereas PAPR is

$$PAPR = \frac{\text{peak power}}{\text{average power}} \tag{3.2}$$

$$\text{Crest factor} = \sqrt{PAPR} \tag{3.3}$$

However for unmodulated single carrier system, the PAPR ratio will be 0 dB , as envelope will have same variation as carrier, whereas its crest factor would be $\frac{\text{peak value}}{\text{peak value}/\sqrt{2}}$ i.e. 3 dB .

In OFDM, as all the carriers are added using an IFFT operation, this may lead to a signal with large peaks and dynamic range in time domain. For an OFDM signal $x(t)$, the PAPR is given as:

$$PAPR\{x(t)\} = \frac{\max_{0 \leq t \leq T} \{|x(t)|^2\}}{E\{|x(t)|^2\}} \quad (3.4)$$

Where: $\max\{x(t)\}^2$ is the peak signal power

$E\{x(t)\}^2$ is the average signal power

If $E\{x(t)\}^2 = 1$, and all the N subcarriers are in same phase, then PAPR will be N . Envelope of an OFDM signal for $N=16$ using 16-QAM for is shown in Fig. 3.1, This fig. shows abrupt peaks in the envelope leading to high peak power.

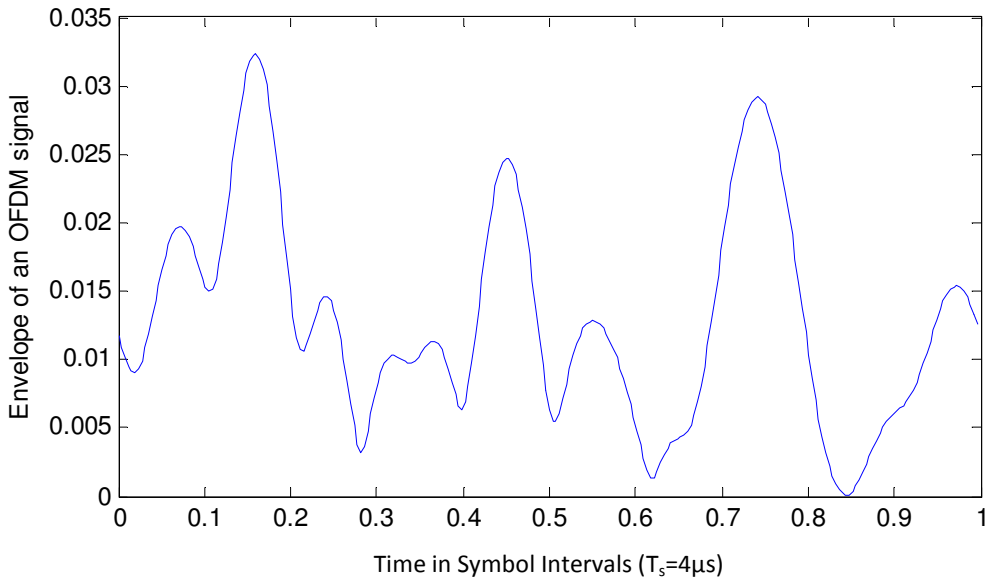


Fig. 3.1 Envelope of an OFDM signal

If OFDM symbol is modulated on carrier, the baseband signal will now be treated as pass band/band pass signal. If QAM mapping is considered then:

$x(t)_{bandpass} = \sqrt{2} \operatorname{Re}\{(x_I(t) + jx_Q(t))e^{j2\pi f_c t}\}$ Where $x_I(t)$, $x_Q(t)$ and f_c are in phase component, quadrature phase component and carrier frequency respectively.

$$\begin{aligned} E\{|x(t)_{bandpass}|^2\} &= \frac{1}{2} E\{|x_I(t)|^2\} + \frac{1}{2} E\{|x_Q(t)|^2\} \\ &= \frac{1}{2} E\{|x(t)|^2\} \end{aligned} \quad (3.5)$$

Considering carrier frequency much higher than $\frac{1}{T_{sym}}$:

$$\max_{0 \leq t \leq T} \{ |x_{bandpass}(t)|^2 \} = \max_{0 \leq t \leq T} \{ |x(t)|^2 \} \quad (3.6)$$

PAPR for band pass signal will be:

$$PAPR_{bandpass} = \frac{\max_{0 \leq t \leq T} \{ |x(t)|^2 \}}{\frac{1}{2} E \{ |x(t)|^2 \}}$$

$$PAPR_{bandpass} = 2 \times PAPR_{baseband} \quad (3.7)$$

As far as the maximum value of $PAPR_{baseband}$ is concerned, it is N or $10 \log(N)$ dB. High value of PAPR is serious concern when OFDM signal pass through nonlinear devices such as in 4G systems where OFDM is a downlink method and on-board high power amplifiers (HPA) have nonlinear input output characteristic [9] at high power values as shown in Fig 3.2.

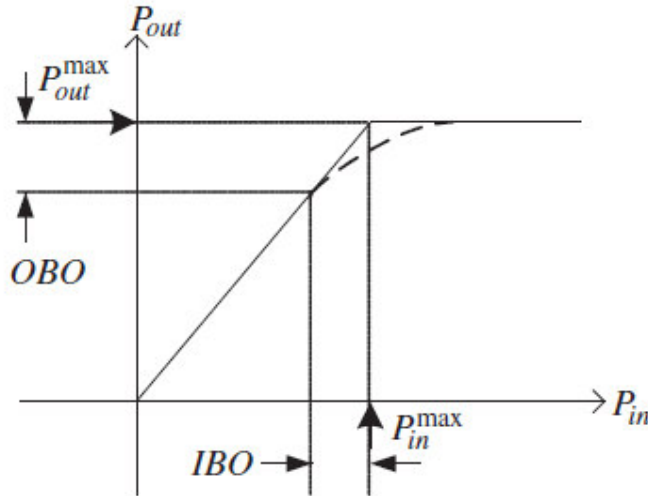


Fig. 3.2 Input output characteristics of a HPA

Fig. 3.2 shows that I/O characteristics are nonlinear after maximum input value P_{in}^{max} . When OFDM with high peak power pass through HPA, it drives the circuit in saturation region i.e beyond P_{in}^{max} , this leads to inter-modulation and generation of harmonics. This spectral regrowth creates in and out-of-band distortion. This distortion leads to carrier offset resulting in ICI, attenuation, rotation and poor bit error rate performance.

However input signal power can be forcefully reduced so that system operates in linear region of the characteristics. Such back-off at input (IBO) and output (OBO) reduce the power efficiency of the circuit. IBO and OBO determine the region of the linear operation. IBO is defined as:

$$IBO = 10 \log_{10} \frac{P_{in}^{max}}{P_{in}} \quad (3.8)$$

However if we try to transmit OFDM signal with large dynamic range, the cost and circuit complexity of ADC, DAC, HPA and other components increase drastically. So PAPR reduction is a must to avoid high cost, complexity of the circuits and distortion generated due to it.

3.1 Measuring PAPR

Complementary cumulative distributing function (CCDF) [8-10] is a standard parameter used in literature to measure the PAPR of OFDM and to evaluate the performance of PAPR reduction technique. *Cumulative distribution function (CDF)* shows how much time signal remain below any given level whereas a *CCDF* curve shows how much time the signal remains at or above a given power level. The percentage of time the signal spends at or above each power level defines the probability for that particular power level. A *CCDF* curve is a plot of relative power levels versus probability, this is shown in Fig. 3.3:

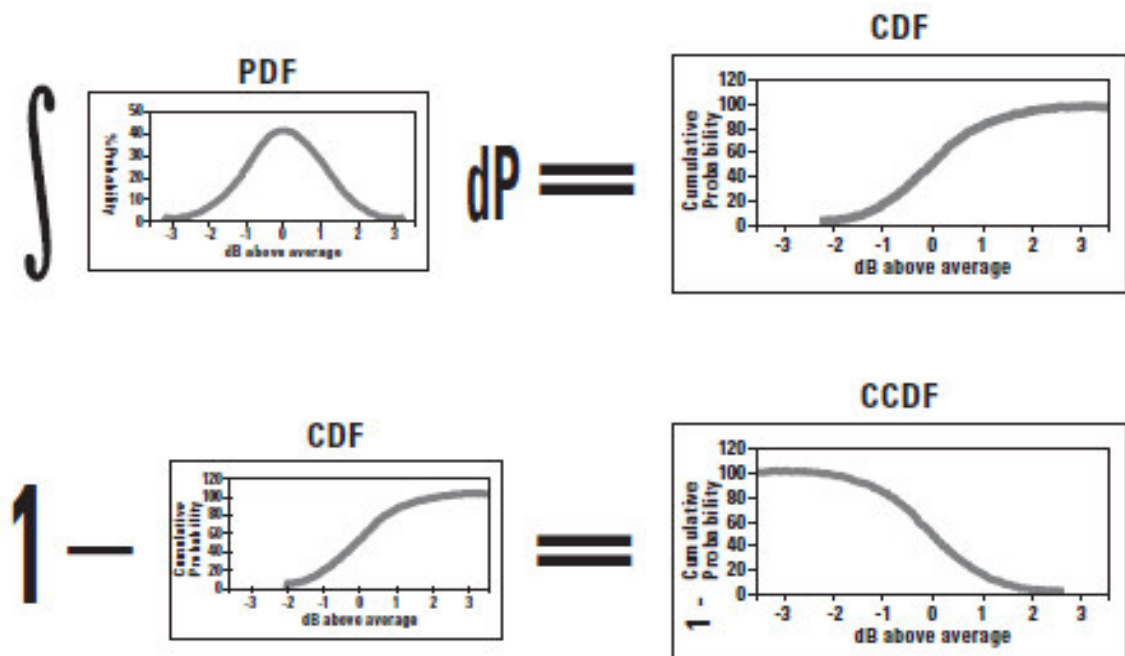


Fig. 3.3 Relation between PDF, CDF and CCDF

Considering large number of sub-carriers, the real and imaginary part of OFDM signal can be considered asymptotically Gaussian. In such case, the envelope of the OFDM signal follow Rayleigh distribution and power follows exponential distribution. Assuming average power of OFDM signal as unity, the normalized Rayleigh distributed OFDM samples will have following probability distribution function (PDF):

$$f_{Z_n}(z) = \frac{z}{\sigma^2} e^{-z^2/2\sigma^2}, n=0, 1, \dots, N-1 \quad (3.9)$$

Since it is normalized to unity power $2\sigma^2 = 1$:

$$f_{Z_n}(z) = \frac{z}{\sigma^2} e^{-z^2/2\sigma^2} = 2ze^{-z^2} \quad (3.10)$$

Then CDF showing the probability that OFDM signal with N subcarriers will have PAPR below certain level z is same as the probability that all the subcarriers are below the power level z , it can be shown as:

$$F(z) = P(Z < z) = P(Z_0 < z) \cdot P(Z_1 < z) \cdot \dots \cdot P(Z_{N-1} < z) \quad (3.11)$$

Now since $P(Z < z) = \int_0^z 2ze^{-z^2} dZ$ to solve this integration we substitute the following:

$$\text{Let } z^2 = t \quad \text{then} \quad 2z \cdot dz = dt$$

New limits of integration will be 0 to z^2 , integration will convert to:

$$P(Z < z) = \int_0^{z^2} 2ze^{-z^2} dZ = (1 - e^{-z^2}) \quad (3.12)$$

Now eq. 3.11 can be written as:

$$CDF = F(z) = (1 - e^{-z^2})^N \quad (3.13)$$

$$\text{Thus } CCDF = P(Z > z) = 1 - CDF = [1 - (1 - e^{-z^2})^N] \quad (3.14)$$

For a discrete time OFDM signal $x(n)$ the PAPR value will not be same as its continuous counterpart $x(t)$ as while sampling most of the peaks may be omitted leading to a lower value of PAPR. However calculating PAPR for baseband OFDM signal is a tedious task since it is

calculated after DAC implementation. So to calculate more precise value of PAPR from discrete OFDM signal, oversampling is done. However after oversampling the samples will not remain mutually independent or uncorrelated to each other, in that case eq. 3.14 is not valid.

The exact expression is very difficult to derive, however a lot of work is done to find the exact expression for oversampled signal. *Van Nee et.al.* [14] gave an empirical solution for oversampled signal, where they considered oversampled signal with N subcarriers equivalent to OFDM signal without oversampling with αN subcarriers :

$$CCDF = P(Z > z) = 1 - CDF = [1 - (1 - e^{-z^2})^{\alpha N}] \quad (3.15)$$

Where $\alpha=2.8$ is found to be more suitable for large number of carriers. However in some of the literature $\alpha=4$ considered as a suitable value.

CCDF curve for 16-QAM OFDM with 64 sub-carriers is shown in Fig. 3.4, on Y-axis the probabilities are given and on X-axis the PAPR values are given in dB. Curve shows that almost 60% of time PAPR values will be near by 6 dB, similar interpretation can be drawn for other value of PAPR from the CCDF.

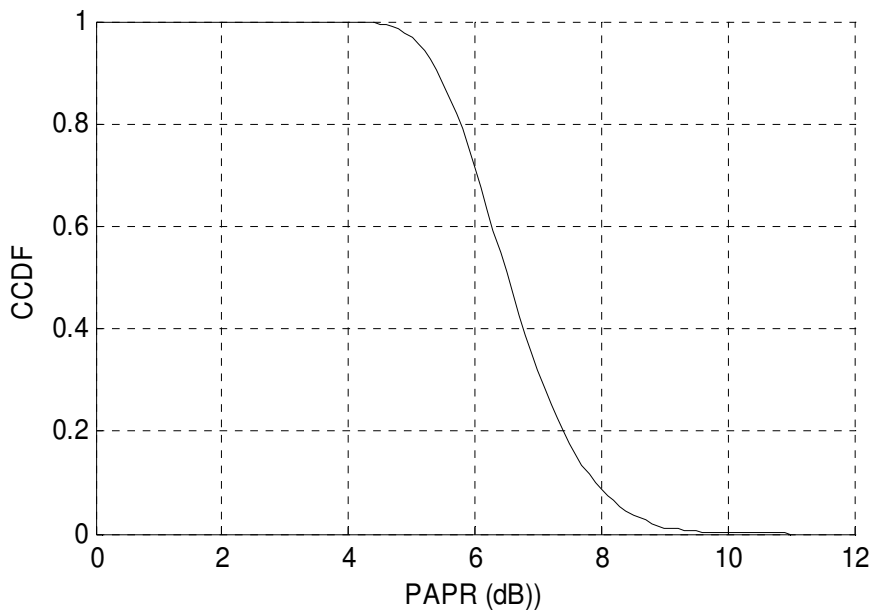


Fig. 3.4 CCDF curve for 16-QAM OFDM with $N=64$

In Fig.3.5, we have simulated CCDF curves for OFDM using BPSK, QPSK, 16-QAM and 64 QAM mapping schemes with $N=512$ subcarriers in MATLAB. CCDF curve shows that PAPR values for BPSK is lower as compared to rest of the mapping schemes. PAPR value is almost same for M-QAM ($M=2, 4, 6$) schemes.

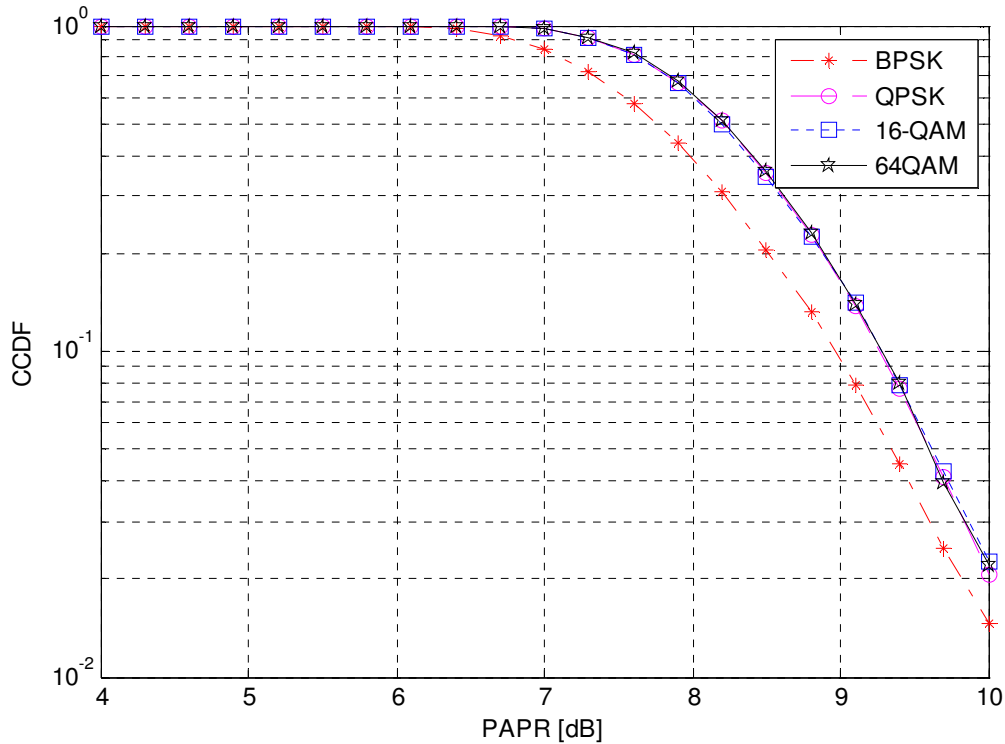


Fig 3.5 CCDF curves for BPSK and M-QAM ($M=2, 4, 6$) using $N=512$

As we increase the number of subcarriers in OFDM system there would be higher probability to get high PAPR as more number of subcarriers are contributing toward envelope peak. In Fig.3.6, we have simulated CCDF curves for OFDM using 16-QAM mapping scheme with $N=64, 128, 256$ and 1024 subcarriers in MATLAB. CCDF curve shows that PAPR values increases when numbers of subcarriers are increased.

Third generation partnership project (3GPP) in recent year has proposed a new parameter to measure envelop variations termed as cubic meter (CM) instead of PAPR. The reason behind the idea is, since major cause of distortion due to nonlinearity of a HPA is contributed by third order spectral components and CM considers such secondary peaks, whereas PAPR considers only major primary peak.

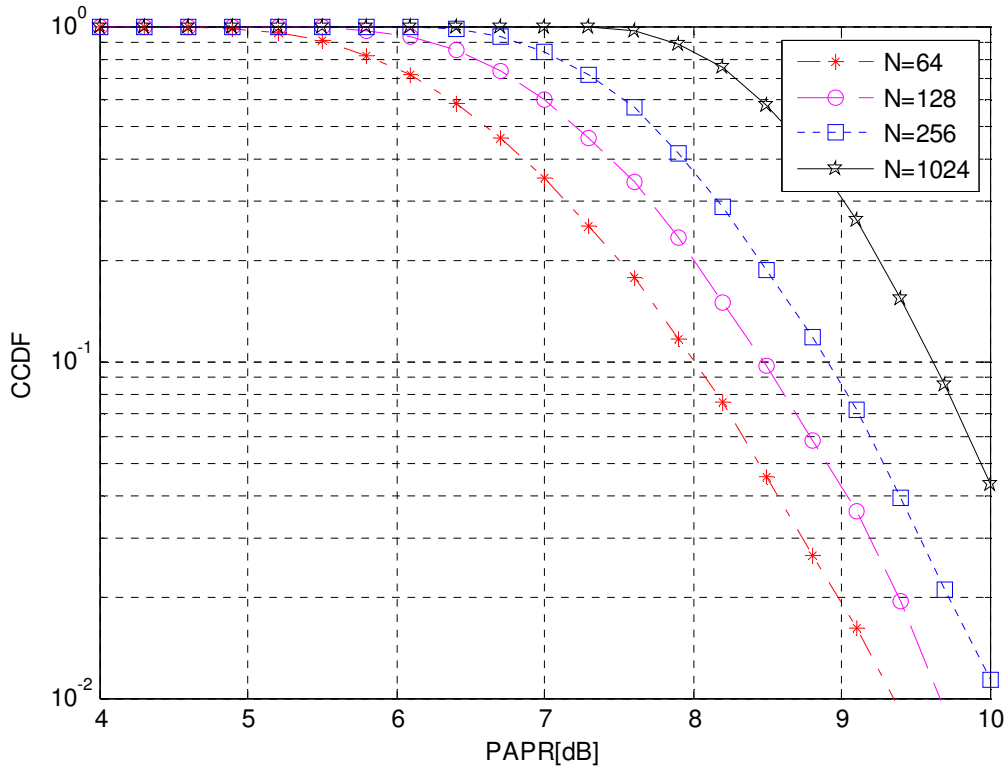


Fig 3.6 CCDF curves for 16-QAM OFDM using N=64, 128, 256, 1024

PAPR reduction is a key issue as it affects cost and complexity of various elements in the OFDM transmitter and receiver as well. There are various PAPR reduction techniques discussed in literature. CCDF is the primary parameter to evaluate the performance of a PAPR reduction scheme. In all these techniques PAPR reduction also affects transmission power required, bit error rate, effective data rate and computational complexity. Following section gives a brief insight of these techniques.

3.2 PAPR Reduction Schemes

PAPR reduction techniques are primarily divided in to methods which create distortion and methods which do not create distortion while performing PAPR reduction.

3.2.1 Clipping and its Modifications

Clipping [18] is the easiest method to avoid high peaks and PAPR. In this technique, a PAPR threshold is considered for deciding the maximum value of envelop. Any envelope peaks going beyond the threshold value is clipped off back to threshold. However signal remains unchanged if the signal level is below the threshold.

$$x_c(t) = \begin{cases} Ke^{j\theta(t)}, & |x(t)| > K \\ x(t), & |x(t)| < K \end{cases} \quad (3.16)$$

Where K is the clipping level and $\theta(t)$ is the phase of the OFDM signal. However clipping can reduce PAPR to any desired level but clipping a signal is a non-linear process which creates in and out-of-band distortion. In band distortion degrades BER performance of the system, however out of band distortion creates interference in the adjacent channels. If signal clipping is performed on standard Nyquist rate sampled OFDM signal, it may lead to aliasing affecting high frequency components. But when OFDM signal is oversampled, BER is less affected if proper filtering is used. In clipping, a parameter called clipping ratio (CR) is defined as follows:

$$CR = \frac{K}{\sigma} \quad (3.17)$$

Fig. 3.7 shows the effect on PAPR level of an OFDM signal using 16-QAM in presence of clipping. The number of carriers used are $N=128$, for $CR = 0.8$ and 1.0 . It clearly shows that clipping reduces PAPR significantly. For smaller value of CR the effect of clipping on the OFDM is more.

Out-of-band distortion can be reduced by employing post filtering [19]. Filtering reduces out-of-band distortion at the cost of spectral regrowth, so PAPR reduction is lesser as compared to when clipping is used alone.

Fig 3.8 compares PAPR of clipped OFDM signal with clipped and filtered OFDM signal. Filter used is a band pass FIR filter with sampling frequency 6 MHz and stop band attenuation ranging to 35-40 dB with frequency vectors varying from 1.3 to 2.5 MHz. It clearly indicates the effect of spectral regrowth after filtering as PAPR is increased.

Some other suggested methods are repeated clipping with filtering [20] to avoid spectral regrowth but it requires a lot of iterations. A clipping method with distortion control is described in [21], which includes setting a proper distortion bound and then repeated clipping and filtering is performed, this scheme achieves significant PAPR reduction at relatively lower BER. Author proposed a clipping-noise guided sign- selection (CGS) algorithm in [22] where an optimal set of subcarriers signs are used. Algorithm iteratively flips the signs of the subcarriers with high level of clipping noise, this scheme provides decent PAPR reduction with lower BER.

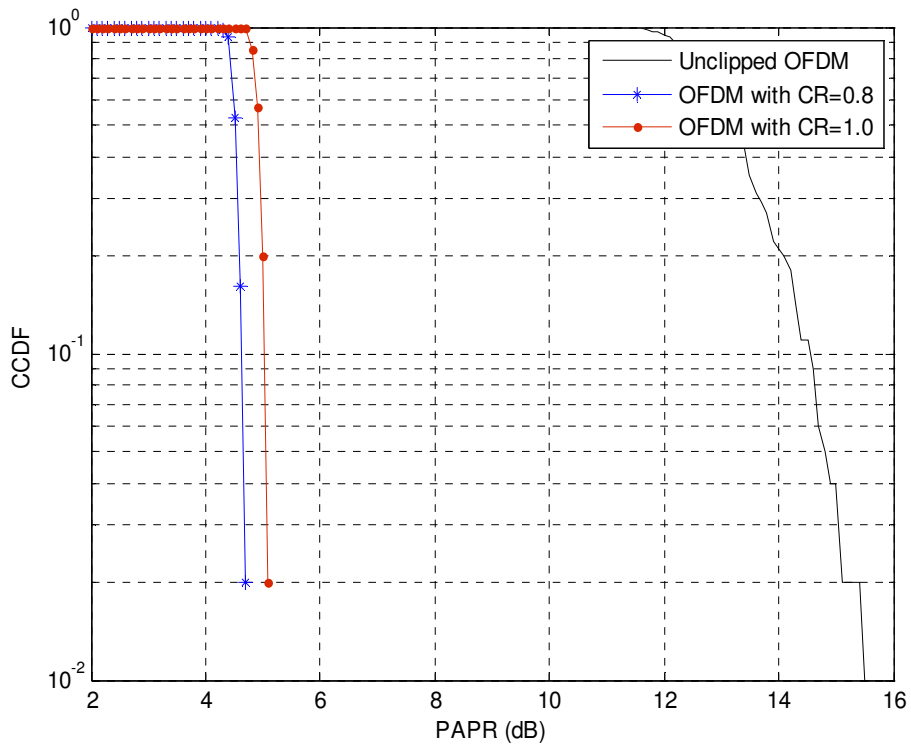


Fig. 3.7 CCDF of OFDM after clipping at CR=0.8 and 1.0

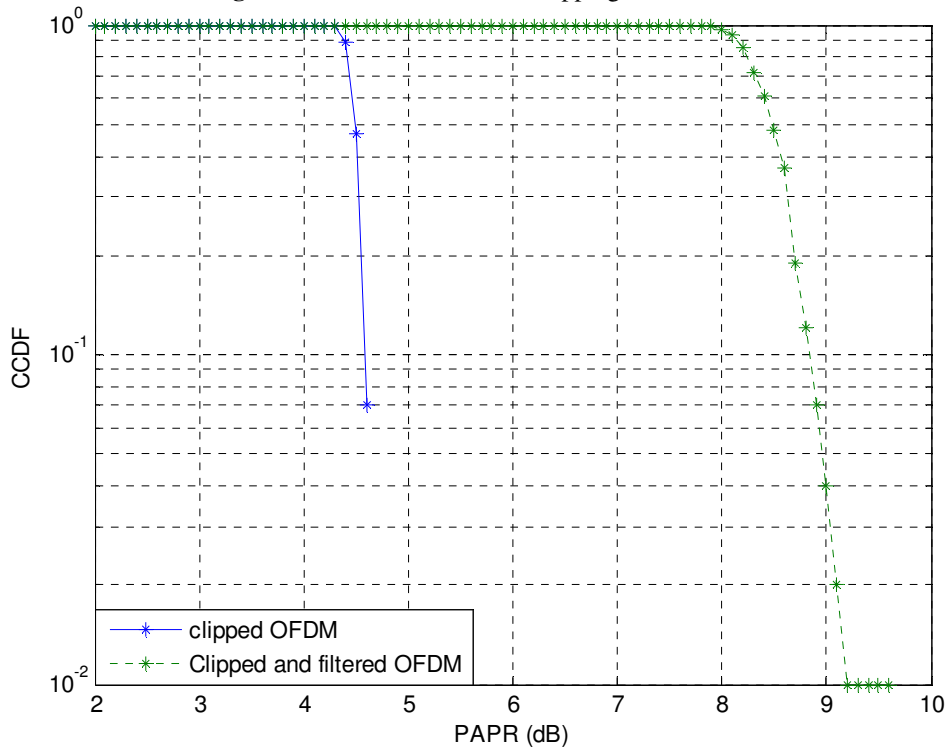


Fig.3.8 CCDF comparison of clipped and clipped-filtered OFDM

A peak cancellation method is described in [23], which utilizes the parabolic peak cancellation (PPC) using the truncated kernel signal, generated from the inverse fast Fourier transform (IFFT) of the shaped peak reduction tones (PRTs). In reference [24] author suggests an adaptive CGS (ACGS) algorithm to accelerate the convergence rate of CGS (clipping-noise guided sign-selection) algorithm. Meanwhile ACGS algorithm adjusts the clipping threshold adaptively in each iteration. An iterative estimation and cancellation of clipping noise is proposed in [25], it assumes that clipping noise is generated by a pre-determined process that can be replicated at the receiver and later on removed.

Clipping is however a simplest approach to reduce sudden peaks in OFDM envelope to lower down PAPR significantly. But using a hard limit threshold introduces distortion causing adjacent channel interference and poor BER performance. Both of these problems are inevitable, rectifying these problems is a tedious task involving high cost and complexity. So clipping is not a good candidate for PAPR reduction.

3.2.2 Companding

Companding includes compression and expansion. Audio signal envelope variations and OFDM signal envelope variation are similar due to the fact that both exhibit infrequent high peak values. Two standard compression method used for speech signals are A -law and μ -law. Companding increases lower signal power levels and keeps higher signal value almost fixed to enhance signal quality.

First in 1999 Wang, Tjhung and C.S.Ng [26] used μ -law companding for PAPR reduction. After that μ -law companding is largely exploited by the researchers for PAPR reduction. The μ -law companding can be expressed as:

$$x_{\mu c}[n] = \frac{A \cdot \text{sgn}(x[n]) \cdot \ln\left(\frac{1 + \mu x[n]}{A}\right)}{\ln(1 + \mu)} \quad (3.18)$$

Where μ is the parameter for compression, A is normalization constant such that $1 \leq \frac{x[n]}{A} \leq 1$.

Let the received signal be:

$$r[n] = x_{\mu c}[n] + N_q[n] + W[n] \quad (3.19)$$

Where $N_q[n]$ is the quantization error in ADC and $W[n]$ is the AWGN noise added in channel. The expanded OFDM signal at the receiver would be:

$$x_{\mu e}[n] = A \frac{e^{\left[\frac{r[n]}{A \cdot \text{sgn}(r[n])} \log(1+\mu) \right]} - 1}{\mu \cdot \text{sgn}(r[n])} \quad (3.20)$$

After companding, the lower peak values are increased but higher peaks remain closely intact. So peak power remains constant but average power is increased which results in PAPR reduction. This is simulated in Fig. 3.9 for 16-QAM OFDM signal at $L=4$ oversampling factor using μ -law companding at $\mu=15$. It clearly shows that after companding only lower peaks are altered. For higher values of μ better PAPR performance is achieved.

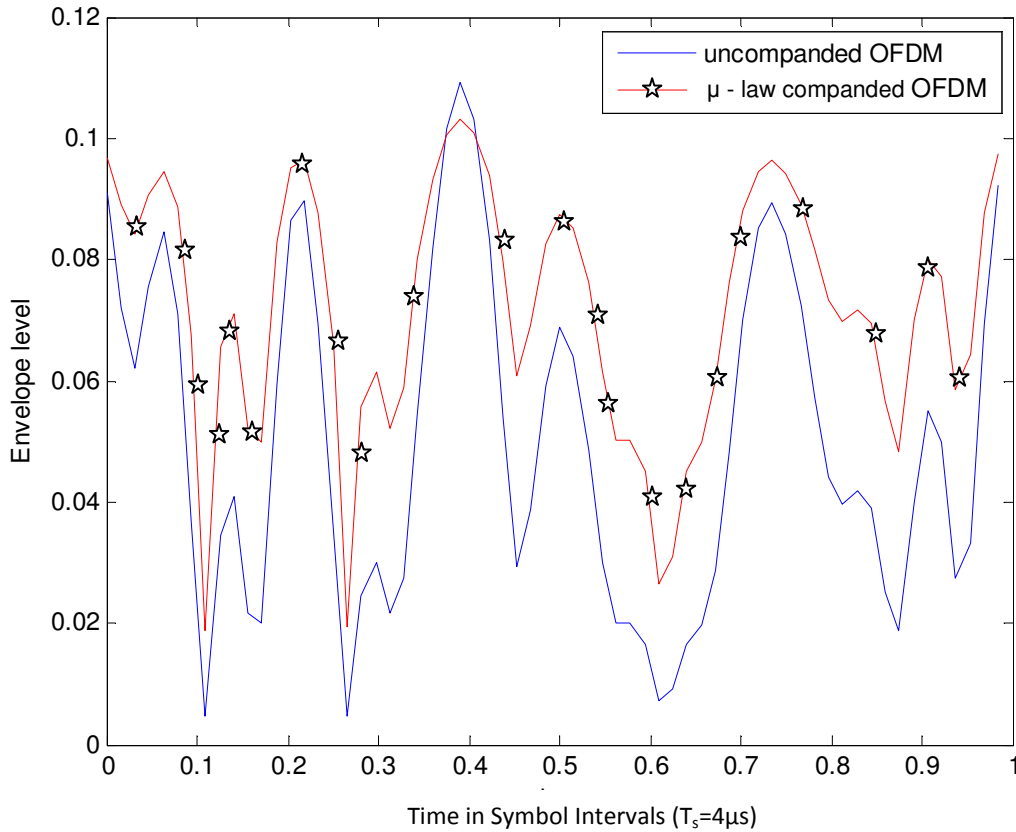


Fig. 3.9 μ -law companded 16-QAM OFDM signal

As far as the BER is concerned it remains undisturbed in absence of channel noise unlike in clipping method. Even when μ is changed BER remains unaltered. But in presence of AWGN the

noise component at the receiver will also experience expansion along with the desired signal which leads to increase in BER. So BER increases with increase in value of μ .

Due to the above fact uncompressed OFDM will always have lower BER than companded OFDM. In Fig. 3.10, effect of companding is shown on probability distribution function (PDF), it indicates that the occurrence of lower amplitude signal is reduced and the OFDM signal is more evenly distributed, thus increasing the average power.

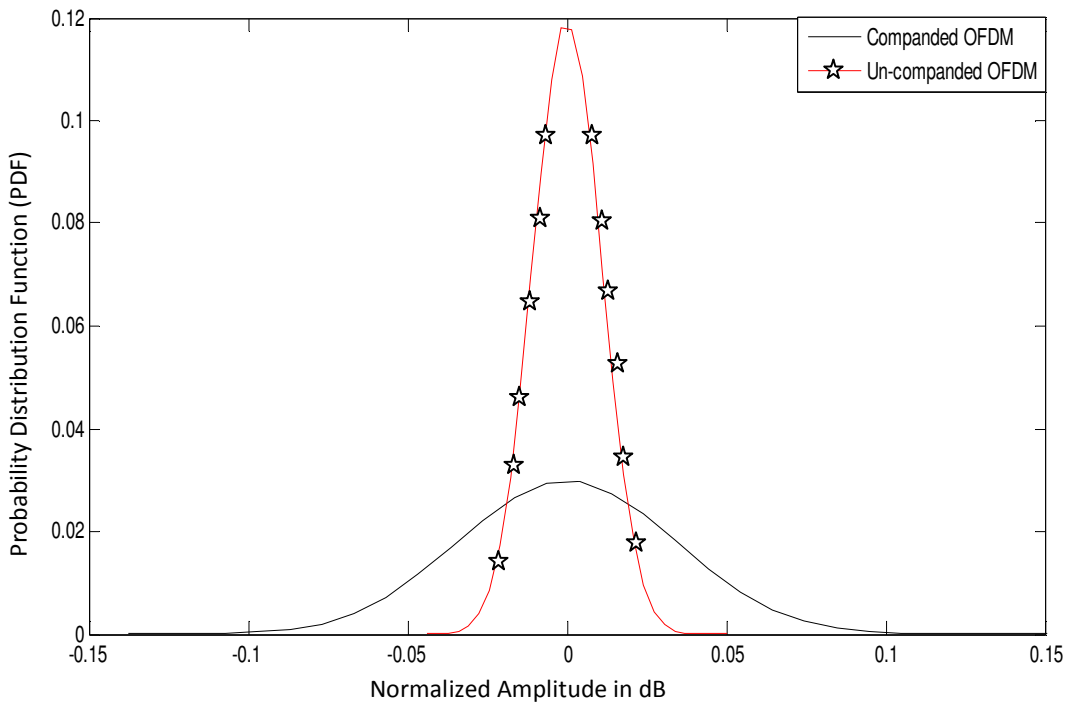


Fig 3.10 Probability distribution function for companded and un-companded OFDM

Author combined clipping with companding to achieve higher PAPR reduction in [27], but since clipping affect BER adversely, author suggested that a trade off between decent PAPR and good BER could be done if proper value of companding parameter is used.

Since average power of OFDM signal is increased to reduce PAPR value, it will put additional burden on transmitter to transmit more power than before. This is a major drawback with companding scheme, and reason why it is not in much use.

3.2.3 Windowing Method

In windowing method, whenever peak of envelope goes beyond a pre-decided threshold they are multiplied by weight governed by a windowing function. The commonly used windowing

functions owing to their good spectral characteristics are Cosine, Hamming, Hanning and Kaiser or Gaussian windows. But Kaiser window is used extensively because it is easy to manipulate the spectrum by changing window length and shape parameter. Kaiser window is given by following function:

$$w(n) = \frac{I_0 \left[\beta \sqrt{1 - \left(\frac{2n}{H+1} - 1 \right)^2} \right]}{I_0(\beta)} \quad (3.21)$$

Where $I_0(.)$ is the 0th order modified Bessel function of first kind

H is the window length

β is the attenuation factor

Shape of Kaiser window can be controlled using parameters L and β .

In [28], author suggested a method where windowing is performed on a clipped and filtered signal repeatedly for PAPR reduction and achieved 7 dB PAPR reduction at CCDF value of 10^{-3} , within 1 dB increase of E_b/N_0 at 10^{-4} BER. In [29], an advanced peak windowing method is discussed in which new weighting coefficients are introduced whenever successive peaks are generated within a half of the window length. Applying the new weighting coefficients, the successive peaks can be restrained to the given threshold level. In [30], author suggested two new peak windowing methods, called sequential asymmetric superposition (SAS) and optimally weighted windowing (OWW) to deal with closely spaced peaks to avoid high PAPR values.

However windowing method gives better performance as compared to clipping as it does not employ hard clipping, but still distortion can't be avoided fully.

Three methods mentioned above in sections 3.2.1, 3.2.2 and 3.2.3 reduces PAPR at the cost of producing distortion, so all of the above methods are not favourites, especially in the situations where E_b/N_0 values are at lower levels and BER is a major concern.

In next few sections, we will discuss those PAPR reduction techniques which are distortionless.

3.2.4 Coding Method

The basic principle is to select a set of code vectors which can be used for data vectors to avoid

high peaks and PAPR. A forward error correction (FEC) code is defined by (n, k) , where n are the data bits and k represents redundant bits, so the idea is to add redundant bit in a manner that overall PAPR value is minimized.

FEC are broadly divided in block codes and run length codes. Block codes uses a block of data bits together to encode them, whereas run length codes employs memory and lower values of n . Linear block codes, Golay complementary codes, Reed Muller, Bose Chaudhuri Hochquenghem (BCH), low density parity check (LDPC) are few block codes which have been used for PAPR reduction, whereas Turbo codes, which are derived from convolution codes is also discussed in literature for PAPR reduction.

In [31-32], first time block codes were proposed to be used for PAPR reduction in a multicarrier transmission system, where linear block codes were used for $N=4$ subcarriers using BPSK mapping. E.g.: in Table-3.1 maximum envelope power value for $N=4$ OFDM is shown for all possible data combinations, considering all the carriers are individually normalized to 1 watt.

Table 3.1 PEP values for OFDM with 4-subcarriers

Data block	Peak envelop power (PEP) (in watts)	Data block	Peak envelop power (PEP) (in watts)
0000	16.0	0001	7.07
1000	7.07	1001	9.45
0100	7.07	0101	16.0
1100	9.45	1101	7.07
0010	7.07	0011	9.45
1010	16.0	1011	7.07
0110	9.45	0111	7.07
1110	7.07	1111	16.0

Now, 4 set of combinations generate a PEP of 16 watts i.e. PAPR of 6.02 dB, 4 set generates a PEP of 9.45 watts i.e. 3.73 dB and rest of the 8 combinations generate a PEP of 7.07 watt i.e. 2.47 dB. If those data combination which are generating PAPR of 6.02 dB and 3.73 dB are avoided in transmission, overall PAPR will become almost 2.47 dB which is much lower than 3.7 dB, achieved otherwise. If we use $(4, 3)$ block codes such that, 3-bit data is converted to a 4-bit

codeword by using 1 redundant bit and all those sequences are avoided which generate high PAPR value, overall PAPR could be decreased. However this scheme requires exhaustive searches for finding the optimum code word when a large number of subcarriers are involved. In [33], block codes were used for PAPR reduction as well as to reduce BER, here (7, 4), (8, 4) and (15, 11) were used for achieving 2.9 dB, 4 dB and 1.26 dB PAPR improvement. The technique employs a weighting vector for creating an offset in the code word set, which is equivalent in terms of error control properties, but PAPR is reduced. This method is further improved in terms of computational complexity and improvement of 4.5 dB is achieved at low computational complexity [34].

Golay complementary sequence [35] could be used to modulate the subcarriers of an OFDM symbol and achieving a maximum PAPR value of just 2. In [36], relation between Golay complementary sequences and second order Reed-Muller code is exploited to achieve low PAPR of almost 3 dB. Golay codes were further investigated for PAPR reduction in [37-42] for various constellation sizes such as 16-QAM and 64-QAM.

A coding schemes derived from dual Bose Chaudhuri Hochquenghem (BCH) codes also been employed for PAPR reduction technique [43], as BCH codes don't have practical realizable decoders and work much below the Shannon limit. In this scheme, the gap in Shannon limit is filled by using turbo structure and PAPR improvement of 7 dB is achieved.

Turbo codes being a capacity approach codes are very popular, these codes are also being used for PAPR reduction. Three turbo coded OFDM system for PAPR reduction were proposed in [44], first using m -sequences for PAPR reduction and short codes for side information, second uses interleaving and third is combination of first two schemes. In [45], a tail-biting turbo coded OFDM system is proposed to generate candidates in a selective mapping scheme, without need of side information protection.

Low density parity check (LDPC) codes were first introduced by Gallager [46-47]. These codes have largely dominated the other forward error correction codes in terms of error correction capabilities with reasonable complexity of encoders they gave performance near to Shannon's limit. LDPC codes are also investigated by the researchers for PAPR reduction [48-49], in [48] it is shown that LDPC codes comes out to be better in terms of PAPR reduction than the Turbo codes.

Coding techniques suffers from a major problem of exhaustive search to find a suitable codeword which can reduce PAPR but at the same time these methods are limited to small number of subcarriers owing to high complexity of encoders and decoders. These methods find it difficult to exploit the error correction capability and PAPR reduction at the same time.

3.2.5 Multiple Signal Representation Techniques

These techniques produce a set of alternative transmit signals generated by same data set by using different set of phase sequences and their permutations, each of the candidate in the set have different PAPR characteristics, finally the candidate with best PAPR performance is selected and transmitted.

(A) Selective Mapping Scheme (SLM)

SLM scheme was proposed way back in 1996 [50], the basic principle is to generate a set of OFDM symbols representing same data sequence by multiplying a set of phase weights, each candidate have different PAPR value, the one with least PAPR is selected for final transmission. The block diagram of the scheme is shown in Fig. 3.11.

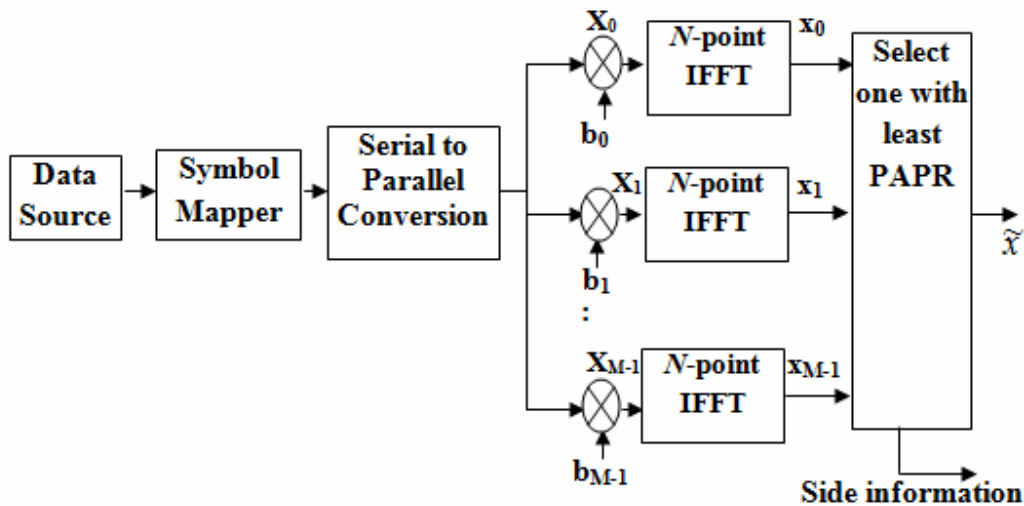


Fig. 3.11 Selective mapping scheme (SLM)

Let the input data block is $X=[X_0, X_1, \dots, X_{N-1}]$, this data block is multiplied with M different phase factors $b_m = [b_m^0, b_m^1, \dots, b_m^{N-1}]$, where $m= 0, 1, 2, \dots, M-1$; $b_m^n = e^{j\theta_m^n}$ and

$\theta_m^n \in [0, 2\pi)$ for $n=0, 1, 2, \dots, N-1$. After taking IFFT, this multiplication generates M sequences in time domain given by:

$$x_m[n] = \sum_{n=0}^{N-1} X_n b_m^n e^{\frac{j \cdot 2 \cdot n \cdot \pi \cdot t}{N}} \quad \text{for } m=0, 1, \dots, M \quad (3.22)$$

Among all of the generated x_m , the one with lowest PAPR is selected for transmission, condition is given by:

$$\tilde{x} = \arg \left(\max_{m=0, 1, \dots, M-1} \left(\max_{n=0, 1, \dots, N-1} |x_m[n]| \right) \right) \quad (3.23)$$

Fig. 3.13 shows the CCDF of SLM technique for $M=4, 8$ using 16-QAM mapping scheme and 64 subcarriers.

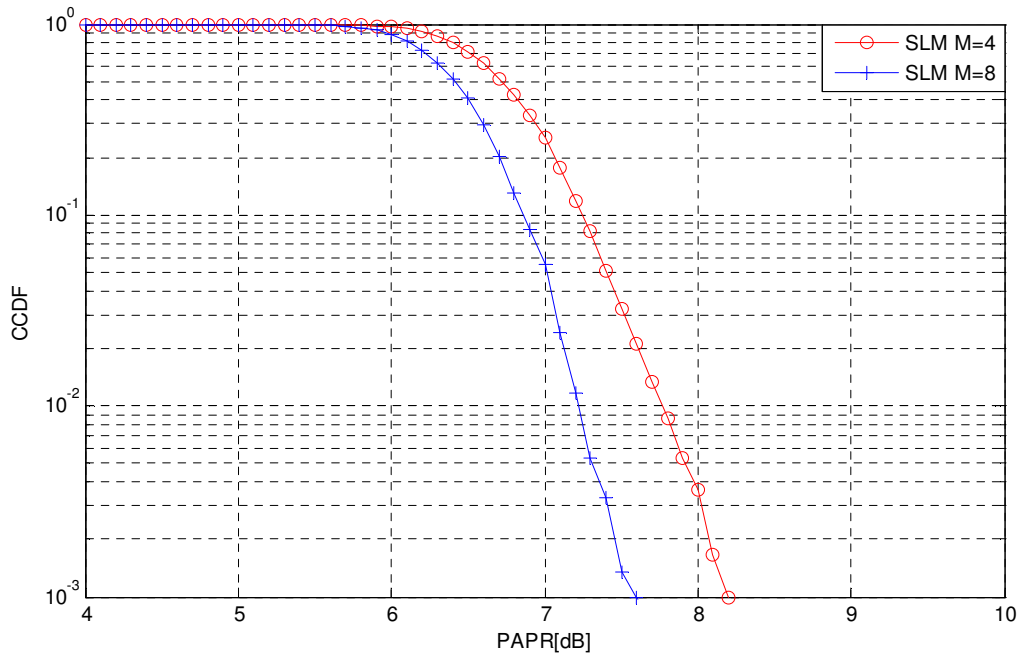


Fig. 3.12 CCDF for SLM technique with $M=8, 10$

To decode the OFDM symbol at the receiver information about the phase factor used at the transmitter need to be transmitted separately in form of side information [SI]. This puts additional burden on the bandwidth. For M phase sequences $\lceil \log_2 M \rceil$, side information bits are required. SLM involves a number of complex multiplications and additions, which makes it costly for

higher value of N and M , e.g. a N -point IFFT involves $\frac{N}{2}\log_2(N)$ complex multiplications and $N \log_2(N)$ additions, these are increased by a factor of L if oversampling is performed. Thus for M -phase sequence SLM, total number of multiplications equal to $L.M.\frac{N}{2}\log_2(LN)$ and total number of additions equal to $L.M.N \log_2(LN)$ will take place. A lot of schemes are available in literature to modify SLM, to address following three issues:

1. Computational complexity
2. PAPR reduction capability and
3. Avoiding SI.

For removing SI in SLM, various methods are proposed out of which few are discussed here, such as in [51] author proposed a scheme where a level is inserted with each candidate as an identifier tag so that phase sequence could be easily decoded at the receiver and scrambling is used to avoid any direct manipulation of SI at the receiver, convolution encoder could be used additionally to enhance the security of SI. Only a small amount of redundancy is added, but hardware implementation cost gets increased. This scheme did not proposed removal of SI, only representation is changed. In [52], a blind SLM receiver is proposed to avoid SI based on few constraints such as data vector is restricted for a given constellation and phase factor set is known at both the end. It simply multiplies the received signal with conjugate of phase factors and calculates the minimum distance from the received signal as follows:

$$D' = \arg \min_{\hat{c}, \hat{p}_m} \left\{ \sum_{n=0}^{N-1} \left| r_n \cdot e^{-j\phi_n^m} - H_n \cdot \hat{c}_n \right|^2 \right\} \quad (3.24)$$

Where D' represents the distance, r_n represents the received signal, H_n is the frequency response of the channel, $e^{-j\phi_n^m}$ is representing the phase sequence for $m=0,1,\dots,M-1$ and \hat{c}_n is the estimated symbol. D' metric is calculated for all values of M and then one with minimum distance is selected. For coded-OFDM system, codes like convolution, trellis codes etc. can use Viterbi decoder to calculate the min distance and could be integrated with receiver. But for uncoded OFDM, to test all the phase sequence for min distance is a tedious problem, thus this scheme suffers from complex receiver design with high computational complexity. This design is

further extended in [53] by the author for PTS as well, in [53], maximum likelihood (ML) method is used to find the transmitted phase factor for a coded OFDM system, Viterbi decoding method is used at the receiver to find likelihood function, however decoder hardware complexity is a challenging issue. In [54], author proposed a method named magnitude scaled-SLM, where a set of envelop function derived from Walsh sequences are used to scale the power profile of OFDM signal and at the receiver envelope function along with a detection matrix could easily identify the used phase at the transmitter. In [55-57], few other blind SLM schemes are proposed. In [55], author proposed use of *m-sequences* and use of a technique quite similar to [52] for detection of SI at the receiver but at transmitter SI is embedded in the sequences with the help of block partitioning and rotation, at the receiver phase factor are chosen from cyclic shifting the *m-sequences* which are derived from a Walsh Hadamard matrix. In [56], author proposed similar scheme for space time block coded (STBC) based multiple input multiple output (MIMO) OFDM system where alternate sequences are generated by cyclically shifting the OFDM signals from different antennas and then linearly combining them using additions/subtractions. At the receiver ML decoder is used to recover the signal and by avoiding IFFT operations at transmitter computational complexity is reduced. Authors suggested embedding the SI information in the phase sequence using offset determined by the biorthogonal vectors for the partitioned sub-blocks [57]. The author also proposed a low complexity ML decoder where the computational complexity is decreased by a factor of $(M - 2)/M$ as compared to the conventional OFDM system. In [58], author proposed a P-SLM method for Alamouti's SFBC MIMO-OFDM systems. Where phase offset is used for the signals from different antennas which corresponds the phase rotation sequences at the receiver, phase offset with minimum Euclidian distance from the received signal is considered as the transmitted phase shift, the PAPR performance is compared with conventional SLM scheme for $M = 4, 8$ and 16 and performance is found to be same. BER for the P-SLM scheme is also similar to conventional SLM above 8 dB SNR. In [59], author proposed a modified SLM scheme where conversion matrices (CM) containing a large set of elements is used to generate alternate OFDM signals and no SI is required due to especial design of CM, PAPR performance is again equivalent to that of conventional SLM.

For large block sizes and large number of phase sequences, choosing the best candidate is complex problem involving a lot of computations. Lot of work has been done to address this issue. In [60], author proposed a method for decreasing computational complexity where an

intermediate k -stage IFFT block is used to partially IFFT the block and then phase sequences are multiplied to it, remaining $n-k$ stage IFFT is done after it. The computational complexity reduction ratio (CCRR) is tabulated for various values of $n-k$, M and N . For lower value of $n-k$ up to 72% CCRR is achieved. For generating larger set of the candidates for better PAPR reduction at reduced complexity, the generated OFDM signals are combined [61], so with same number of IFFT operations a larger set of candidate is derived, author demonstrated generation of M^2 new candidates for only M IFFT blocks, however there is a increase in amount of SI. For multiplication, a CCRR of 63.7% is achieved with 2048 subcarriers. In [62], a low complexity SLM scheme is proposed for SFBC MIMO system, it reduces number of IFFT operations by exploiting time domain correlation between an antenna signals pair, as compared to the conventional SLM this scheme requires only 4.22% complex multiplications and 11.72% complex multiplications at a CCDF of 10^{-3} , using four phase weights $\{\pm 1, \pm j\}$. In [63], candidate signals are generated by combining OFDM signals and its cyclically delayed version of varying delay and phase, same PAPR performance is achieved at reduced complexity of 50% to 76%. In [64], proposed scheme uses additive sequence for generation of the new candidates from the existing one, scheme achieves a CCRR up to 88 % for the multiplication and 78% for addition at $M=40$. In [65], the proposed scheme uses intermediate IFFT stages, however in place of multiplying phase rotation, the proposed scheme generates OFDM candidates by cyclically shifting the connections at intermediate IFFT stage, achieved CCRR for multiplications and addition is 70% for 1024 subcarriers and $M=8$. In [66], author proposes a hybrid method for detection of SLM signal which is a combination of pilot-aided channel estimation and ML detection. Scheme offers a CCRR of 97.53% for multiplication and 99.69% for addition when using 64-QAM with $M=16$.

(B) Partial Transmit Sequence (PTS)

PTS [67-68] is one of the most preferred techniques for PAPR reduction in OFDM; typical building blocks of the scheme are shown in Fig.3.13. Here, the input frequency domain data block of length N is first partitioned into disjoint sub-blocks. Then each of the sub-blocks are padded with zeros appropriately and weighted by complex phase factors. The phase factor is the key for reduction of PAPR.

The data vector $X = [x_0, x_1, x_2, \dots, x_{N-1}]^T$ is divided in V disjoint sets, $\{X_v, v = 1, 2, \dots, V\}$, using same number of carrier for each group, the alternative frequency domain signal sequence is given by:

$$X' = \sum_{v=1}^V X_v b_v \quad (3.25)$$

Where $b_v = e^{j\phi_v}$ are the phase factors and $\phi_v = 2\pi i / W, i = 0, 1, \dots, W-1$. In time domain x_v , IFFT of X_v is called partial transmit sequence. The phase factor is chosen such that PAPR of candidate signal x' is minimum.

$$[\tilde{b}_1, \dots, \tilde{b}_V] = \arg \min_{[b_1, \dots, b_V]} \left(\max_{n=0, 1, \dots, N-1} \left| \sum_{v=1}^V b_v x_v[n] \right| \right) \quad (3.26)$$

Corresponding time domain signal with lowest PAPR is:

$$x' = \sum_{v=1}^V \tilde{b}_v x_v \quad (3.27)$$

For V sub-blocks with W phase weights total number of phase weights which need to be analyzed are W^{V-1} , as for the first block phase factor is always chosen as 1. The PTS scheme for weights $W = \{1, -1\}$ can be described as follows:

Step-1: Partition the input data block into V sub-blocks.

Step-2: Set all the phase factors equal to 1 and find PAPR of generated candidate and record this value.

Step-3: Now set the phase factor for $v=2$ as -1, and recalculate the PAPR. Compare the PAPR value to PAPR calculated in step 2, keep the lower one and discard the higher value. If value is lower then keep the phase factor unchanged otherwise switch it back to 1.

Step-4: Repeat the process till all values of v are exhausted, and record the phase factor value which generates the candidate with minimum PAPR. This set will be treated as optimized phase set.

For W phase weights, we have to search W^{V-1} possible candidate to get the one with least PAPR value. In calculation of each candidate $V-1$ additions and multiplication takes place.

So total number of complex additions and multiplication can be given by:

$$\text{Complex additions} = (V - 1) \times W^{V-1} \quad (3.28)$$

$$\text{Complex multiplications} = (V - 1) \times W^{V-1} \quad (3.29)$$

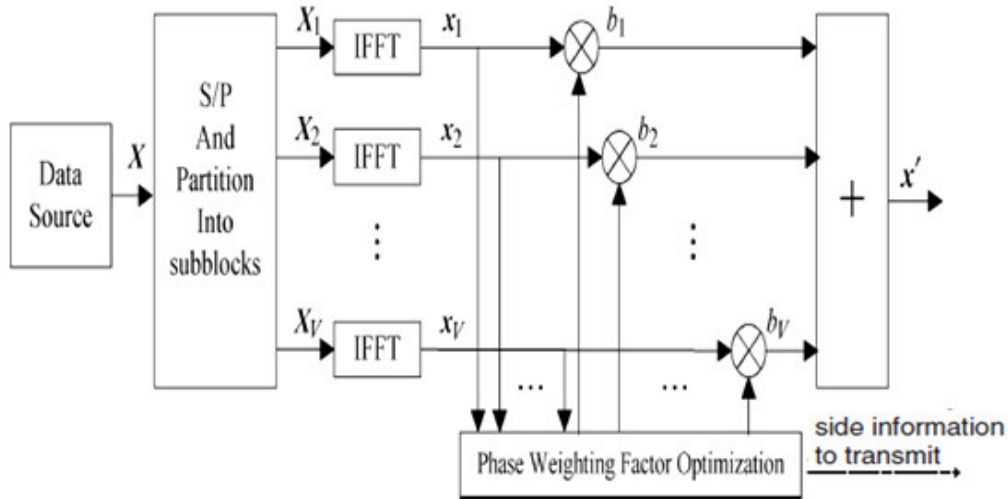


Fig. 3.13 Block diagram of PTS technique

Considering oversampling factor of L and block size N the above eq. 3.27 and 3.28 would be scaled by a factor of NL .

$$\text{Complex additions} = N.L.(V - 1) \times W^{V-1} \quad (3.30)$$

$$\text{Complex multiplications} = N.L.(V - 1) \times W^{V-1} \quad (3.31)$$

E.g for $V=4$ and $W=2$ i.e. +1 and -1, the phase sequences are b_1, b_2, b_3, b_4 , since b_1 is always 1, rest of the phase factors b_2, b_3, b_4 will have $8 = 2^3 = W^{V-1}$ possible permutations, given in Table 3.2:

Table 3.2 Phase factor combinations for $W=2$ and $V=4$

b_2	1	1	1	1	-1	-1	-1	-1
b_3	1	1	-1	-1	1	1	-1	-1
b_4	1	-1	1	-1	1	-1	1	-1

← $W^{V-1} = 8$ Combinations →

Candidate sequences are calculated as $X = b_1 \times x_1 + b_2 \times x_2 + b_3 \times x_3 + b_4 \times x_4$ so each candidate requires $V-1$ additions and multiplications, b_l is always 1 so it is not included in complexity calculation.

At the receiver end, to recover the OFDM signal back, we need to send the side information regarding the optimized phase factor, the number of bits in SI will be $\lceil \log_2 W^v \rceil$. This again is a burden on required bandwidth and also reduces bandwidth efficiency of the system.

The PAPR performance of PTS scheme for sub-block sizes $V = 4, 5, 6, 7, 8$ and without OFDM is shown in Fig.3.14, for 128 subcarriers and 16-QAM mapping scheme. It clearly shows that PAPR performance gets improve when block size is increased. Poor PAPR performance without PTS is clearly visible. For higher value of V , more number of candidates signal will be generated resulting in better PAPR performance.

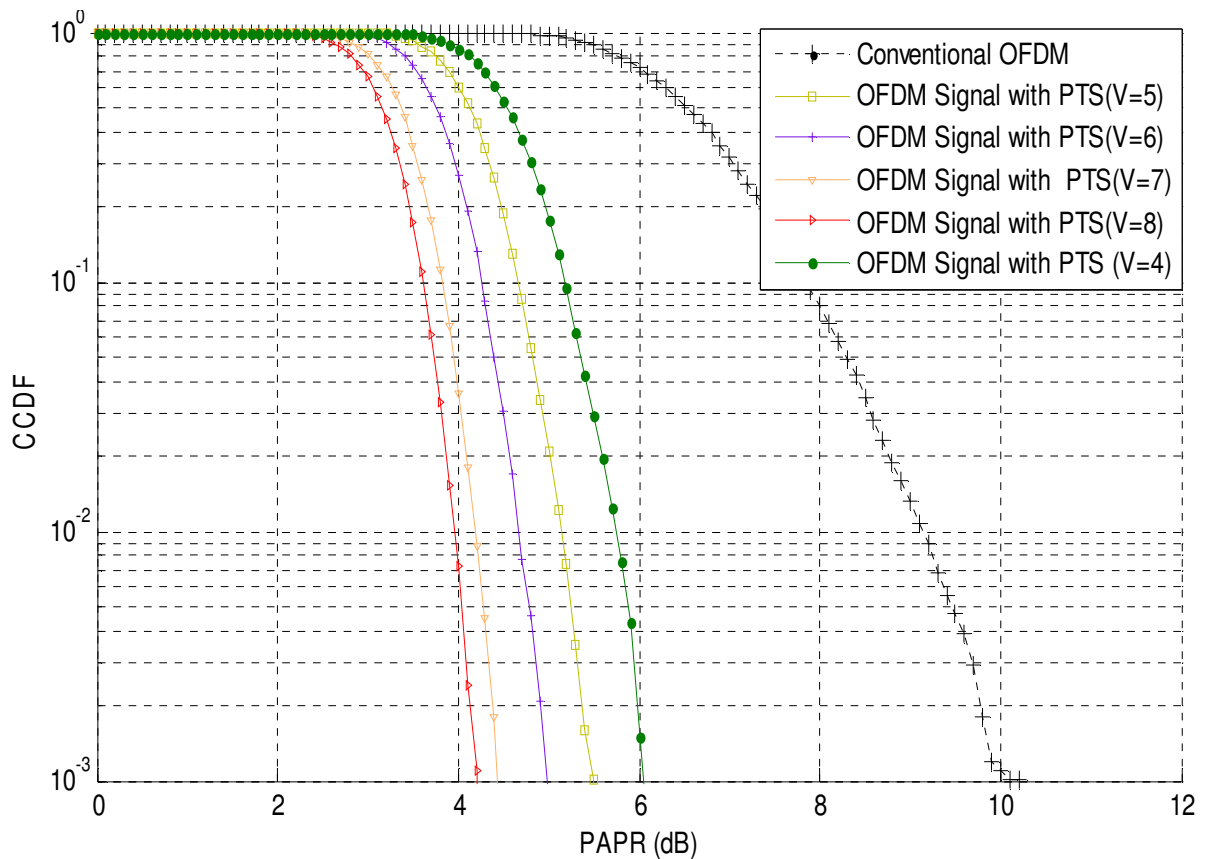


Fig. 3.14 CCDF comparison of OFDM systems with and without PTS

In PTS division of the data block in disjoint sub-blocks is done in three ways:

- (A) Adjacent Partitioning
- (B) Interleaved Partitioning
- (C) Pseudo-random Partitioning

In conventional OFDM scheme, adjacent partitioning scheme is widely used. In adjacent partitioning scheme, the entire data block/subcarrier space is subdivided in almost equal sub-blocks of N/V size and consecutive data symbols/sub channels are placed in the same sub-block. In interleaved partitioning, all the symbols or sub channels separated by V are assigned in the same sub-block. In pseudo random partitioning, any sub channel can be allocated to any of the sub-block. Fig. 3.15, 3.16 and 3.17 show adjacent, interleaved and pseudo random partitioning schemes simulated in MATLAB for arbitrary values of subcarrier-index n and block size V .

Out of these three schemes Pseudo random interleaving is proved to be the best [68], however its implementation on hardware is pretty complex, interleaved techniques is more complex as compare to adjacent as unnecessary. It involves unnecessary multiplications and addition with zeros takes place which can be easily avoided in adjacent partitioning.

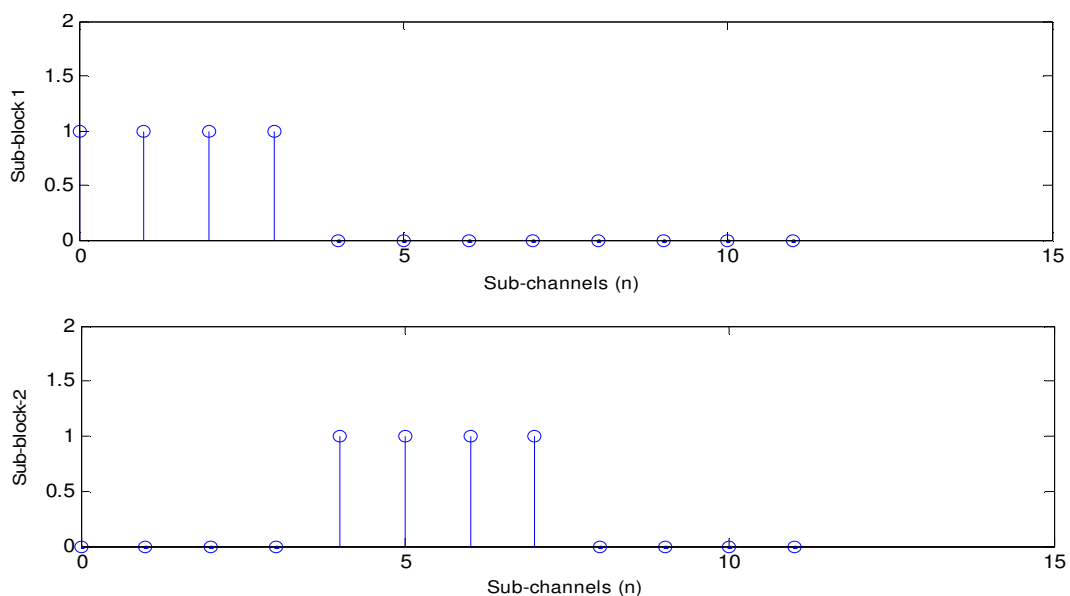


Fig 3.15 Adjacent partitioning

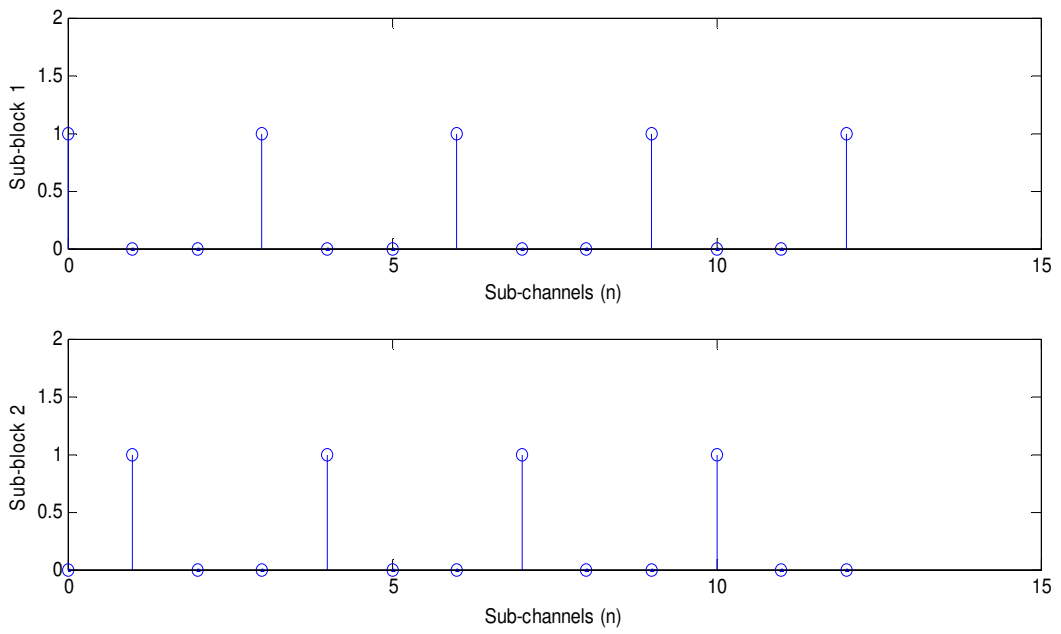


Fig. 3.16 Interleaved Partitioning

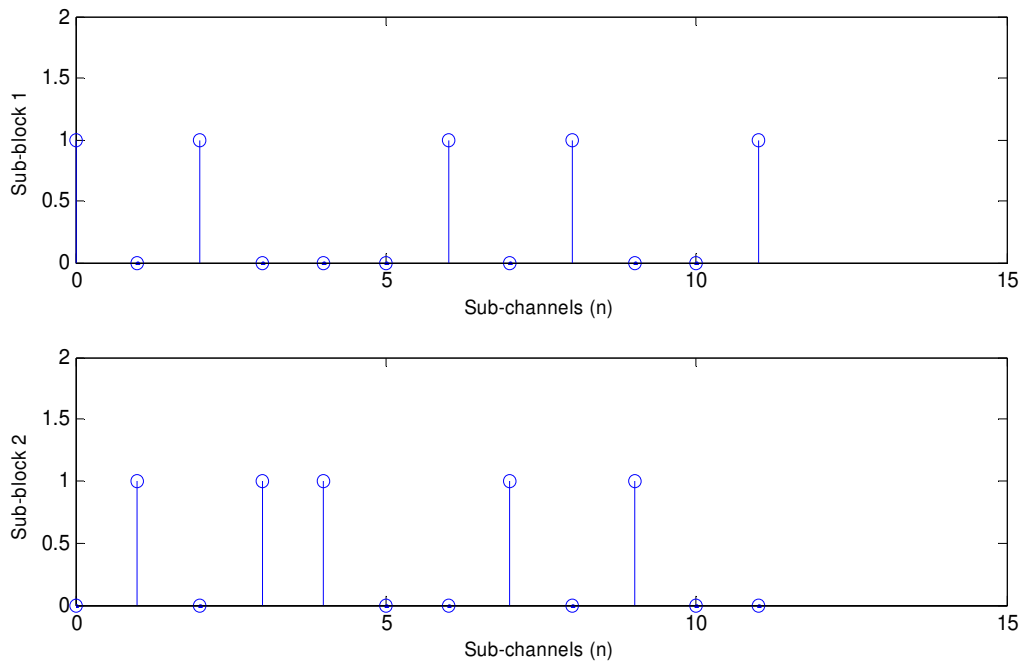


Fig. 3.17 Pseudo random partitioning

Most of the literature available on PTS targets following three issues associated with it:

- A) Reduction of exhaustive searches to find the optimum phase sequence
- B) Reduction of computational complexity
- C) Avoiding need of SI

In next few chapters, we will take up the issues associate with PTS and will discuss the literature available targeting these issues and new proposed schemes.

SLM and PTS both are however best sought methods for PAPR reduction, but both are affected by high computational complexity and data rate loss due to SI. However PAPR performance of SLM is better than PTS, but PTS is preferred due to its low computational complexity [69-72].

(C) Interleaving Technique

This technique is quite similar to the SLM technique discussed above, however to get multiple representation or permutations of the OFDM signal, block interleavers are used. Interleavers are devices which simply scramble or change the arrangement of the symbols [17, 73-78]. After taking IFFT, PAPR for each of the block is calculated and compared to the unchanged OFDM symbol, and then one with the least PAPR value is transmitted. Fig 3.18 shows the basic building blocks of the interleaved OFDM.

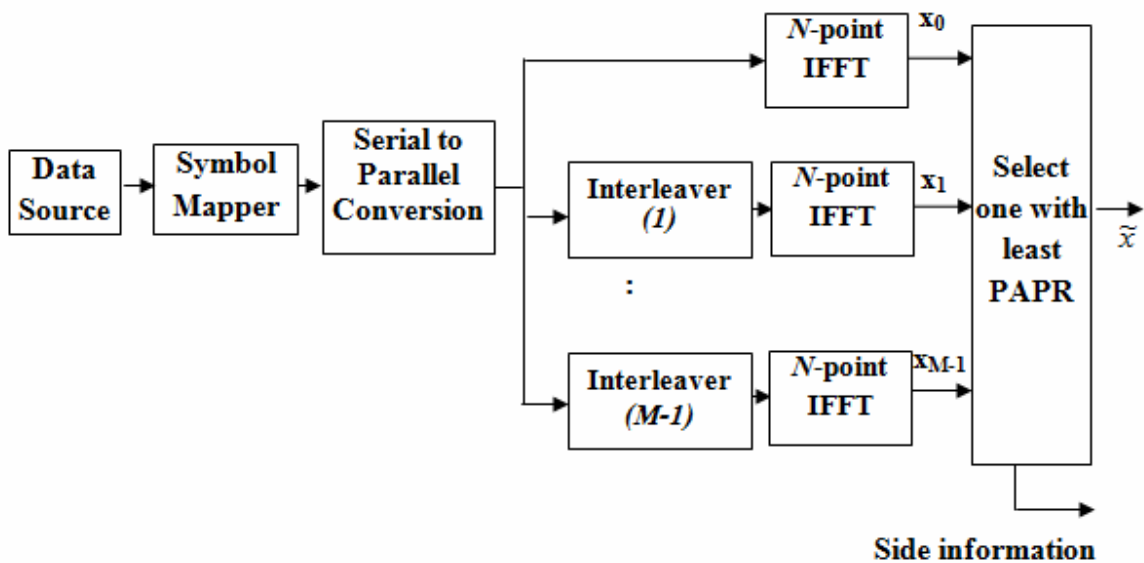


Fig. 3.18 Interleaved OFDM Techniques

Interleavers and de-Interleavers are usually denoted by the symbol π and π^{-1} , e.g. If $X = [X_0, X_1, \dots, X_{N-1}]$ after interleaving it can be written as $X(\pi) = [X_{\pi(1)}, X_{\pi(3)}, \dots, X_{\pi(N-2)}]$ i.e. X_0 is replaced by X_1 , X_1 is replaced by X_3 and so on, in the interleaved version. Fig. 3.19 shows a simple block interleaver.

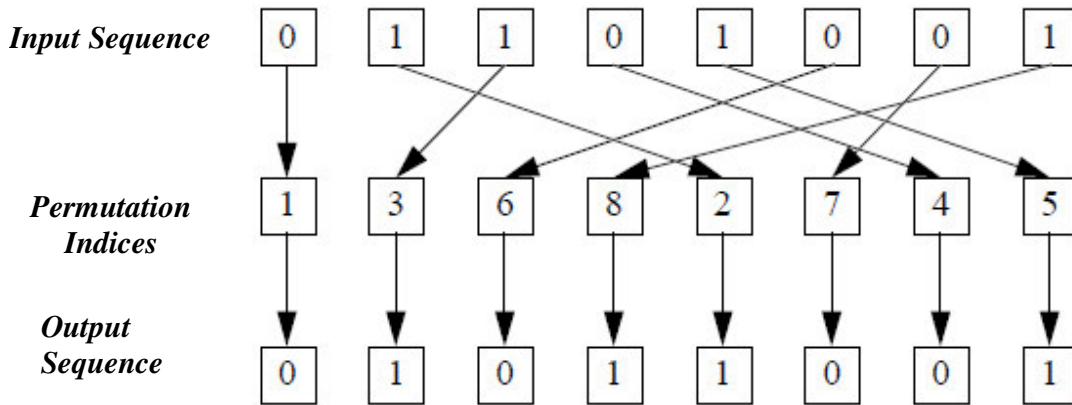


Fig. 3.19 Block interleaver

Fig. 3.19 shows that an input sequence is permuted using permutation indices 1, 3, 6, 8, 2, 7, 4, 5. Since there are M interleavers used (including unchanged data block), at the receiver to recover the original signal back, information regarding interleaver used at transmitter is required. So a total number of $\lceil \log_2 M \rceil$ bits of side information required. Both the transmitter and receiver keep a copy of permutation indices to make the interleaving and de-interleaving simpler. PAPR reduction depends on number of interleavers used and their architecture.

All the three techniques mentioned above are however distortion less techniques, but all of them have some serious implementation issues. SLM, PTS and interleaved techniques require transmission of side information causing reduced B.W efficiency and loss in data rate. All the three schemes also suffer from optimization problem in searching best PAPR candidate. Computational complexity also makes implementation a tedious task.

3.2.6 Constellation Modification Methods

In these methods, the constellation of OFDM signal is modified in such a way that resultant OFDM signal have low PAPR value. These methods are discussed in the following section.

(A) Tone Reservation Technique

In tone reservation (TR) [79-81] technique, a set of peak reduction tones or peak reduction carriers (PRT/PRC) are reserved and added to the existing OFDM symbols so that summation has lower PAPR values, at the receiver these PRT's/ PRC's are removed. So the objective is to add a data block with original data block in time domain, which changes the distribution of OFDM signal such that PAPR is reduced. If in frequency domain a block of PRC's denoted by $C = [C_0, C_1, \dots, C_{N-1}]$ is added with original OFDM signal block $X = [X_0, X_1, \dots, X_{N-1}]$, the new signal can be written as:

$$\hat{X} = X + C, \text{ in time domain it can be written as } IDFT(X + C) = x + c = \hat{x} \quad (3.32)$$

The PRC block C and X are chosen from disjointed frequency sub-space. PRC are low SNR signals which do not carry any information, but due to their orthogonality they do not interfere with subcarriers carrying data information. The objective is to find an optimum set of PRC's satisfying following condition:

$$\hat{x} = \arg \min_c [\max \{IDFT(X + C)\}] \quad (3.33)$$

Since X and C belong to disjoint space i.e $X_n = 0, n \in \{i_1, i_2 \dots i_S\}$ then $C_n \neq 0, n \in \{i_1, i_2, \dots, i_S\}$. These S nonzero tones/carriers are PRC's. Finding the optimum value of C_n is a complex problem which can be solved by treating it as a linear programming problem of complexity order $O(S.N^2)$. The typical block diagram of a tone reservation technique is shown in Fig. 3.20 and symbolic representation of signals shown in Fig. 3.21. PAPR reduction depends on the number of PRC used, their location in frequency subspace, location of PRC should be known at the receiver increasing overhead data bits. The addition of PRC actually reduces the data rate since PRC do not carry data bits. The data rate loss [79] could be given as:

$$Data\ Rate\ Loss = \frac{\sum_{k=1}^S b_{i_k}}{\sum_{k=0}^{N-1} b_k} \quad (3.34)$$

Where b represents the number of bits in the respective tone. We can reduce the data rate loss by choosing lower value of b_{i_k} .

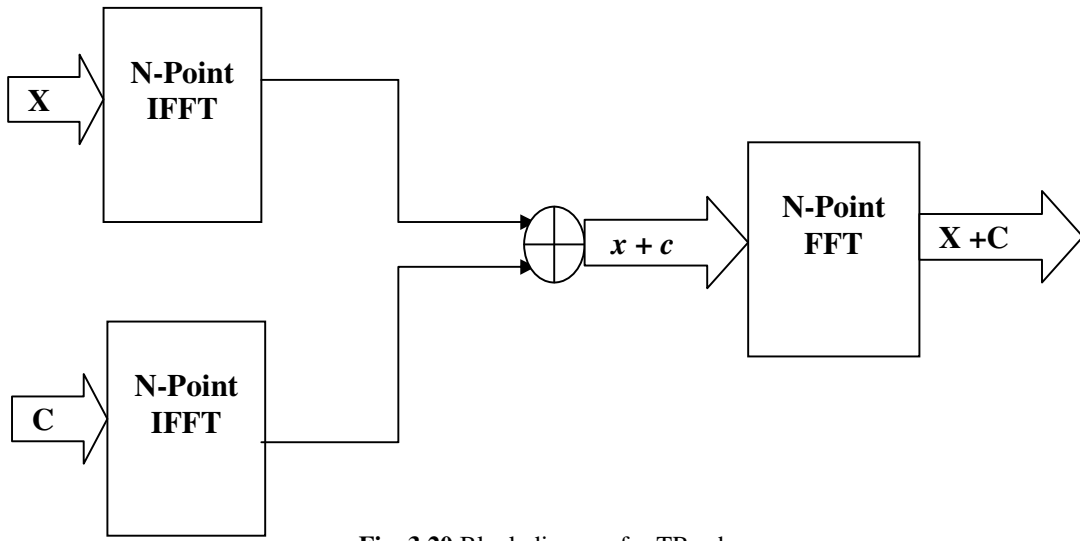


Fig. 3.20 Block diagram for TR scheme

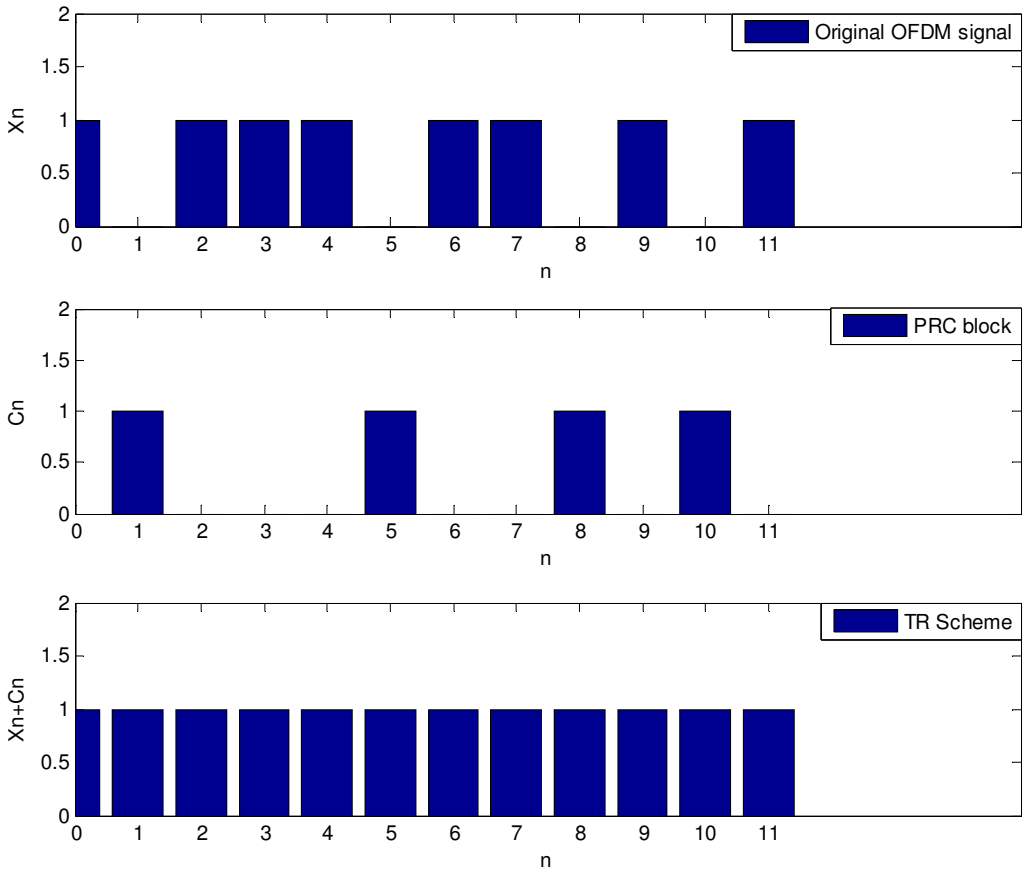


Fig. 3.21 TR scheme for PAPR reduction in OFDM

Various literatures are available mainly focusing on complexity reduction of optimization problem. A gradient algorithm is proposed in [79], where the gradient of clipping noise mean square error is calculated and optimization of signal to clipping noise ratio is done in place of PAPR and order of complexity is $O(N)$. In [82], author proposed a truncated IDFT algorithm where in place of calculating entire IDFT values, it calculates on maximal IDFT element thus reducing complexity of optimization process. The basic idea is to divide the group in two halves of $N/2$ and leave the half with lesser energy and move in similar way till we reach the maximum energy element, however the result may not always give correct maximal IDFT element, it also costs in lower PAPR reduction. Author however tried to improve it by carrying two best estimates to next level, rather than just one. In [83], a modification for pseudo noise code for PRC selection based system is proposed, to minimize the overheads required to send the information regarding PRC between transmitter and receiver, here PRC sequence is generated by finding the starting point of first PRC using bit reversing algorithm and then gradually increasing the offsets from first point to find rest of the PRC position. A q -stage linear feedback register is used to generate PN sequence, with q memory elements and s modulo-2 adder each having $q-1$ inputs, where $N=2^q$ and length of the sequence is 2^q-1 . Initial state of linear feedback register is shared between transmitter and receiver, then using bit reversing method first PRC is determined and offset give rest of the PRC information. In [84], for designing the peak cancelling signal clipping noise is analyzed and several iterations of clipping and filtering is used till desired peak cancellation signal is generated. Author also proposed constant-scaling algorithm and an adaptive-scaling algorithm for tone reservation. These algorithms scale the filtered clipping noise by a constant or an adaptively calculated factor to generate a peak-cancelling signal. A LSA-TR method with fast convergence is proposed in [85], which is based on least square approximation and used to find the peak cancelling signal faster than clipping control TR method, here filtered clipping noise signal generates peak cancelling signal after multiplication with a optimization factor, this method gives decent PAPR reduction even after the first iterations, here an optimization factor p needs to be determined which satisfies the following condition:

$$\min \left\{ \sum_{n \in \mathfrak{X}} [p \cdot |c_n| - |f(n)|]^2 \right\} \quad (3.35)$$

Where \mathfrak{R} is the set of the tones for which the amplitude of the signals exceed the desired threshold level, $f(n)$ is the clipping noise, $c(n)$ is the peak cancellation signal and p is the optimization factor.

Cross entropy (CE) method is proposed in [86], to find the set of optimal PRC's for PAPR reduction, the CE method proposed in [87] solve rare event estimation problem and widely used for the constrained combinatorial optimization problem, the basic principal of the CE method is to construct a random sequence of sample space of solution based on previous iteration's distribution, in every iteration based on the Kullback Leibler (KL) distance or cross entropy between associated density and the optimal importance sampling density parameters are adjusted to give better solution set and distribution in next iteration, scheme [86] gives a PAPR of 9 dB for 1024 subcarriers with 32 PRC's and 8.75 dB for 64 PRC's at a CCDF value of 10^{-4} . In [88], genetic algorithm is used to find the optimal PRC set, it also discuss an adaptive amplitude clipping tone reservation algorithm (AAC-TR) to solve the optimization problem in clipping control TR method. In [89], a curve fitting based tone reservation method is proposed using clipping noise introduced by clipping to generate a peak-cancellation signal, proposed scheme need just one IFFT operation thus reducing the computational complexity by huge margin, here the peak cancellation signal is fitted over the signal generating clipping noise, this reduces number of iterations too. Scheme requires a power increase of just 0.607 dB at CCDF value of 10^{-4} for $N=1024$ and 64 PRC's, this scheme requires just 2 iterations as compared to other efficient scheme such as LSA-TR needing 6 iterations, however AAC-TR also need 2 iterations.

In TR scheme data rate loss incurs due to addition of PRC's, as due to low SNR they do not carry information, thus can only solve the purpose of PAPR reduction at the cost of low data rate especially for lower value of N . Apart from this finding, an optimize set of PRC's increase the complexity at the transmitter, however adding PRC increases required transmission power.

(B) Tone Injection

The basic principle behind the tone injection scheme (TI) [79-80] is to extend the constellation of original OFDM signal, such that each point in the original constellation can be mapped in to an alternate one from larger set of constellation points available. This additional degree of freedom can be utilized for PAPR reduction i.e. in time domain, the PAPR reduction data block and original data block can be combined to generate low PAPR OFDM signal. Let $C[n]$, $n=0, 1 \dots N$,

represents the PAPR reduction data block in frequency domain. Then combined OFDM signal will be:

$$x(k) = \sum_{n=0}^{N-1} \{X[n] + C[n]\} \cdot e^{j \cdot 2\pi \cdot k \cdot n / N} \quad (3.36)$$

Where $C[n] = p[n] \cdot D + jq[n] \cdot D$; p, q are integers and D is a real positive number which remains constant. The values of p and q are adjusted in such a way that PAPR of combined signal is reduced, however D is a known parameter at the receiver and performing a *modulo-D* operation at the receiver can easily remove PAPR reduction data block from the combined signal. Adding C to the data block is equivalent to injecting a tone of appropriate phase and frequency, this is the reason of naming the technique as tone injection technique. Typical building block of a TI scheme is shown in Fig. 3.22

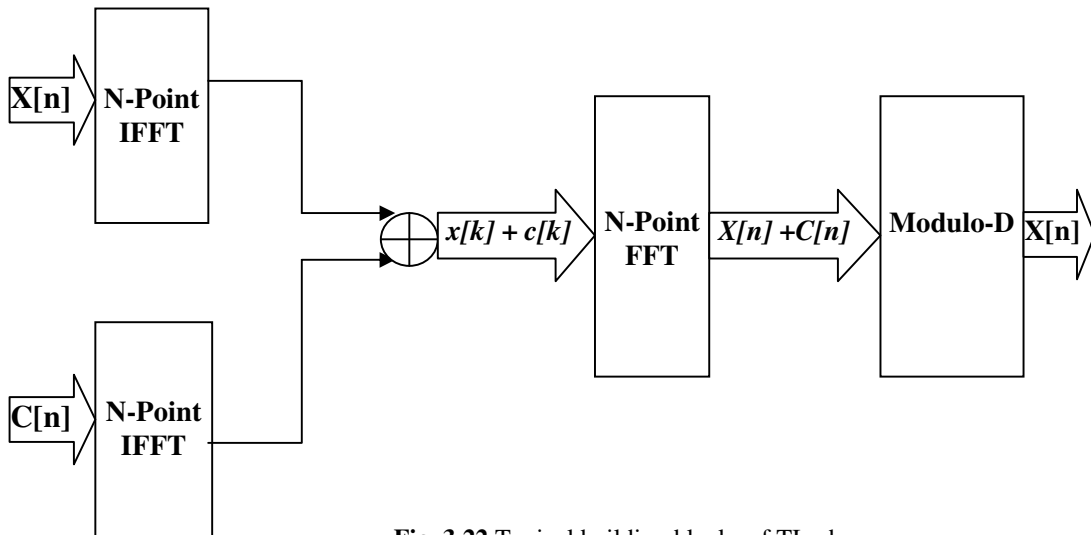


Fig. 3.22 Typical building blocks of TI scheme

Unlike TR scheme, in TI scheme X and C subspace need not be disjoint and orthogonal, both occupies the same frequency space, however in absence of orthogonality *mod-D* operation allows the separation of X and C at the receiver. The extended constellation of a constellation point in QPSK/4-QAM is shown in Fig. 3.23. In Fig. 3.23 distance between the constellation point is d , in such case real and imaginary parts of the symbol X_n can take value $(\sqrt{M} - 1) \cdot d/2$, where M is the number levels in M-QAM. These points could be extended to new points by TI, the distance between the original and extended points is D , it should be chosen such that BER at

the receiver should remain unaltered. Usually the value of D is $\rho.d.\sqrt{M}$, where $\rho \geq 1$. D is an important parameter as it affects the transmission power as well as the BER. Higher value of D increases the average power but BER will be low, lower value of D causes poor BER as constellation points come close to each other.

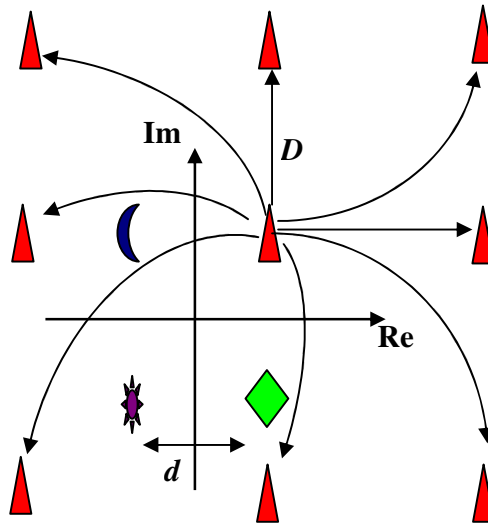


Fig. 3.23 Extended constellation in QPSK

In [90], use of hexagonal constellation is proposed in place of QAM constellation, as hexagonal geometry allows more number of signal points to be spaced uniformly in same area as compared to QAM constellation and the average magnitude is less than average value of QAM constellation, thus requires less transmission power than corresponding QAM constellation. In [91], author proposes use of cross entropy method to solve the problem of large number of searches to find optimum constellation. In [92], author proposes a low complexity TI scheme that uses the clipping noise to find the optimal equivalent constellation and is based on minimum mean error between the clipping noise and possible constellation points. In [93], author proposed a method of tone injection optimization for PAPR reduction and a linear programming algorithm which closely approximates the original tone injection optimization problem which is used for achieving low complexity, the algorithm is based on compressive sensing.

In TI scheme, unlike TR scheme there is no loss of data, as both X and C share the same frequency space, however finding a suitable set of solutions for $p[n]$ and $q[n]$ is again a complex problem. But there is no requirement of side information since at the receiver only Mod- D

operation is required to decode the signal back. TI scheme also require high transmission power due to addition of tones.

(C) Active Constellation Extension

In active constellation scheme (ACE) scheme [94-97], similar to the TI scheme the constellation of a OFDM signal is modified such that resultant signal will have a lower value of PAPR without any adverse affect on the BER. In ACE only the outer constellation points are dynamically extended away from the original constellation. Outer points are chosen for extension as extending them away from the decision boundary increases the spacing between the constellation points thus reducing BER and if it is adjusted properly, PAPR could also be reduced, as new signals cancels out the time domain peaks. In Fig. 3.24 regions of feasible extension are shown by shaded region for a QPSK constellation, original constellation point is extended to these regions.

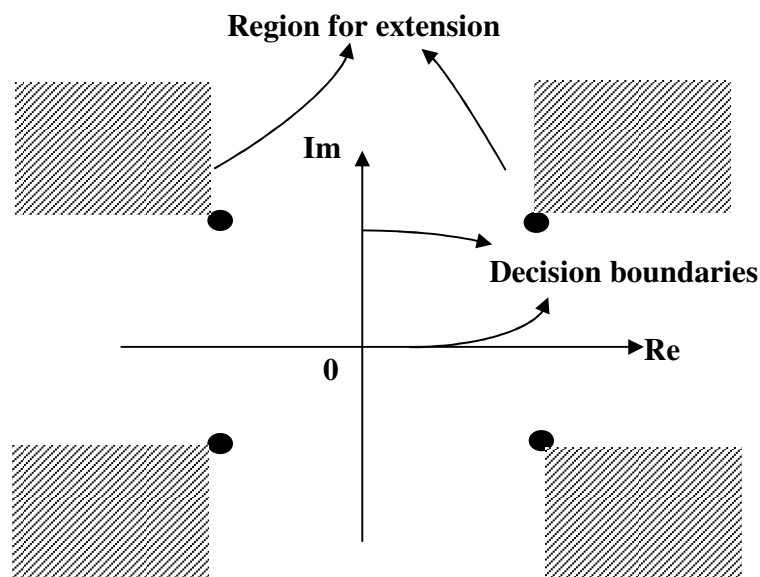


Fig. 3.24 ACE for QPSK mapping

For QPSK the quadrant boundaries are the decision boundaries, so any point far from these boundaries will definitely have a lower BER as its distance from other points will be more, the regions are chosen such that any extended constellation point will bound to have low BER and increment in the transmission power will be minimal.

Extensive work is available in the literature on ACE and suggested modification. In [98], author focuses on poor BER performance due to clipping used in ACE. Author gives a generalization of the ACE constraints to limit BER degradation. In [99], author uses pre-distortion technique in place of clipping based ACE (CB-ACE), the metric pre-distort those frequency domain symbols which have large contribution to output thus to PAPR. In [100], author proposes an adaptive clipping control algorithm to achieve better PAPR as compared PAPR reduction achieved in clipping based ACE at reduced number of iterations.

ACE however offers dual advantage of BER and PAPR reduction. ACE scheme do not require transmission of side information too, so there is no data rate loss too. But the major disadvantage is the increase in transmission power requirement. Thus the use of this scheme is limited to smaller constellation sizes only.

In all the above mentioned schemes, Partial transmit sequence found to be most suitable candidate for PAPR reduction especially in latest technology such as 4G LTE and WiMAX systems. However it also has certain issued such as high computational complexity, need of side information. However SLM gives better PAPR performance than PTS but not used much due to higher complexity. PTS is the most sought research area in PAPR reduction due to its application in 4G systems. Our next few chapters will discuss the issues associated with PTS, solutions suggested in recent years to tackle these issues and proposed schemes.

PARTIAL TRANSMIT SEQUENCE TECHNIQUE WITH LOW COMPUTATIONAL COMPLEXITY

This chapter deals with computational complexity issue of PTS scheme used for PAPR reduction in OFDM system. In this chapter, various schemes available in literature for computational complexity reduction are discussed and finally a new scheme is proposed for low complexity PTS system.

In PTS, while generating the candidate signals a number of complex additions and multiplications take place. For a PTS scheme with V sub-block, W phase weights and L oversampling factor, the number of complex additions and multiplication are given by:

$$\text{Complex additions} = N.L.(V - 1) \times W^{V-1} \tag{4.1}$$

$$\text{Complex multiplications} = N.L.(V - 1) \times W^{V-1} \tag{4.2}$$

To measure the performance of proposed scheme in terms of complexity reduction capability, we calculate *Computational Complexity Reduction Ratio* (CCRR), given by:

$$CCRR = \left(1 - \frac{\text{Computations for new Scheme}}{\text{Computations for conventional PTS}} \right) \times 100 \tag{4.3}$$

To reduce the computational complexity various schemes are proposed [101-120]. But either solution is not optimum or they suggest reducing the number of candidates.

In [101], binary phase weights $\{+1, -1\}$ are considered, all initial V phases are set as +1 and PAPR is calculated, next b_l is made equal to -1, PAPR is calculated again and if PAPR comes out to be less than the previous PAPR value, then only current phase factor is retained otherwise flipped back to +1, this continues till all the V positions have been explored. Scheme offers a PAPR of 7.8dB as compared to 6.8 dB in case of ordinary PTS for CCDF of 10^{-2} for $N=256$ and QPSK mapping scheme, however number of complex additions and multiplications reduces to just 16. In [102], author proposed an iterative adaptive scheme for PAPR reduction which is quite similar to [101], where the iterations stops when the threshold PAPR is achieved, author used binary phase weights $\{+1, -1\}$ and set the initial phase weights to +1, since maximum number of iteration is $\leq 2^{V-1}$, if after first iteration the PAPR is less than the threshold iteration stops, if not b_l is changed to -1, PAPR is calculated again and compared to the threshold, if it is less than the threshold then $b_l = -1$ becomes part of

optimized phase set and iteration stops other wise iteration continues. The result shows that for $M=8$, $CCDF \leq 10^{-2}$, scheme require only 16 iterations as compared to 128 in the conventional PTS, reducing the complexity by almost 83 %. For PAPR threshold of 7.4, 7.25 and 7.0 dB, scheme requires 22, 36 and 71 iterations thus reducing the complexity up to 83, 12 and 44%, respectively. However in this scheme maximum number of iteration could go up to 2^{V-1} as in conventional PTS. In [103], the algorithm is inspired from [101-102] however here the amplitude of the input symbols are first arranged in descending order and there alternated phases are varied by a offset of π , here the number of iterations are reduced to $L.N$ from W^{V-1} , this scheme is not restricted to binary phase weights only. In [104], a gradient descent approach is used for finding the optimum phase factors, the scheme initiates the phase sequence to a pre determined value and finds an updated phase set in the neighbourhood of radius r , where neighbourhood is defined as the set of phase sequences having hamming distance equal to or less than r . The condition for phase weight updation from b to b' is:

$$b' = \arg \left\{ \max_{\|b'-b\|_H \leq r} (PAPR_b - PAPR_{b'}) \right\} \quad (4.4)$$

Where $\| \cdot \|_H$ denotes the Hamming weight. For $r = M$ number of searches is same as the ordinary PTS. Search complexity get increased when r is increased, for $1 \leq r \leq M$, the complexity reduction is achieved at the cost of degraded PAPR performance. The scheme work as follows:

- 1) Partition of data blocks into sub-blocks.
- 2) Set all phase weights as 1 and iteration count to 1.
- 3) Among the phase factors set in the neighbourhood, find the one that gives best PAPR performance.
- 4) If the phase weight gives better PAPR performance than previous, then update the phase set, otherwise exit.
- 5) Increase the iteration number if it is less than maximum value otherwise exit.

For 128 subcarrier, 8 sub-blocks, four phase weights at a CCDF of 10^{-1} , PAPR is 5.90 dB with ordinary PTS, where as proposed scheme offers a degraded 7.0 dB PAPR performance, however the search complexity is reduced by a factor of 6% for $r=2$.

In [105], author proposed a search scheme using sphere decoding algorithm, algorithm is inspired by shortest vector problem in the lattice. Here the algorithm searches only those

vectors which are inside a sphere of radius $\alpha^2.V + \mu^2$, where μ is the sphere radius, α and μ are the coefficients depending on the PAPR threshold, set to be achieved. For $V=8$, binary phase weights and 512 subcarriers using 8-PSK modulation scheme offers a PAPR reduction of almost 2 dB poorer than the conventional PTS scheme, however offers a reduction in search complexity by 50-65%

In [106], the author proposed a scheme where IFFT is performed in more than one stage, for $N=2^n$, the N -point IFFT is divided in two parts, first l stage IFFT is performed on the data block, this intermediate sequence generates V new sequence after $n-l$ stage IFFT takes place and each one is multiplied with a rotation phase sequence and then summed up sequence with lowest PAPR is chosen as the final candidate. The side information is added in form of index in the data only once, after the last stage of IFFT. For $n-l$ values of 3, 4, 5 and 6, computational complexity reduction ratio (CCRR) is calculated for $V=2, 4$ and 8 using $N = 256, 2048$ and 8192. Results show that for $n-l=6$ and $V=8$, the maximum CCRR is just 47.1 ($N=8192$) which is poorer as compared to lower values of $n-l$, it increases with N and V . However for $V=3$ with $N=8192$ maximum CCRR of 67.3 is achieved. The PAPR performance of the scheme is poorer by 0.2 dB at CCDF of 10^{-4} than conventional PTS scheme, achieving a CCRR of 48 % for $N=2048, l=6$ and $V=8$.

In [107] to optimize the search process a new scheme is proposed which is based on nonlinear optimization called simulated annealing (SA). The SA scheme is derived from physical annealing of the solids. SA works on following concept:

For a solution vector b the fitness function $f(b)$ is calculated, another vector \hat{b} is accepted only when $\Delta E = f(\hat{b}) - f(b)$ is less than 0, otherwise accepted only when the acceptance probability is greater than a random number between 0 and 1. This takes place iteratively till crystal settles down to its lowest energy state. For PAPR reduction, the b represents the phase array and $f(b)$ represents the PAPR. For $N=256, V= 16$, 16-QAM mapping scheme, and $W= \{+1,-1\}$, at a CCDF value of 10^{-4} the PAPR is 8.17 dB as compared to 6.80 dB in conventional PTS scheme. However numbers of searches are just 10 as compared to conventional PTS which requires approximately 2^{16} searches. For 1000 iterations SA method gives a PAPR of 7 dB.

In [108], an IFFT based PAPR reduction technique is discussed, where signals are taken from middle stages of N -point radix IFFT. Here decimation in frequency is used in place of decimation in time due to lower multiplicative complexity for final stages, since the IDFT can

be obtained by taking the complex conjugate of the input and output sequences while using the same parameters. FFT algorithm reduces the N -point DFT computation to $r \times N / r$ -point DFTs repeating in $m = \log_r N$ stages, where r is the radix of r -FFT algorithm. As a consequence, the computational complexity is reduced from $O(N^2)$ to $O(N \cdot \log_r N)$ and sub-blocking or portioning is done at intermediated stage signal and $m-v$ stages take place after it. For 256 sub-carriers and $V=8$ sub-blocks the multiplication and additions decreases up to maximum 74 % and 60 %, however PAPR reduction is poorer as compared to conventional PTS. In [109], author proposed a low complexity which exploits the correlation between the generated candidates. Correlation between the two candidates generated between two candidate signals is calculated by:

$$\mathfrak{R}_{a,b} = \frac{\text{cov}(x_a, x_b)}{\sqrt{\text{var}(x_a) \cdot \text{var}(x_b)}} \quad (4.5)$$

High correlation between the signals can be used to calculate PAPR of one candidate from one another, only high amplitude signal points above a preset threshold are considered as they are major contributor to PAPR, rather than considering all the N points. If in x_a , D points are considered, in x_b also only the D points are considered thus reducing the computational complexity. All the candidate signals are divided in groups with significant correlation. For 16-QAM OFDM signal with $V=2$, $W=4$ and $N=1024$, the complexity reduction of 65% is achieved, whereas for $N=4096$ only 54% reduction is achieved but at a poorer PAPR performance as compared to conventional PTS.

In [110], author proposed an artificial bee colony algorithm for phase optimization. The artificial bee colony (ABC) algorithm for optimization is given in [111-112], however ABC algorithm is suitable only for continuously numerical optimization problem, for phase factors ABC algorithm is modified, for a CCDF of 10^{-3} , $V=16$, $W=2$ ABC-PTS scheme provides a PAPR of 6.8 dB as compared to 6.45 dB in conventional PTS but number of searches reduces from $W^{V-1}=2^{15}=32768$ to just 900 searches in ABC-PTS. In [113], author uses the correlation among the generated PTS signals. Scheme first set a generator matrix or array (basis vector) for phase sets and the rest of the phase factors are searched with just flipping the signs of the basis vector, as follows:

For $V=2$ and $W=2$ i.e. $\{1,-1\}$, phase weights the phase sequences will be $\{1,1\}$ and $\{1,-1\}$, now the basis vector are calculated by removing the sign of the these sequences i.e $B=\{1,1\}$,

similarly for $V=2$, and $W=4$ i.e. $\{\pm 1, \pm j\}$, the phase sequences will be $\{1, 1\}$, $\{1, -1\}$, $\{1, j\}$, $\{1, -j\}$ the basis vector will be $B_1 = \{1, 1\}$ and $B_2 = \{1, j\}$. Now all the phase sequences could be calculated by creating a table by following set of rules.

1. Basis vectors are put in the first row of the column, such that adjacent column varies by just one element. First element of the basis vector is always one.
2. In each column, rest of the phase sequences are derived from the basis vector by just changing sign of one element and placing them in the same column.
3. The signs of elements in last sequence of a column are same as the signs of the elements in the first sequence of the next column.

For $V=2$ and $W=4$, total number of phase weights = $W^{V-1} = 4$ are shown in Table 4.1 along with the signs of the elements in the vector.

Table 4.1 Phase factors for $V=2$ and $W=4$

$B_1 = \{1, 1\}$		$B_2 = \{1, j\}$	
$b_{B1,1} = \{1, 1\}$	$\{+, +\}$	$b_{B2,1} = \{1, -j\}$	$\{+, -\}$
$b_{B1,2} = \{1, -1\}$	$\{+, -\}$	$b_{B2,2} = \{1, j\}$	$\{+, +\}$

For $V=3$ and $W=4$, total number of phase weights = $W^{V-1} = 16$ are shown in Table 4.2 along with the signs of the elements in the vector.

Table 4.2 Phase factors for $V=3$ and $W=4$

$B_1 = \{1, 1, 1\}$	$B_2 = \{1, 1, j\}$	$B_3 = \{1, j, j\}$	$B_4 = \{1, j, 1\}$
$b_{B1,1} = \{1, 1, 1\}$ $\{+, +, +\}$	$b_{B2,1} = \{1, 1, -j\}$ $\{+, +, -\}$	$b_{B3,1} = \{1, j, -j\}$ $\{+, +, +\}$	$b_{B4,1} = \{1, j, -1\}$ $\{+, +, -\}$
$b_{B1,2} = \{1, -1, 1\}$ $\{+, -, +\}$	$b_{B2,2} = \{1, -1, j\}$ $\{+, -, -\}$	$b_{B3,2} = \{1, -j, j\}$ $\{+, -, +\}$	$b_{B4,2} = \{1, -j, -1\}$ $\{+, -, -\}$
$b_{B1,3} = \{1, -1, -1\}$ $\{+, -, -\}$	$b_{B2,3} = \{1, -1, -j\}$ $\{+, -, +\}$	$b_{B3,3} = \{1, -j, -j\}$ $\{+, -, -\}$	$b_{B4,3} = \{1, -j, 1\}$ $\{+, -, +\}$
$b_{B1,4} = \{1, 1, -1\}$ $\{+, +, -\}$	$b_{B2,4} = \{1, 1, j\}$ $\{+, +, +\}$	$b_{B3,4} = \{1, j, j\}$ $\{+, +, -\}$	$b_{B4,4} = \{1, j, 1\}$ $\{+, +, +\}$

Since there is significant correlation between the columns e.g. column 1 and 2 are same except the last element.

While generating the candidate PTS this correlation can be exploited e.g. using step 2, we can derive one candidate from other:

$$\begin{aligned}\tilde{x}^1 &= b_{B1,1,1}.x_1 + b_{B1,1,2}.x_2 + b_{B1,1,3}.x_3 \\ &= \text{sign}(b_{B1,1,1}).x_1 + \text{sign}(b_{B1,1,2}).x_2 + \text{sign}(b_{B1,1,3}).x_3\end{aligned}\quad (4.6)$$

$$\begin{aligned}\tilde{x}^2 &= b_{B1,2,1}.x_1 + b_{B1,2,2}.x_2 + b_{B1,2,3}.x_3 \\ &= \text{sign}(b_{B1,2,1}).x_1 + \text{sign}(b_{B1,2,2}).x_2 + \text{sign}(b_{B1,2,3}).x_3 \\ &= \tilde{x}^1 - \text{sign}(b_{B1,1,2}).2.x_2\end{aligned}\quad (4.7)$$

In this manner complexity could be reduced, author assume that Table 4.1 and 4.2 are created first before generating the PTS candidates and are available at transmitter and receiver both. For $W=4$, $V=4$ and $V=6$, the complexity of multiplication is reduced to just 8% and 2% respectively. However, only those multiplications are counted in computational complexity evaluation, where the phase weight is other than +1. Which actually is not correct since only for x_1 the phase weight remain unchanged to +1, so we can leave inclusion of the multiplication by +1 for the first block only, but for rest of the blocks the multiplication by +1 should be included, for precise and justified calculation of computational complexity.

In [114], author proposed a low complexity PTS scheme without SI, here the candidate PTS can be generated through cyclically shifting each sub-block sequence in time domain and combining them in a recursive manner. In this paper, author used interleaved partitioning in place of better PAPR performing techniques of pseudo random and adjacent partitioning method due to lower complexity when applying Cooley-Tukey FFT algorithm [115], since poor PAPR performance of interleaved partitioning can be improved by making the candidate in interleaved PTS more independent from each other [116]. In place of applying phase shifts to sub-block sequences, new candidate are generated by cyclically shifting some of the sequences and combining them with others. E.g. Let x_v represents the sub-block signal for $v=1, 2 \dots V$, after applying k -cyclic shifts the shifted sequence would be:

$$\hat{x}_v(k) = [x_v(k), \dots, x_v(0), \dots, x_v(k-1)]$$

The first candidate would be $x^1 = \sum_{v=1}^V x_v$ (4.8)

The next candidate would be $x^2 = x^1 - (x_v - \hat{x}_v(k))$ (4.9)

Then rest of the candidates can be generated from above equation using recursive method. Since there is no need of multiplying the phase sequences as candidates are generated by cyclic shifting, resulting in lower computational complexity. Since each cyclic shifted signal will have different phase constellation in frequency domain, so at the receiver using this phase information we can determine the shift k in the sub-block v . For 4-QAM, the best CCRR value achieved is 86.67% for $V=16$ and $N=128, 256, 512$ and 1024 . CCRR of 86.66% is achieved for 16-QAM. This scheme gives same performance with interleaved and pseudo random based convention PTS scheme. However implementing cyclic shift enhances the hardware implementation complexity at both transmitter and receiver.

In [117], author proposed three PTS schemes with grouping, recursive phase weighting method and combination of the two and shown that in all the three methods computational complexity is reduced. In group phase weighting method, the candidate sequence is divided in to groups first as:

$$x' = \sum_{v=1}^V b_v \cdot x_v = \sum_{v=1}^{r_1} b_v x_v + \sum_{v=r_1+1}^{r_2} b_v x_v + \dots + \sum_{v=r_{R-1}+1}^V b_v x_v \quad (4.10)$$

Where r is representing the group number, a group would be defined as G_k , $k = 1, 2, \dots, R$.

Now the candidate sequence can be written as:

$$x' = \sum_{v=r_0}^{r_1} b_v x_v + \sum_{v=r_1+1}^{r_2} b_v x_v + \dots + \sum_{v=r_{R-1}+1}^{V=r_R} b_v = G_0 + G_1 + \dots + G_R \quad (4.11)$$

Using given phase weighting sequences and these subgroups, all the candidates can be generated e.g.

If $W=2$ i.e. $\{1, -1\}$, $V=4$ and $R=2$ groups are divided as follows after considering the phase sequences:

$$G_{1,1} = x_1 + x_2, G_{1,2} = x_1 - x_2, G_{2,2} = x_3 + x_4, G_{2,3} = -x_3 + x_4, G_{2,4} = -x_3 - x_4 \quad (4.12)$$

Using these sequences, all the 2^{V-1} candidates can be generated. Similar concept is applied in case of recursive phase weighting method by exploiting high degree of correlation between the phase sequences. For $V=4$ and $W=2$, these scheme provides CCRR for multiplication as 58.3% and as 81.3% for $W=4$, for group phase weighting method and for recursive phase weight method it is fix at 75%, for any values of the parameter. However, combining the two methods give a CCRR of 87.5% and 94.5 % for $V=4$ and $W=2, 4$ respectively.

In [118], to reduce the search complexity parallel tabu search based PTS scheme is proposed, where parallel tabu search (TS) is used to find the optimal phase factors. Tabu search uses a memory which keeps the solution of previous iterations. TS work as follows:

- (1) Take a randomly generated initial candidate as solution.
- (2) Select the best solution out of a set of vectors which is not in the list.
- (3) Update the current solution in the list if it is better than present solution. Repeat the process till threshold criteria for the fitness function is satisfied.

From the initial solution set, a set of solutions created by applying a slight modification to it and fitness function (PAPR in this case) is calculated for all the sets. However, to avoid local minima some time modification may lead to a solution which gives poor fitness than the current solution, such moves are restricted and kept in a tabu list. Based on the tabu list subsets of solution are created and fitness is calculated for them, best candidate replaces the current set. The iteration continues till a threshold PAPR performance is achieved. In parallel tabu search crossover operation of genetic algorithm is used to update the initial set of solutions and pass the information between two parallel TS. It creates two new solutions from two existing ones. For $V=16$, $W=2$ with maximum 11 iteration and 4 parallel TS the scheme requires 1000 searches compared to almost 65536 searches in conventional PTS with PAPR values of 6.93 dB and 6.74 dB respectively.

In [119], a low complexity PTS scheme is proposed based on successive local search using Kasami sequences [120]. Proposed method involves two steps. In the first step set of sequences with very low cross correlation are chosen as initial phase vectors. For this purpose, Kasami sequences are used, which have very low correlation properties. In second step, out of the initial set those vectors are chosen, which generate low PAPR value. From these chosen vectors new phase sequences are generated using local search method. For $V=16$, $W=2$, $N=256$ these scheme requires just 0.42 % of complexity as compared to what involved in conventional PTS.

In [121], a tree based search mechanism is used for reducing the search complexity involved in PTS. A W -way tree is created, with nodes representing the phase factors and layers representing the sub-blocks, all PTS candidate will be generated by combining layers and the nodes while traversing the entire tree. The W -way tree is created as follows:

Tree will have total V layers equal to number of sub-blocks. At each layer, every node will be father of W nodes in next layer. All the nodes in a layer will be arranged as a sequence with

period of $2.W$ with bilateral symmetry in group of W . All the PTS candidates can be obtained by the combination of the sub-blocks and the related phase factors on the paths from root to leaves. Since there is a difference of only one weighting factor from root to neighbour, if difference signal is added to a candidate signal it will lead to next PTS candidate. When transition is taking place from $i-1$ to i^{th} node, the difference signal at layer v will be: $d_{v,i} = (b_{v,i} - b_{v,i-1}).x_v$, where b represents the phase factor and the x_v represents the PTS candidate signal.

The scheme achieves a CCRR of almost 95%, 97% and 98 % for multiplications and 65%, 66% for additions, when $V=4$ and $W=4, 6, 8$ respectively. PAPR reduction is same as achieved with the convention OFDM.

In [122], a low complexity PTS scheme is proposed which is based on cross correlation as parameter to optimize the phase sets. Here, the nonlinear model used for HPA and correlation of its output along with input helps in finding the optimized vector. There are two models Rapp and polynomial [123] used for mathematical representation of HPA. Phase sequence need to be selected such that cross correlation between the input (the PTS sequence) and output of the HPA is maximum. Scheme offers a CCRR of 80% and 90% for additions and multiplications.

In [124], a segmental PTS scheme is proposed for offset quadrature amplitude modulation based orthogonal frequency division multiplexing (OQAM-OFDM) systems. OQAM-OFDM system offers better data rate and spectral efficiency as compared to conventional OFDM due to lower number of side lobes and absence of cyclic prefix. OQAM-OFDM improve data rate by almost 13% than conventional OFDM systems. OQAM-OFDM systems are less affected by ICI due to frequency offsets as these systems are less sensitive to offsets. The overlapped OQAM-OFDM signal is divided in segments and in each of them some disjoint sub-blocks are partitioned and rotated by the phase factors. Scheme offers a CCRR of 85%, for $V=8$.

4.1 Proposed Low Complexity PTS Scheme

To reduce the complexity, we try to generate candidate signals from one another in the form of a weighted sequence as they exhibits high degree of correlation among them. For a given weight set and block size, candidate signals can be generated using a set of seed matrices. The analysis is done for $V=4, 5, 6, 7$ and 8 , which are considered as standard values of partitioning, however this can be extended to any value of V . For number of sub block $V=4$

and weighting factor $W=2$ i.e. 1 and -1. The candidate sequences eligible for transmission are given by:

$$Y_1 = X_1 + X_2 + X_3 + X_4$$

$$Y_2 = X_1 + X_2 + X_3 - X_4$$

$$Y_3 = X_1 + X_2 - X_3 + X_4$$

$$Y_4 = X_1 + X_2 - X_3 - X_4$$

$$Y_5 = X_1 - X_2 + X_3 + X_4$$

$$Y_6 = X_1 - X_2 + X_3 - X_4$$

$$Y_7 = X_1 - X_2 - X_3 + X_4$$

$$Y_8 = X_1 - X_2 - X_3 - X_4$$

Therefore, each term in the candidate sequence denotes one complex multiplication and addition each, except for the first term for which phase weight is always one.

Total complex multiplications in conventional PTS ($V=4$) = $W^{(V-1)} * (V - 1) = 24$

Total complex additions in conventional PTS ($V=4$) = $W^{(V-1)} * (V - 1) = 24$.

In proposed scheme, to reduce the complex number of additions and multiplications, we define following seeds or generator G :

$$G^1 = \begin{bmatrix} X_1 + X_2 \\ X_1 - X_2 \end{bmatrix}$$

Complex additions =2; multiplications =2 (as X_2 is considered to be multiplied by 1 and -1 respectively producing $+X_2$ and $-X_2$).

$$G^2 = \begin{bmatrix} X_3 + X_4 \\ X_3 - X_4 \end{bmatrix}$$

Complex additions =2; multiplications =4

Now, the same candidate sequences for PTS can be generated by grouping elements of the defined matrices as follows:

$$Y_1 = G_1^1 + G_1^2 \quad \text{Complex additions =1; multiplications =0}$$

$Y_2 = G_1^1 + G_2^2$	Complex additions =1; multiplications =0
$Y_3 = G_1^1 - G_2^2$	Complex additions =1; multiplications =0
$Y_4 = G_1^1 - G_1^2$	Complex additions =1; multiplications =0
$Y_5 = G_2^1 + G_1^2$	Complex additions =1; multiplications =0
$Y_6 = G_2^1 + G_2^2$	Complex additions =1; multiplications =0
$Y_7 = G_2^1 - G_2^2$	Complex additions =1; multiplications =0
$Y_8 = G_2^1 - G_1^2$	Complex additions =1; multiplications =0

Where G_i^j is the i^{th} element of j^{th} seed matrix

From the above equations in the new scheme:

Total number of complex additions =12

Total number of complex multiplications = 6

This is much less than the 24 complex additions and multiplications used in conventional PTS. *CCRR* values for complex additions and multiplications in the proposed scheme are:

$$CCRR^+ =50 \quad \text{and} \quad CCRR^x =75$$

While calculating *CCRR*, terms *N.L* is cancelled at numerator and denominator. So when mentioning the number of multiplication and additions *N.L* is not considered as it does not affect the *CCRR* values.

For no. of sub-blocks $V=5$

Candidate signals are:

$$Y_1 = X_1 + X_2 + X_3 + X_4 + X_5$$

$$Y_2 = X_1 + X_2 + X_3 + X_4 - X_5$$

$$Y_3 = X_1 + X_2 + X_3 - X_4 + X_5$$

$$Y_4 = X_1 + X_2 - X_3 + X_4 + X_5$$

$$Y_5 = X_1 - X_2 + X_3 + X_4 + X_5$$

$$Y_6 = X_1 + X_2 + X_3 - X_4 - X_5$$

$$Y_7 = X_1 + X_2 - X_3 + X_4 - X_5$$

$$Y_8 = X_1 - X_2 + X_3 + X_4 - X_5$$

$$Y_9 = X_1 + X_2 - X_3 - X_4 + X_5$$

$$Y_{10} = X_1 - X_2 + X_3 - X_4 + X_5$$

$$Y_{11} = X_1 - X_2 - X_3 + X_4 + X_5$$

$$Y_{12} = X_1 + X_2 - X_3 - X_4 - X_5$$

$$Y_{13} = X_1 - X_2 + X_3 - X_4 - X_5$$

$$Y_{14} = X_1 - X_2 - X_3 - X_4 + X_5$$

$$Y_{15} = X_1 - X_2 - X_3 + X_4 - X_5$$

$$Y_{16} = X_1 - X_2 - X_3 - X_4 - X_5$$

The seed or generator matrices are:

$$G^1 = \begin{bmatrix} X_1 + X_2 \\ X_1 - X_2 \end{bmatrix} \quad \text{Complex additions =2; multiplications =2}$$

$$G^2 = \begin{bmatrix} X_3 + X_4 \\ X_3 - X_4 \end{bmatrix} \quad \text{Complex additions =2; multiplications =4}$$

$$G^3 = [X_5] \quad \text{Complex additions =0; multiplications =1}$$

With the help of above generator matrices, all the possible candidates can be derived as following:

$$Y_1 = G_1^1 + G_1^2 + G^3 \quad \text{Complex additions =2 and multiplications =0}$$

$$Y_2 = G_1^1 + G_1^2 - G^3 \quad \text{Complex additions =2 and multiplications =0}$$

$$Y_3 = G_1^1 + G_2^2 + G^3 \quad \text{Complex additions =2 and multiplications =0}$$

$$Y_4 = G_1^1 + G_2^2 - G^3 \quad \text{Complex additions =2 and multiplications =0}$$

$$Y_5 = G_2^1 - G_1^2 + G^3 \quad \text{Complex additions =2 and multiplications =0}$$

$$Y_6 = G_1^1 - G_2^2 - G^3 \quad \text{Complex additions =2 and multiplications =0}$$

$$Y_7 = G_1^1 - G_1^2 + G^3 \quad \text{Complex additions =2 and multiplications =0}$$

$$Y_8 = G_1^1 - G_1^2 - G^3 \quad \text{Complex additions =2 and multiplications =0}$$

$$Y_9 = G_2^1 + G_1^2 + G^3 \quad \text{Complex additions =2 and multiplications =0}$$

$$Y_{10} = G_2^1 + G_1^2 - G^3 \quad \text{Complex additions =2 and multiplications =0}$$

$$Y_{11} = G_2^1 + G_2^2 + G^3 \quad \text{Complex additions =2 and multiplications =0}$$

$$Y_{12} = G_2^1 + G_2^2 - G^3 \quad \text{Complex additions =2 and multiplications =0}$$

$$Y_{13} = G_2^1 - G_2^2 + G^3 \quad \text{Complex additions =2 and multiplications =0}$$

$$Y_{14} = G_2^1 - G_2^2 - G^3 \quad \text{Complex additions =2 and multiplications =0}$$

$$Y_{15} = G_2^1 - G_1^2 + G^3 \quad \text{Complex additions =2 and multiplications =0}$$

$$Y_{16} = G_2^1 - G_1^2 - G^3 \quad \text{Complex additions =2 and multiplications =0}$$

Total complex additions in conventional PTS ($V=5$) = $W^{(V-1)} * (V-1) = 64$

Total complex multiplications in conventional PTS ($V=5$) = $W^{(V-1)} * (V-1) = 64$

Total complex additions in proposed scheme=36

Total complex multiplications in proposed scheme =7

Therefore, in proposed scheme $CCRR^+ = 43.75$ and $CCRR^x = 89.06$

For number of sub-blocks V=6

The seed or generator matrices are:

$$G^1 = \begin{bmatrix} X_1 + X_2 \\ X_1 - X_2 \end{bmatrix} \quad \text{Complex additions =2; multiplications =2}$$

$$G^2 = \begin{bmatrix} X_3 + X_4 \\ X_3 - X_4 \end{bmatrix} \quad \text{Complex additions =2; multiplications =4}$$

$$G^3 = \begin{bmatrix} X_5 + X_6 \\ X_5 - X_6 \end{bmatrix} \quad \text{Complex additions =2; multiplications =4}$$

The possible candidate signals can be derived as following:

$$Y_1 = G_1^1 + G_1^2 + G_1^3 \quad \text{Complex additions =2 and multiplications =0}$$

$$Y_2 = G_1^1 + G_1^2 + G_2^3 \quad \text{Complex additions =2 and multiplications =0}$$

.....

$$Y_{31} = G_2^1 - G_1^2 - G_2^3 \quad \text{Complex additions =2 and multiplications =0}$$

$$Y_{32} = G_2^1 - G_1^2 - G_1^3 \quad \text{Complex additions =2 and multiplications =0}$$

Total complex additions in conventional PTS ($V=6$) = $W^{(V-1)} * (V-1) = 160$

Total complex multiplications in conventional PTS ($V=6$) = $W^{(V-1)} * (V-1) = 160$

Total complex additions in proposed scheme = 70

Total complex multiplications in proposed scheme = 10

Therefore in proposed scheme $CCRR^+ = 56.25$ and $CCRR^x = 93.75$

For number of sub-blocks $V=7$

The seed or generator matrices are:

$$G^1 = \begin{bmatrix} X_1 + X_2 \\ X_1 - X_2 \end{bmatrix} \quad \text{Complex additions =2; multiplications =2}$$

$$G^2 = \begin{bmatrix} X_3 + X_4 \\ X_3 - X_4 \end{bmatrix} \quad \text{Complex additions =2; multiplications =4}$$

$$G^3 = \begin{bmatrix} X_5 + X_6 \\ X_5 - X_6 \end{bmatrix} \quad \text{Complex additions =2; multiplications =4}$$

$$G^4 = [X_7] \quad \text{Complex additions =0; multiplications =1}$$

Corresponding candidate signals are:

$$Y_1 = G_1^1 + G_1^2 + G_1^3 + G^4 \quad \text{Complex additions =3 and multiplications =0}$$

$$Y_2 = G_1^1 + G_1^2 + G_1^3 - G^4 \quad \text{Complex additions =3 and multiplications =0}$$

.....

.....

$$Y_{63} = G_2^1 - G_1^2 - G_1^3 + G^4 \quad \text{Complex additions =3 and multiplications =0}$$

$$Y_{64} = G_2^1 - G_1^2 + G_1^3 - G^4 \quad \text{Complex additions =3 and multiplications =0}$$

Total complex additions in conventional PTS (V=7) = $W^{(V-1)} * (V-1) = 384$

Total complex multiplications in conventional PTS (V=7) = $W^{(V-1)} * (V-1) = 384$

Total complex additions in proposed scheme=198

Total complex multiplications in proposed scheme = 11

Therefore, in proposed scheme $CCRR^+ = 48.4$ and $CCRR^x = 97.13$

For number of sub-blocks V=8

The seed or generator matrices are:

$$G^1 = \begin{bmatrix} X_1 + X_2 \\ X_1 - X_2 \end{bmatrix} \quad \text{Complex additions =2; multiplications =2}$$

$$G^2 = \begin{bmatrix} X_3 + X_4 \\ X_3 - X_4 \end{bmatrix} \quad \text{Complex additions =2; multiplications =4}$$

$$G^3 = \begin{bmatrix} X_5 + X_6 \\ X_5 - X_6 \end{bmatrix} \quad \text{Complex additions =2; multiplications =4}$$

$$G^4 = \begin{bmatrix} X_7 + X_8 \\ X_7 - X_8 \end{bmatrix} \quad \text{Complex additions =2; multiplications =4}$$

Corresponding candidate signals are:

$$Y_1 = G_1^1 + G_1^2 + G_1^3 + G_1^4 \quad \text{Complex additions =3 and multiplications =0}$$

$$Y_2 = G_1^1 + G_1^2 + G_1^3 - G_2^4 \quad \text{Complex additions =3 and multiplications =0}$$

.....

.....

$$Y_{127} = G_2^1 - G_1^2 - G_1^3 + G_2^4 \quad \text{Complex additions =3 and multiplications =0}$$

$$Y_{128} = G_2^1 - G_1^2 + G_1^3 - G_1^4 \quad \text{Complex additions =3 and multiplications =0}$$

Total complex additions in conventional PTS ($V=8$) = $W^{(V-1)} * (V - 1) = 896$

Total complex multiplications in conventional PTS ($V=8$) = $W^{(V-1)} * (V - 1) = 896$

Total complex additions in proposed scheme=392

Total complex multiplications in proposed scheme =14

Therefore, in proposed scheme $CCRR^+ = 56.25$ and $CCRR^x=98.4$

4.2 Performance of Proposed Scheme and its Comparison with Existing Schemes

The computational complexity reduction in new scheme in terms of CCRR is given below in Table 1. The results show that there is significant reduction in computational complexity which is reflected in terms of high value of CCRR as compared to conventional PTS system ($CCRR=0$).

Table 4.3 CCRR of proposed scheme

No. of Sub-blocks (V) for $W=2$	$CCRR^x$ (CCRR Multiplication)	$CCRR^+$ (CCRR Addition)
4	75	50
5	89.06	43.75
6	93.75	56.25
7	97.13	48.4
8	98.4	56.25

The scheme proposed here exploits the correlation among the candidate PTS signals to reduce computational complexity. So without reducing the number of candidate signal this scheme achieves same PAPR reduction as C-PTS scheme but at reduced complexity. The computational complexity decreases more when we increase number of sub-blocks used. In [105], the $CCRR^x$ is 50.4%. In [124], only 85 % CCRR for $V=8$ is achieved as compared to 98.4 % in our scheme. In [110], [118] and [119], it has been found that CCRR is 98% but at higher block size of $V=16$, which is more complex to implement than for $V=8$.

Findings

The increased computational complexity directly affects the design complexity and cost of the hardware needed to implement the PTS scheme since high computational complexity requires

higher processing capacity units to perform required multiplications and additions for generation of PTS candidates.

In proposed scheme the reduction in computational complexity is remarkable. The results suggest that there is significant reduction in computational complexity in terms of high value of CCRR as compared to conventional PTS system (CCRR=0). Results show that a minimum of 75% to a maximum of 98.4% reduction in complex multiplications can be achieved, whereas a reduction of 50-56 % in complex additions can be achieved.

Reducing the number of candidate signal is a general approach to reduce the computational complexity in conventional PTS based OFDM systems, however this result in performance degradation in terms of PAPR reduction. In proposed scheme the computation complexity reduction is achieved while keeping number of sub-carriers intact.

PARTIAL TRANSMIT SEQUENCE TECHNIQUE WITHOUT NEED OF SIDE INFORMATION

This chapter deals with transmission of side information (SI) in partial transmit sequence technique and review of the work done to avoid need of SI and a proposed octagonal mapping based PTS scheme which avoids the need of SI in PTS.

In partial transmit sequence technique, once the optimum phase sequence which generates the least PAPR partial transmit sequence is found, the information regarding the phase sequence must be transmitted to the receiver so that OFDM signal could be decoded correctly. This information regarding the phase sequences is sent in form of side information. Need of SI burdens the bandwidth and reduces the bandwidth efficiency of the system.

For V sub-blocks and W phase weights, total number of phase sequences would be W^{V-1} , in such case maximum number of side information bits would be $\lceil \log_2 W^V \rceil$. Avoiding SI can help out in saving extra bandwidth and thus making system more efficient. Extensive work has been done for avoiding the need of side information. Some of the key work is discussed here.

In [125], author proposed a scheme where the side information is embedded in the transmitted data. A marker is used to identify the side information embedded in the data. The marker is generated in following manner: for phase weights 1, no rotation take place so do nothing, for phase weights -1 entire sub-block is rotated by $\pi/4$. Scheme puts a marker on the rotated sub-blocks. At the receiver, after the de-mapping following formula is used for detection:

$$R = \sum_{i=1}^{(N/V)-1} Y_{i,v} \cdot Y_{i+1,v}^* \quad (5.1)$$

Where $Y_{i,v}$ is representing the i^{th} subcarrier in the v^{th} sub-block and Y^* is representing the conjugate of Y .

If there is no rotation, the received vector R will be $(N/V)-1$, otherwise there is rotation took place, this simple method can detect the phase sequences at the receiver. This scheme uses Walsh codes sequences as the phase sequences and the PAPR reduction achieved by this scheme is 1 dB poorer than conventional PTS scheme.

In reference [126], author proposed a novel way to send the side information at the receiver, since typically the first sub-block remains unaltered in PTS as for it phase weight is always 1. Side information for the symbol could be placed in first sub-block of next OFDM symbol, so the first OFDM symbol is transmitted without any SI and for the last symbol, additional dummy OFDM symbol is needed to carry SI. Since SI will be received in the next symbol at the receiver, there would be delay of one OFDM symbol in decoding the data. So the OFDM symbol is represented as $[S_{i-1,0}, \dots, S_{i-1,c-1}, X_{i,c}, \dots, X_{i,N-1}]$, where S represents the subcarrier carrying the SI of the previous symbol, rest of the subcarrier carries data symbol. However, sending SI in the same OFDM symbol requires additional IFFT operations. This scheme offers better PAPR performance than conventional PTS with SI. BER performance is also improved since now it is easier to detect SI, but this scheme does not offer removal of SI.

In [53], author proposes use of maximum likelihood (ML) detector at the receiver to find the optimum phase sequence used, based on the following condition:

$$D'^v = \min_{v \in \{0,1,\dots,V-1\}} \sum_{n=N_V/V}^{N(v+1)/(V-1)} \min_{\hat{c}_n} |r_n - \hat{H}_n \hat{c}_n \hat{b}_v|^2 \quad (5.2)$$

Where D' represents the Euclidian distance, r_n is the received symbol, \hat{H}_n is the estimated channel, \hat{b}_v is the estimated phase sequence and \hat{c}_n is the estimated symbol at the receiver. Based on the distance metric receiver decides upon the transmitted phase sequence. However, implementing ML decoder itself increases the hardware complexity of the receiver circuit especially for higher order constellations. PAPR reduction performance of the scheme is same as achieved with conventional PTS system with SI.

In [127], author proposed a PTS without SI scheme, here pilot tones are used to identify the side information, in each sub block one pilot tone is added. At the receiver, a minimum distance criterion is used to identify the phase sequences, as following:

$$b = \min_{b_1} |a_1 - b_1' \cdot r_1| \quad (5.3)$$

Where $|\cdot|$ represents the square of Euclidian distance, a_1 is the transmitted tone, r_1 is the received symbol and b_1' represents the estimated phase factor. All the phase sequences are applied and the one with minimum Euclidian distance is selected. However, for larger set of phase sequences a larger set of pilot tones may be needed which results in the loss of data rate. In [128], author proposed a scheme for embedding the side information; however it does

not offer removal of SI, but offers decent BER at the receiver. In [129], author proposed an extended scheme based on the scheme proposed in [127], again pilot tones are used to determine the phase weights at the receiver using minimum distance criteria. Let at

transmitter the phase factor is b_i , then at the receiver $b_i' = \frac{1}{b_i}$ is used for detection. Then the

Euclidian distance is calculated as $M_1^i = \left(|a_1 - b_i' r_1| \right)^2$ where $i=1, 2, \dots, W$. M_1 is calculated

for all the possible phase weights, author suggested use of phase weights $b_i \{1, j\}$, at receiver the weight used will be $\{1, -j\}$. In that case, two values M_1 and M_2 will be calculated. To find the correct M , difference D is calculated as $D = M_1 - M_2$. A circuit to calculate D is also mentioned in the paper. However, the hardware implementation is pretty complex for the proposed scheme.

In [130], author proposed a new constellation extension scheme for avoiding side information in PTS, scheme is proposed for phase weights $\{\pm 1, \pm j\}$. The scheme exploits the fact that when a quaternary phase point is multiplied with these phase weights, the product will produce four new points which will lie on the vertices of a square. Thus a 4-QAM signal will generate 16 new points in the extended constellation, these are divided in 4 groups and each corresponds to quaternary point transmitted, at the receiver a look up table is created containing all these 16 points divided in the groups. Any decoded symbol at the receiver will be matched to the groups in the table thus decoding the correct symbol without any SI. The PAPR performance is same as the conventional PTS scheme, but the scheme is limited to only four phase weights.

In [131], author employed the same constellation extension scheme as in [6] but for binary phase weights $\{+1, -1\}$. Here, each symbol $X(k)$ is mapped to one of the two points $\hat{X}(k)$ and $\tilde{X}(k)$ after rotation by $+1$ or -1 . Out of these, one generating lower PAPR will be selected for transmission. Since at the transmitter, one of the point is chosen from the two constellation depending on the PAPR value, so at the receiver, there is no need to know that the points are from which of the constellation for de-mapping purpose of the symbol. The scheme offer 1.1 dB and 0.6 dB better PAPR performance than conventional PTS for $V=4$ and 8 respectively using 16-QAM OFDM with $N=256$ subcarriers, but it is limited to two phase factors only.

In [132], a combination of PTS scheme with channel estimation is introduced. A virtual channel frequency response is proposed which is the combination of channel's frequency response and the phase factors used in PTS. So channel estimation itself could decode the OFDM symbol without any additional SI. A special pilot tone arrangement makes channel estimation process easier. Each sub-block contains at least one of the pilot tones. The estimation takes place as follows:

Let $\mathcal{X}^P = \{i_0, i_1, \dots, i_P\}$ represents the set containing pilot tones location, where P is the number of pilots. $X(k)$ represents the data symbol if $k \in \mathcal{X}^{P^c}$ (complementary set of \mathcal{X}^P), otherwise represents the pilot symbol. Transmitted signal will be:

$$X(k) = X_d(k) + X_p(k) = \begin{cases} X_d(k); k \in \mathcal{X}^{P^c} \\ X_p(k); k \in \mathcal{X}^P \end{cases} \quad (5.4)$$

Received frequency domain symbol will be:

$$R(k) = X(k).H(k) + W(k) \quad (5.5)$$

Where $H(k)$ is the frequency response of the channel and $W(k)$ is the noise component.

An estimated version of frequency response at the receiver is given by:

$$\hat{H}(k) = \hat{H}_d(k) + \hat{H}_p(k) \quad (5.6)$$

Where $\hat{H}_p(k) = \frac{R(k)}{X_p(k)}$; $k \in \mathcal{X}^P$ and $\hat{H}_d(k)$ can be calculated by interpolation, the

estimated data symbol would be:

$$\hat{X}_d(k) = \frac{R(k)}{\hat{H}_d(k)}; k \in \mathcal{X}^{P^c} \quad (5.7)$$

For $W=2$ and $V=8$, it offers 5.2 dB at a CCDF of 10^{-4} which is 0.2 dB better than conventional PTS scheme. However, BER rate is poorer than conventional PTS scheme with SI.

In [133], a PTS scheme without SI is proposed, here in each sub-block a pilot symbol is inserted at the end and channel estimation is done at the receiver using known pilots which helps in symbol detection without any SI. Total numbers of subcarriers are $N = N_p + N_{data}$, representing pilots and data respectively. This scheme offers similar PAPR and BER

performance as conventional PTS. Since in this technique, additional pilots are added, it leads to higher transmission power requirement and loss of data rate.

In [134], a PTS scheme without SI is proposed which is based on constellation extension. In this scheme, the data block X is used to create a difference vector D , which is the difference between the original and the extended constellation points and then D is partitioned into several disjoint sub-blocks. Combination of IFFT of X and IFFT of sub-blocks of D used to generate signal with low PAPR. At the receiver, extended constellation is used to detect the signal back. Scheme offers same PAPR performance as conventional PTS. But due to extended constellation, additional transmission power is required for the transmission. However, this system works better with binary phase weights only.

In [114], author suggested an interleaved partitioned PTS scheme using cyclic shift in sub-blocks to generate candidate signal in place of multiplying phase rotations. At receiver, the received signal is partitioned again using interleaved partitioning. The decision metric is Euclidian distance, which is calculated at the receiver as following:

$$\tilde{r}_m(n) = \min_{k \in \mathfrak{R}(v,k)} \sum_{n=N_v(1)}^{N_v(N/V)} \min \left| \frac{r(n).e^{-j.2.\pi k.n/LN}}{\tilde{h}(n)} - \tilde{X}(n) \right|^2 \quad (5.8)$$

Where \mathfrak{R} represent the set containing sub-block and cyclic shifts k , N_v represents the subcarriers in interleaved block v , $\tilde{h}(n)$ is the estimated channel response. The $\tilde{X}(n)$ generating minimum distance is stored, this is done for all the sub-blocks and their subcarriers, and thus generating shift value of cyclic shift is estimated for each sub-block. However, this scheme suffers from higher implementation complexity. In [135], scheme of [114] is used again, only difference is that pseudo random partitioning is used in place of interleaved.

In [136], a PTS scheme without SI is proposed for Alamouti's multiple inputs and multiple output system. Here, a phase offset along with phase factor is used and at receiver minimum Euclidian distance decoder is used. The PAPR performance of conventional PTS scheme is same as the proposed one, for CCDF= 10^{-4} , PAPR reduction of 2.7 dB and 3.8 dB is achieved for $V=4$ and 8.

5.1 Proposed PTS Scheme without SI

We have proposed a octagonal mapping based PTS scheme (OM-PTS) where set of eight phase weights $\left\{1, \frac{1}{\sqrt{2}}(1+j), j, \frac{1}{\sqrt{2}}(-1+j), -1, \frac{1}{\sqrt{2}}(-1-j), -j, \frac{1}{\sqrt{2}}(1-j)\right\}$ are considered for better and precise PAPR performance evaluation.

In OM-PTS the input data stream is converted in to quaternary data, each laying in one of the four different quadrants. When initially mapped symbols are rotated by these phase weights they get remapped on the edge of an octagon. Fig. 5.1 shows the mapping of quaternary point $1+2j$ to eight different constellation points in four quadrants, new constellation points are $1+2j$; $-0.707+2.12j$; $-2+j$; $-2.12-0.707j$; $-1-2j$; $0.707-2.12j$; $2-j$; $2.12+0.707j$ resulted from rotation due to weights $\left\{1, \frac{1}{\sqrt{2}}(1+j), j, \frac{1}{\sqrt{2}}(-1+j), -1, \frac{1}{\sqrt{2}}(-1-j), -j, \frac{1}{\sqrt{2}}(1-j)\right\}$ respectively. These eight points lie on the vertices of an octagon, as shown in Fig. 5.2.

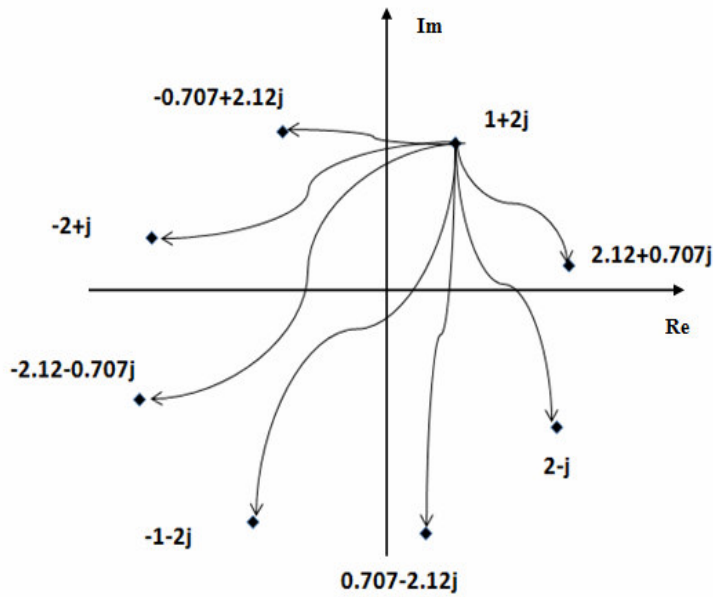


Fig. 5.1 Mapping of symbols due to rotation by eight phase weights

The proposed scheme can be described in following steps:

Step 1): Convert the input data bit stream in to quaternary points.

Step 2): Divide the entire constellation in to four groups Gr_1 , Gr_2 , Gr_3 and Gr_4 .

Step 3): Quaternary points are mapped to eight new points representing vertices of an octagon, when multiplied by eight phase weights.

Step 4): Select the signal with lowest PAPR using conventional PTS method.

Let the four quaternary points $0, 1, 2, 3$ are representing complex symbols $1+2j$, $-0.8+1.5j$, $-0.4-1.2j$ and $1.1-1.6j$ after rotation by eight phases, they get mapped to eight new constellation points creating an octagon.

These 32 constellation points are divided in four groups Gr_1 , Gr_2 , Gr_3 and Gr_4 , representing extended constellation octagonal mapped points corresponding to quaternary points $0, 1, 2$ and 3 respectively. This entire mapping procedure is shown in Table 5.1.

At the receiver end, reception of any symbol belonging to a certain group correctly decodes the original symbol and quaternary points, e.g. if decoded symbol at the receiver is $2.12+0.707j$, which belongs to group Gr_1 . This shows that transmitted quaternary symbol is 0 representing complex symbol $1+2j$. So without sending the side information regarding the used phases sequence at the transmitter i.e. $\left\{1, \frac{1}{\sqrt{2}}(1+j), j, \frac{1}{\sqrt{2}}(-1+j), -1, \frac{1}{\sqrt{2}}(-1-j), -j, \frac{1}{\sqrt{2}}(1-j)\right\}$, we can detect the transmitted OFDM symbol correctly. Table 5.2 shows the decoding process at the receiver.

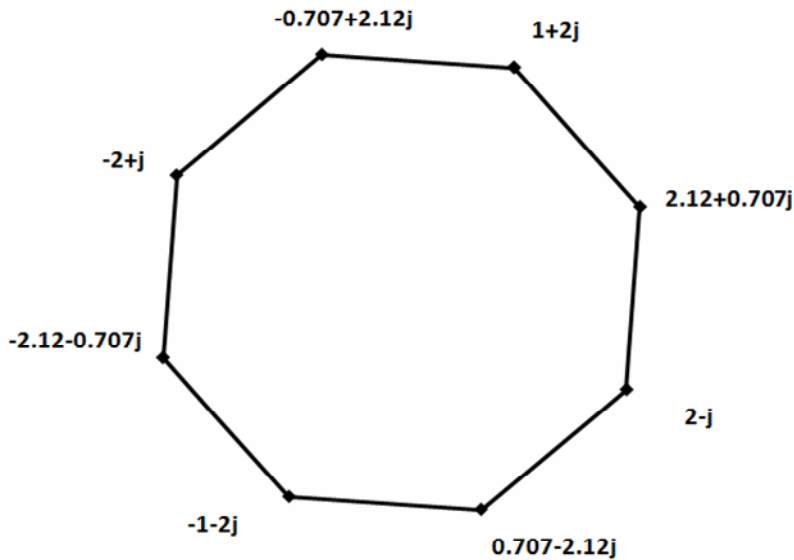


Fig.5.2 Octagon representing remapping of quaternary points

However, above description is for quaternary data, the same scheme can be further applied for hexadecimal data but extended constellation after rotation by phase weights is divided in to 16-groups.

Table 5.1 Octagonal mapping at transmitter

Quaternary symbols and Groups	Initial mapping	Constellation points after multiplication with phase factors (in $\pm X \pm jY$ form)							
		1	$\frac{1}{\sqrt{2}}(1+j)$	j	$\frac{1}{\sqrt{2}}(-1+j)$	-1	$\frac{1}{\sqrt{2}}(-1-j)$	$-j$	$\frac{1}{\sqrt{2}}(1-j)$
0 (G_1)	$1+2j$	$1+2j$	$-0.707+2.12j$	$-2+j$	$-2.12-0.707j$	$-1-2j$	$0.707-2.12j$	$2-j$	$2.12+0.707j$
1 (G_2)	$-0.8+1.5j$	$-0.8+1.5j$	$-1.62+0.49j$	$-1.5-0.8j$	$-0.49-1.62j$	$0.8-1.5j$	$1.62-0.49j$	$1.5+0.8j$	$0.49+1.62j$
2 (G_3)	$-0.4-1.2j$	$-0.4-1.2j$	$0.56-1.13j$	$1.2-0.4j$	$1.13+0.56j$	$0.4+1.2j$	$-0.56+1.13j$	$-1.2+0.4j$	$-1.13-0.56j$
3 (G_4)	$1.1-1.6j$	$1.1-1.6j$	$1.9-0.35j$	$1.6+1.1j$	$0.35+1.9j$	$-1.1+1.6j$	$-1.9+0.35j$	$-1.6-1.1j$	$-0.35-1.9j$

Table 5.2 De-mapping at receiver

Demodulated symbol group	De-mapped constellation symbol	Decoded quaternary data
G_1	$1+2j$	0
G_2	$-0.8+1.5j$	1
G_3	$-0.4-1.2j$	2
G_4	$1.1-1.6j$	3

5.2 Performance of Proposed Scheme without SI

For PAPR performance, simulation we have generated 1000 OFDM symbols with $N=256$ sub carriers, using 16-QAM mapping scheme. Fig. 6 compares the PAPR performance in terms of CCDF for plain-OFDM, OFDM with conventional PTS (C-PTS) and OFDM with OM-PTS for various sub-blocking sizes $V= 4, 5, 6, 7, 8$. Phase weights used are

$$\left\{1, \frac{1}{\sqrt{2}}(1+j), j, \frac{1}{\sqrt{2}}(-1+j), -1, \frac{1}{\sqrt{2}}(-1-j), -j, \frac{1}{\sqrt{2}}(1-j)\right\}.$$

Fig. 5.3 shows that for $N=256$ and 16-QAM the CCDF curves for C-PTS and OM-PTS are almost overlapping, indicating that OM-PTS gives same PAPR reduction performance as C-PTS but without the need of side information. The OFDM system without any PAPR

reduction techniques gives poor PAPR reduction performance as compared to C-PTS and OM-PTS. The values of PAPR are in the range of 4-6 dB which matches the standard values of PAPR in 4-G. The values of PAPR in dB for $CCDF=10^{-2}$ are given in Table 5.3 indicating that the performance of OM-PTS and C-PTS is almost same.

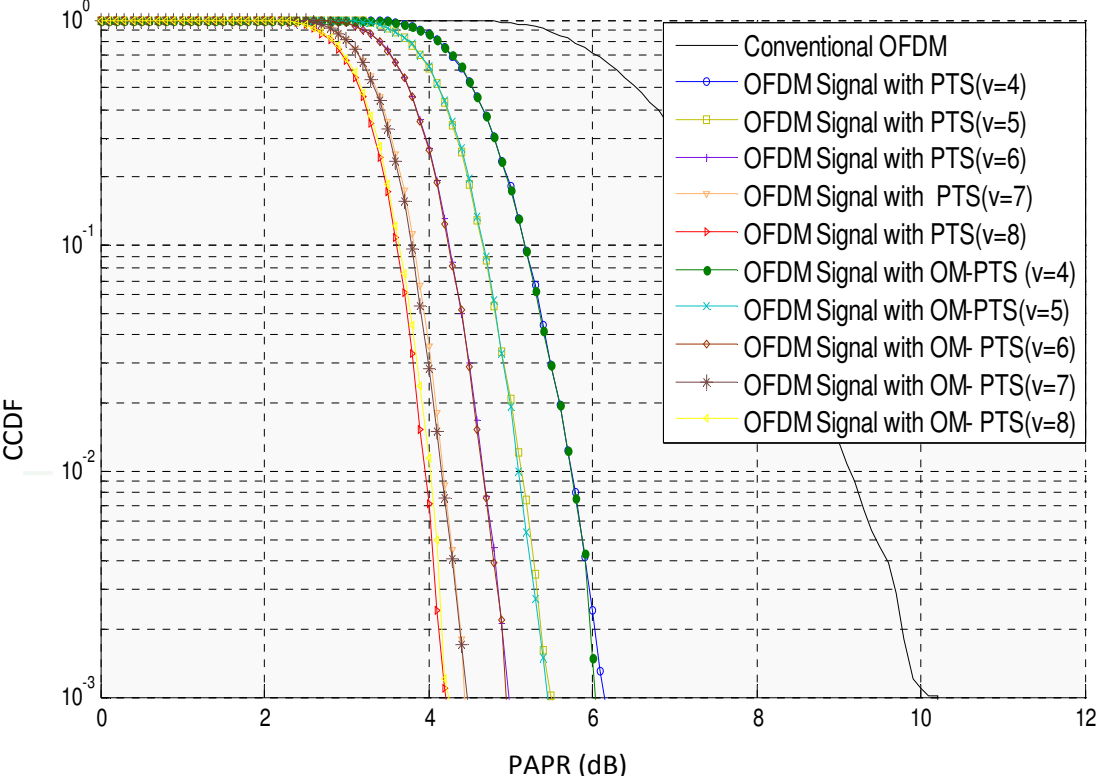


Fig. 5.3 PAPR comparison of OM-PTS and C-PTS for sub-blocks sizes V= 4, 5, 6, 7, 8

Table 5.3 PAPR values and their comparison

Sub-block Size (V)	PAPR (dB)		
	C-PTS	OM-PTS	Conventional OFDM
4	5.85	5.84	9.25 (without any PAPR reduction technique)
5	5.54	5.55	
6	4.90	4.91	
7	4.33	4.38	
8	3.9	3.8	

5.3 Comparison with Existing PTS Schemes without SI

In [129], it is assumed that all permissible weighting factors are known at receiver and it requires transmission of certain number of pilot tones in each sub-block to identify the phase

factor which has been multiplied with the sub-block, at receiver Euclidian distance is calculated to find the transmitted pilot and respective phase factor. Transmission of pilot tone for SI and calculation of Euclidian distance makes system more cumbersome and complex. In [53], maximum likelihood algorithm based receiver is used for avoiding SI transmission, but owing to high complexity of receiver, the authors proposed to reduce the number of candidate signals for PAPR evaluation, which again limits the system's PAPR reduction performance. In [128], the scheme requires transmission of few bits per sub-block for correct SI detection, so it does not offer complete SI removal. In [125], an embedded marking scheme in data sequence is used for SI transmission purpose, when using PTS with 16 sub-blocks, Walsh codes are used as phase sequences. At the receiver, Euclidian distance of detected symbol is calculated with each Walsh code of length 16 and code with minimum hamming distance is chosen as transmitted phase sequence. However, for lower block sizes such as $V=4, 5$ the Walsh code required will be of lower length with lower hamming distance leading to increased error in SI detection, so it is not a good choice for PAPR reduction for lower sub-block sizes. In [114,135], cyclic shifting of sub-blocks is required to generate candidate signals which make its transmitter and receiver more complex to implement and [130-131] limited to only four and two phase weights respectively.

Findings:

Being a most widely accepted technique for PAPR reduction, avoiding side information in PTS can release burden on the transmission bandwidth requirement.

The proposed OM-PTS scheme offers optimum PAPR reduction which is almost same as offered by conventional PTS scheme. However in the proposed scheme there is no need of side information transmission, which is an added advantage in terms of better B.W efficiency than conventional PTS. This scheme does not require any complex receiver unlike existing schemes and at the same time there is no reduction in number of sub-carrier, so there would be no loss of data rate.

The proposed scheme could be very useful in downlink for LTE and WiMaX systems as the PAPR values achieved are slightly better than standard values of PAPR (6 dB) recorded till now for 4G systems and the proposed scheme OM-PTS also saves more in terms of bandwidth by avoiding need of side information.

PERFORMANCE ANALYSIS OF OFDM SYSTEMS IN FADING CHANNELS WITH CHANNEL CODING SCHEMES

This chapter deals with bit error rate performance of an OFDM system in fading channels and its improvement using concatenated channel codes. BER performance of the coded OFDM system using serial concatenation (Reed-Solomon and convolution codes) and parallel concatenation (Turbo codes) is analyzed in various fading channels.

In wireless channels, the signal is received at the receiver via multiple paths with different attenuation and delays. Multipath phenomenon (Fig. 6.1) occurs majorly due to three physical phenomenons

1. Reflection
2. Diffraction
3. Scattering

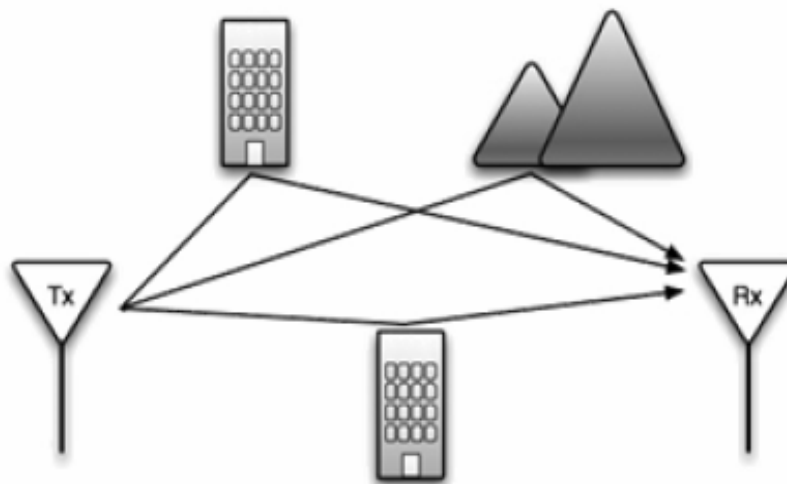


Fig. 6.1 Multipath propagation in wireless channels

When these signals are combined at the receiver the superposition may lead to constructive as well as destructive superposition. So there is rapid fluctuation in the received signal level in short duration or distance, called small scale fading or fading [137]. Fading may completely destroy the received signal or may affect some frequency components. R.M.S delay spread and coherence bandwidths are the parameters used for describing the time dispersive nature of the channel.

R.m.s delay spread is given by the formula:

$$\sigma_{\tau} = \sqrt{\overline{\tau^2} - (\bar{\tau})^2} \quad (6.1)$$

Where $\bar{\tau}$ is the mean delay spread and $\overline{\tau^2}$ is the mean square value. Conventionally, if the $T_{symbol} \geq 10 \cdot \sigma_{\tau}$, then there is no need of equalizers to compensate for the ISI since effect of dispersion is very low.

Coherence bandwidth (B_c) is the range of frequencies over which channel behaves flat i.e channel has constant gain and linear phase response. In coherence bandwidth, the frequency components have strong correlation. It is defined as:

$$B_c \approx \frac{1}{50 \cdot \sigma_{\tau}} \quad \text{For 90\% correlation}$$

$$B_c \approx \frac{1}{5 \cdot \sigma_{\tau}} \quad \text{For 50\% correlation} \quad (6.2)$$

Multipath delay spread leads time dispersion and frequency selective fading categorized in flat and frequency selective fading.

- ❖ *Flat fading*: In flat fading, the spectral characteristics of the transmitted signal remains intact at the receiver. The condition for flat fading is :

$$\text{Signal B.W} < \text{Coherence B.W} \quad \text{OR} \quad \text{Delay spread} \ll \text{Symbol period}$$

- ❖ *Frequency selective fading*: It is due to time dispersion of the symbol in the channel resulting in ISI. The condition for Frequency selective fading is :

$$\text{Signal B.W} > \text{Coherence B.W} \quad \text{OR} \quad \text{Delay spread} > \text{Symbol period}$$

In mobile communication, there is relative motion between transmitter and receiver, even the surrounding objects could also be moving. In such case, channel has a time varying nature.

Time varying nature of the channel is described by Doppler spread and coherence time. Doppler spread (f_d) is a measure of spread in a given frequency signal i.e. a signal of frequency f_c gets mapped in to components $f_c + f_d$ and $f_c - f_d$. Doppler spread could be derived from coherence time (T_c).

Coherence time (T_c) is defined as time duration over which channel impulse response remain invariant or unchanged. Within this interval, signals will have high correlation among them.

It is given as:

$$T_C = \sqrt{\frac{9}{16 \cdot \pi \cdot f_m^2}} \quad (6.3)$$

Where f_m is the maximum Doppler shift.

Doppler spread causes frequency dispersion in time selective fading, defined as follows:

- ❖ *Fast fading*: In fast fading, channel impulse response varies at higher rate than signal variation. The condition for fast fading is :

$$\text{Symbol period} > \text{Coherence time} \quad \text{OR} \quad \text{Signal Bandwidth} < \text{Doppler shift}$$

- ❖ *Slow fading*: In slow fading channel impulse response varies at lower rate than signal variation. The condition for slow fading is :

$$\text{Symbol period} \ll \text{Coherence time} \quad \text{OR} \quad \text{Signal Bandwidth} \gg \text{Doppler shift}$$

There are various distributions derived for wireless channels depending upon the radio environment, out of them Rayleigh, Rician and Nakagami-m [138-139] are most widely used.

6.1 Fading Channels

Following fading channels are considered for the study in the thesis:

6.1.1 Rayleigh Distribution

It is generally used to describe the time varying nature of the received signal envelope. If in a signal the real and imaginary part has Gaussian distribution then resultant signal have Rayleigh envelope. This can be defined as the following:

Let the mobile antenna receives N replicas of same signal. In case of an unmodulated carrier, the transmitted signal at frequency ω_c reaches the receiver via number of paths. The amplitude and phase of the i^{th} path are a_i and φ_i . If there is no direct path or line-of sight (LOS) component, the received signal $s(t)$ can be expressed as:

$$s(t) = \sum_{i=1}^N a_i \cos(\omega_c t + \varphi_i) \quad (6.4)$$

If there is a relative motion between transmitter and receiver the Doppler shift has to be considered. If ω_{d_i} represents the shift for i^{th} component, the received signal can be expressed as:

$$s(t) = \sum_{i=1}^N a_i \cos(\omega_c t + \omega_{d_i} t + \varphi_i) \quad (6.5)$$

The phase φ_i is assumed to be uniformly distributed over $[0, 2\pi]$. If N is large, the in-phase and quadrature components of received signal becomes zero mean Gaussian with standard deviation σ . The probability density function (P.D.F) of the received signal envelope can be given as:

$$f(r) = \frac{r}{\sigma^2} \left\{ \frac{-r^2}{2\sigma^2} \right\} \quad r \geq 0 \quad (6.6)$$

6.1.2 Rician Distribution

It is similar to Rayleigh except for the fact that there exists a strong line of sight component along with reflected waves. In presence of such a path, if k_d is the strength of the LOS component and ω_d is the Doppler shift along the LOS path, then the transmitted signal will be:

$$s(t) = \sum_{i=1}^{N-1} a_i \cos(\omega_c t + \omega_{d_i} t + \varphi_i) + k_d \cos(\omega_c t + \omega_d t) \quad (6.7)$$

The envelope in this case has a Rician density function given by

$$f(r) = \frac{r}{\sigma^2} \left\{ -\frac{r^2 + k_d^2}{2\sigma^2} \right\} I_0 \left\{ \frac{rk_d}{\sigma^2} \right\}, \quad r \geq 0 \quad (6.8)$$

Where $I_0(\cdot)$ is the 0th order modified Bessel function of the first kind.

6.1.3 Nakagami-m Distribution

The Nakagami distribution [139], also known as the “m-distribution,” provides greater flexibility in matching experimental data. Nakagami distribution fits in experimental data better than Rayleigh or Rician distributions. The fading model for the received signal envelope, proposed by Nakagami, has the P.D.F given by:

$$f(r) = \frac{2}{\Gamma(m)} \left(\frac{m}{\Omega} \right)^m r^{2m-1} e^{-mr^2/\Omega}, \quad \Omega \text{ and } r \geq 0 \quad (6.9)$$

where m is shape parameter ($m \geq 1/2$), Ω is the second moment of r and $\Gamma(\cdot)$ is the gamma function. The parameter Ω controls the spread of the distribution. In the range $0.5 \leq m \leq 1$, the Nakagami distribution models high frequency channels where the fading is more severe than the Rayleigh fading. When $m=1$ the distribution become Rayleigh distribution.

For $m \geq 1$, the effect of fading is less severe. There is no fading effect when $m = \infty$. For $1 < m < 2$, Nakagami distribution fits into Rician distribution. In our paper, we used following method [140] for simulating Nakagami-m distribution:

Let $x_i(t)$ and $y_i(t)$ are zero mean Gaussian processes. The variables $x_i(t)$ and $y_i(t)$ are random variables corresponding to these processes respectively. For fixed t , $E[x_i] = E[y_i] = 0$ and $E[x_i^2] = E[y_i^2]$. Let $r_0^2 = x_0^2$ (equivalently $r_0^2 = y_0^2$) and $r_i^2 = x_i^2 + y_i^2$, where i is any positive integer and r_i is Rayleigh distributed. We note that r_0 variable is semi-positive Gaussian distributed. It can be shown that the Nakagami fading model with parameter m of the envelope r is defined as:

$$r = \frac{1}{m} \sqrt{\sum_{i=1}^m x_i^2 + y_i^2} \quad (6.10)$$

In OFDM, due to narrow band channels and long symbol duration the effect of fading is less. However, ICI is still an important factor affecting the performance of OFDM especially in crowded radio environment and severe fading conditions. To improve the BER performance of the OFDM system, channel coding methods could be used in conjunction, such systems are called coded-OFDM (COFDM) system.

Channel codes helps in successful transmission of data, it facilitates the error detection/correction at the receiver in a noisy environment. Channel codes are represented by (n, k) , where n represents the code word bits or symbols, k represents the data bits or symbols, $(n - k)$ is the number of parity bits or redundancy added and $r = k/n$ is called the code rate. Hamming distance between the two code words is the number of bits which change from one to other code. Higher the hamming distance between the two valid code words lower would be the bit error at the receiver.

6.2 Concatenated Channel Codes

Concatenated codes are the combination of two channel codes creating codes of larger length [141] with better performance, but at descent complexity. These codes are divided in to two categories:

6.2.1 Serial Concatenation

Both the encoders are connected in series, one working as inner and other as outer code encoder, dealing with both random and burst errors. The block diagram is shown in Fig. 6.2. Usually an interleaver is also incorporated between these two blocks to spread the burst

errors. Total code rate of a serial concatenation is product of the individual code rate of the two encoders. Usually Reed Solomon codes are used as the outer code and convolution encoder used as the inner code.

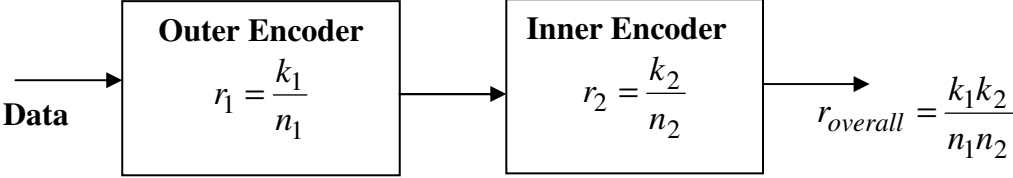


Fig. 6.2 Serial concatenation

(A) Reed Solomon Code Implementation

Reed Solomon codes [142-143] are considered for the outer code owing to following properties:

- Excellent burst error correction capability.
- Can operate at high data rate from 2 to 12 Mbps.
- Can generate large block code length.
- RS codes have capability to remove erasures.
- RS codes are almost perfect as they use minimum redundancy.
- RS codes are maximum distance separable codes i.e. they have maximum value of minimum hamming distance for a given set of (n, k) .

However, it uses hard decision so do not consider soft decision information, to exploit the soft information convolution encoder is used along with viterbi decoder at the receiver. Convolution codes works at lower code rate that’s why they are used in concatenation, but they pass on the soft information to other decoder so that entire system gives best possible estimation of the transmitted symbol. RS codes parameters are chosen from the Table. 6.1 given below:

Table 6.1 RS code parameters

Parameter	Value	Range
w	Number of bits/ Symbol	3-16
n	Symbols/ Code word	$3-2^{w-1}$
k	Symbols/ Data word	$k < n$ ($n-k$ should be even)
t	Number of errors	$(n-k)/2$

The mapping schemes BPSK, QPSK, 16-QAM uses (15, 13) RS codes and 64-QAM uses (60, 58) which are the nearest values of (n, k) as per Table 6.1. For generation of RS codes symbols, Galois fields (GF) are used. $GF(p)$ represents a finite field with p -element, where p is a prime number. This field could be extended to a field containing p^w elements, denoted by $GF(p^w)$.

$GF(2)$ represents binary field, the extension field $GF(2^w)$ contains elements represented by α and its higher power. Such field would have infinite element, to find the finite field out of it, following condition is applied:

$$\alpha^{2^w-1} = \alpha^0 = 1 \quad (6.11)$$

Now the $GF(2^w) = \{0, \alpha^0, \alpha^1, \alpha^2, \dots, \alpha^{2^w-2}\}$. To define the GF , an irreducible primitive polynomial of order m is required and each element of GF can be represented in the form of this polynomial only.

E.g. for $GF(2^3)$, the primitive polynomial is $f(x) = x^3 + x + 1$ and $f(\alpha) = 0$. The various elements of the field are calculated as follows:

Since $f(\alpha) = 0$ i.e. $\alpha^3 + \alpha + 1 = 0$ or $\alpha^3 = \alpha + 1$

The elements of the field would be $\{0, \alpha^0, \alpha^1, \alpha^2, \alpha^3, \alpha^4, \alpha^5, \alpha^6\}$, these element can be calculated recursively as follows:

$$\alpha^4 = \alpha.\alpha^3 = \alpha.(\alpha + 1) = \alpha^2 + \alpha = x^2 + x$$

$$\alpha^5 = \alpha.\alpha^4 = \alpha.(\alpha^2 + \alpha) = \alpha^3 + \alpha^2 = \alpha + 1 + \alpha^2 = x^2 + x + 1$$

$$\alpha^6 = \alpha.\alpha^5 = \alpha.(\alpha^2 + \alpha + 1) = \alpha^3 + \alpha^2 + \alpha = \alpha + 1 + \alpha^2 + \alpha = \alpha^2 + 1 = x^2 + 1$$

$$\alpha^7 = \alpha.\alpha^6 = \alpha.(\alpha^2 + 1) = \alpha^3 + \alpha = 1 = \alpha^0$$

These $2^3 = 8$ elements from the Galois field are shown in table 6.2.

In RS code, all the arithmetic operations take place within the GF . The generator polynomial is calculated as follows:

$$g(x) = (x + \alpha).(x + \alpha^2).(x + \alpha^3)..(x + \alpha^{2^t}) \text{ Mod-2} \quad (6.12)$$

For (7, 4) code word the generator polynomial would be given as:

$$g(x) = (x + \alpha).(x + \alpha^2).(x + \alpha^3) \quad (6.13)$$

Non-systematic code word $C(x)$ for a data vector $d(x)$ could be calculated as:

$$C(x) = d(x).g(x) \quad (6.14)$$

The value of symbols for $C(x)$ can be taken from the elements calculated for GF . However, systematic codes are more in use as it is easier to separate data and parity bits in systematic code word.

Table 6.2 Elements in $GF(2^3)$

Elements	x^2	x^1	x^0
0	0	0	0
α^0	0	0	1
α^1	0	1	0
α^2	1	0	0
α^3	0	1	1
α^4	1	1	0
α^5	1	1	1
α^6	1	0	1

Systematic codes can be generated by using equation 6.15:

$$C(x) = \rho(x) + x^{n-k}.d(x) \quad (6.15)$$

$$\text{Where } \rho(x) = \text{rem} \frac{x^{n-k}.d(x)}{g(x)}$$

At the receiver received signal would be $r(x) = C(x) + e(x)$ (6.16)

Where $r(x)$ is the received vector and $e(x)$ is the error vector.

The error vector can be mapped with the help of syndrome which is given by:

$$S = \frac{r(x)}{g(x)} \quad (6.17)$$

For RS code generation and detection, we need divider circuitries as hardware for implementation.

(B) Convolution Code Implementation

Unlike block codes, in convolution code [143] encoder have memory and data bits are encoded one by one that's why these codes are also termed as run length codes. Input depends on present state of the memory element and the current input.

Here, k bits are at input, n bits are at output, where k & n are very small. The number of bits which affects current output code is called constraint length K . This is defined as:

$$K = \text{code memory} + k \quad (6.18)$$

The convolution code encoders that we have implemented (shown in Figs. 6.3- 6.4) are defined as following:

For 1/2 convolution code

- 1) Constraint length: 7
- 2) Feedback connections: $(171)_8$ & $(133)_8$

For 2/3 convolution codes

- 1) Constraint length (5, 4)
- 2) Feedback connections: $(23, 35, 0:0, 5, 13)_8$

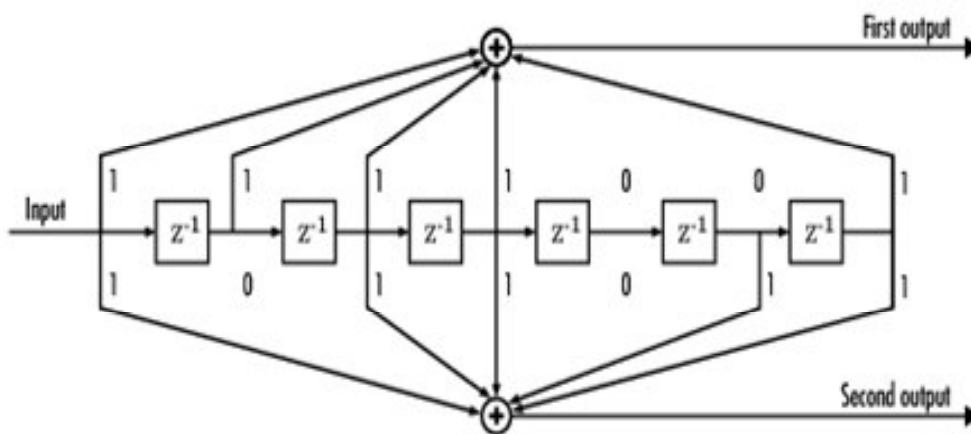


Fig. 6.3 1/2 Convolution code encoder

Viterbi decoding is a standard decoding method for decoding convolution codes. Convolution codes work on maximum likelihood decoding principle. The hamming distance between the received sequence and the estimated sequence is calculated and the sequence with minimum hamming distance is treated as the transmitted sequence. Minimum value of hamming distance is also called as free distance. Hamming distance between two valid code words C_1 and C_2 is calculated as:

$$D_H = \sum_{i=1}^n C_{1,i} \oplus C_{2,i} \quad (6.19)$$

To implement viterbi decoding method first trellis diagram is created for the code. Trellis is usually derived from the state diagram of the encoder, at any time state of an encoder is the content of the memory elements when a data bit enters in it.

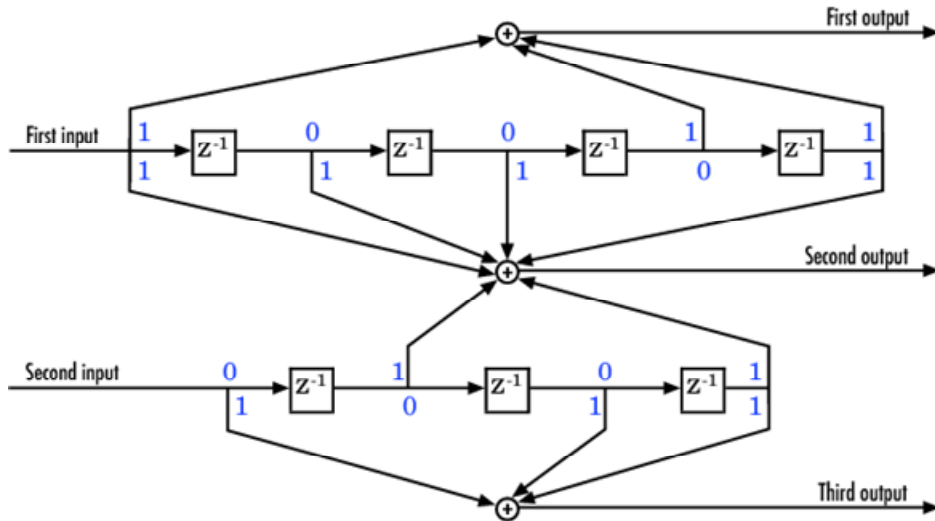


Fig. 6.4 2/3 Convolution code encoder

The trellis is traversed in all possible levels and nodes, at each level the hamming distance of the received code word is measured from all the possible paths in the trellis, the path or estimated sequence with minimum hamming distance is selected as the survivor path. This process continues till the entire trellis is exhausted and there remains only single survivor. From the survivor path we can decode the transmitted bits.

6.2.2 Parallel Concatenation

In parallel concatenation, the encoders are connected in the parallel generating overall code rate of $\frac{k}{n_1 + n_2}$. The block diagram of the scheme is shown in Fig. 6.5. But receiver in the parallel concatenation is usually a serial decoder structure, since parallel decoder works independently so they do not share the soft information. Turbo codes [144-146] use the parallel concatenated structure.

(A) Turbo Code Implementation

Recursive systematic convolution (RSC) encoder is obtained from the non recursive non-systematic (conventional) convolution encoder by feeding one of its inputs back to the input.

Turbo codes encoder use the parallel concatenated encoding scheme as shown in Fig.6.6.

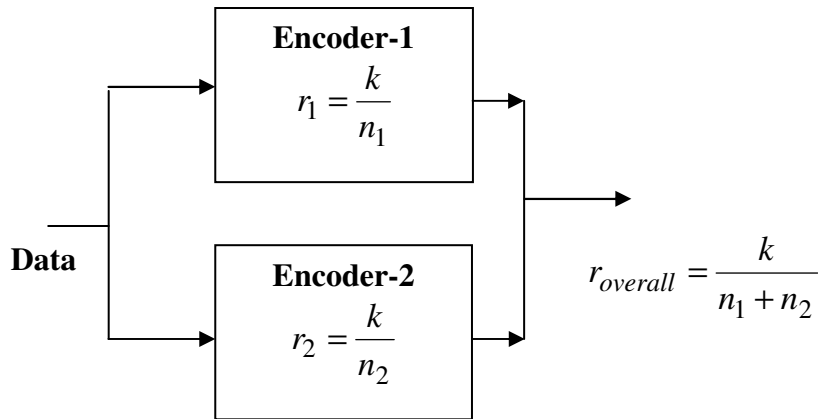


Fig. 6.5 Parallel concatenation

The input sequence \mathbf{x} produces a low-weight convolution code sequence \mathbf{c}_2 for RSC encoder-1 and systematic output \mathbf{c}_1 . To avoid having RSC encoder-2, produce another low-weight output sequence, the interleaver permutes the input sequence \mathbf{x} to obtain a different sequence that hopefully produces a high weight convolution code sequence \mathbf{c}_3 .

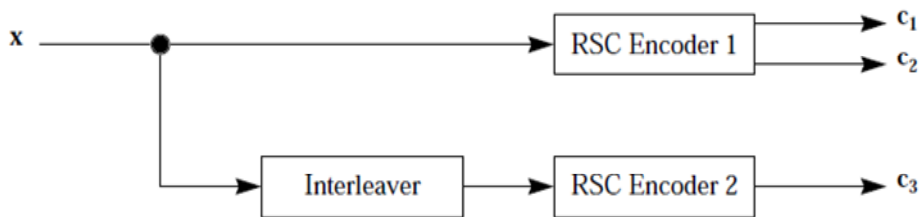


Fig. 6.6 Turbo encoder

The generator used are $[1, g_2/g_1]$ and $[1, g_3/g_4]$ where $g_1 = [1 \ 1 \ 1]$, $g_2 = [1 \ 0 \ 1]$, $g_3 = [1 \ 1 \ 1]$, $g_4 = [1 \ 0 \ 1]$. The constituent components producing 1/3 code rate are given in Fig. 6.7.

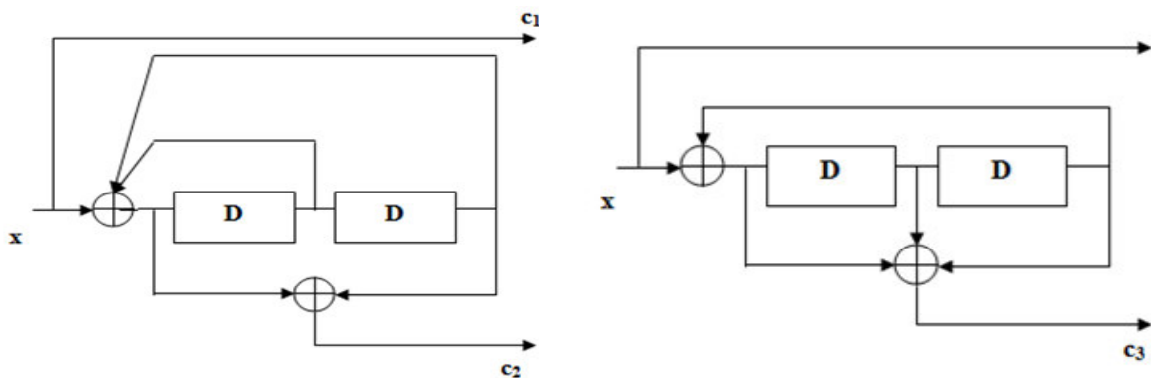
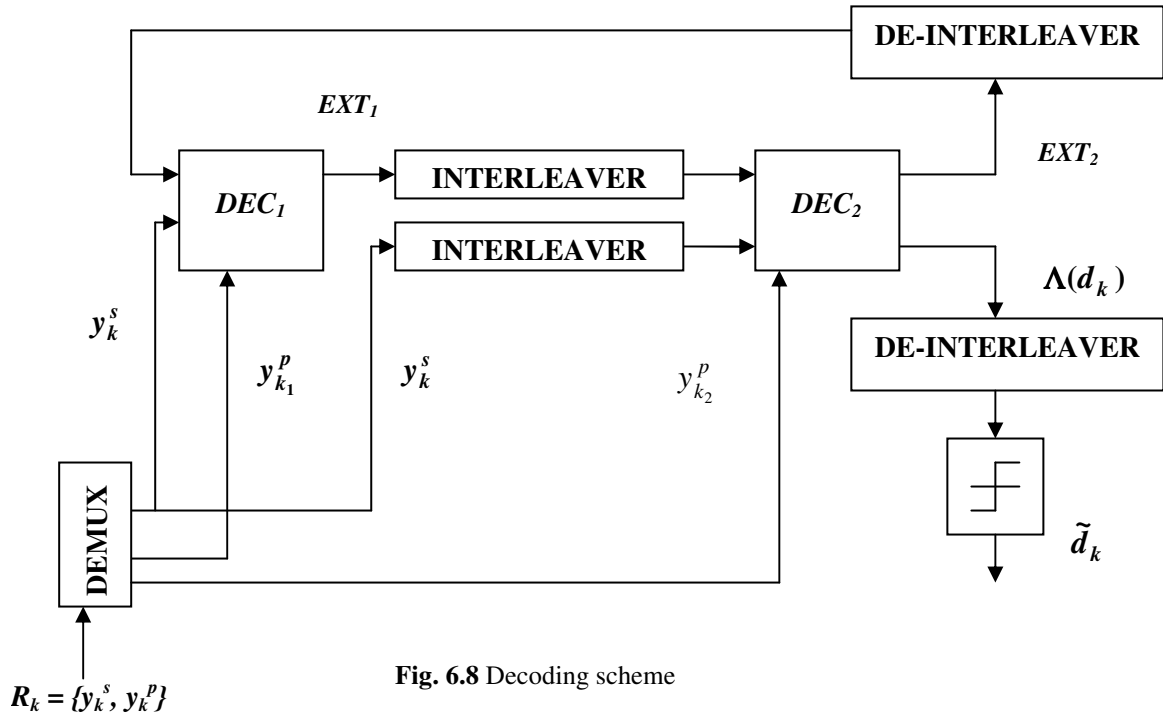


Fig.6.7 RSC encoders used for Turbo code generation

(B) Turbo Code Decoding

Turbo code uses Bahl, Cocke, Jelinek and Raviv (BCJR) [147] also termed as Maximum A Posteriori (MAP) based decoder. This algorithm is based on posteriori probabilities. BCJR algorithm uses log-likelihood ratio (LLR) as metric for decoding the transmitted symbol. The decoder block diagram is shown in Fig. 6.8.



Let d_k be the data input bit which can take values 1 or 0 i.e. +1 or -1, X is the vector containing n bit code words. The log likelihood ratio is given as:

$$\Lambda(d_k) = \ln \frac{P(d_k = +1)}{P(d_k = -1)} \quad (6.20)$$

Where $P(d_k)$ is priori probability that d_k can take value +1 or -1.

The basic working principle of the MAP decoder given in Fig 6.8 is sharing the soft outputs recursively in form of the LLR's. EXT represents the extrinsic information, information which does not contain any redundancy i.e. in each iteration from LLR, the information already processed is subtracted so that EXT does not contain any past information. Inputs to decoder1 (DEC_1) are the systematic output y_k^s and parity bit $y_{k_1}^p$. Extrinsic information EXT_1 from DEC_1 is interleaved and given to DEC_2 . Inputs to DEC_2 are

systematic output y_k^s and parity bit $y_{k_2}^p$. The EXT_2 from DEC_2 is given back to DEC_1 after de-interleaving. This process continues till a predefined number of iterations take place. Then the final LLR is compared to threshold in a hard limiter, giving the estimate \tilde{d}_k .

In noisy environment, let the received vector be y , to find the estimate of the transmitted data bit, posteriori log-likelihood ratio is calculated which is defined as:

$$\Lambda(d_k|y) = \ln \frac{P(d_k = +1|y)}{P(d_k = -1|y)} \quad (6.21)$$

Where $P(d_k = +1|y)$ is called conditional or posteriori probability. The log-likelihood ratio $\Lambda(d_k|y)$ decides the favourable depending on its value, if $\Lambda(d_k|y) > 0$ then decision is likely to go in favour of +1 and if $\Lambda(d_k|y) < 0$ decision is likely to go in favour of -1. However, before taking a hard decision on estimated d_k , several iterations of calculation of $\Lambda(d_k|y)$ take place and finally after gaining sufficient confidence in the estimate a hard decision takes place for deciding whether the transmitted bit d_k is 0 or 1. BCJR is quite a complex algorithm for which simplified versions [147-149] are derived. The algorithm works on trellis as follows:

In trellis there would be two transitions from one each state to next, corresponding to data bit 1 or 0, as shown in Fig. 6.9.

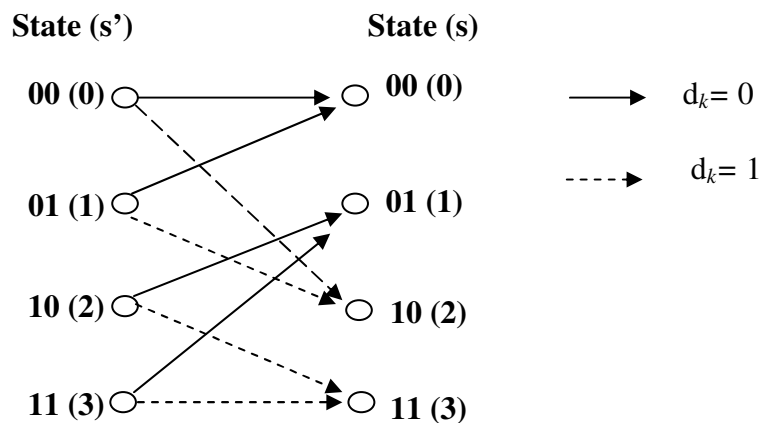


Fig. 6.9 Trellis transition

Let the system is in state s' at $k-1$ instant and make a transition to the next state s at instant k . In this case the posteriori LLR will be:

$$\Lambda(d_k|y) = \ln \frac{\sum_0 P(s', s, y)}{\sum_0 P(s', s, y)} = \ln \frac{\sum_0 \alpha_{k-1}(s') \cdot \gamma_k(s', s) \cdot \beta_k(s)}{\sum_0 \alpha_{k-1}(s') \cdot \gamma_k(s', s) \cdot \beta_k(s)} \quad (6.22)$$

Where $P(s', s, y)$ shows the probability of s' being previous state, s is the current state when sequence y is received. $\sum_0(\cdot)$ and $\sum_1(\cdot)$ represent summation over all the transition caused by $d_k=0$ and 1 respectively. γ_k is the branch transition probability, α_k is called forward and β_k is called backward pass probability, both are associated with the state of trellis. These probabilities are calculated as follows:

$$\alpha_k(s) = \sum_{s'} \alpha_{k-1}(s') \cdot \gamma_k(s', s) \quad (6.23)$$

This probability can directly be calculated from the trellis as follows:

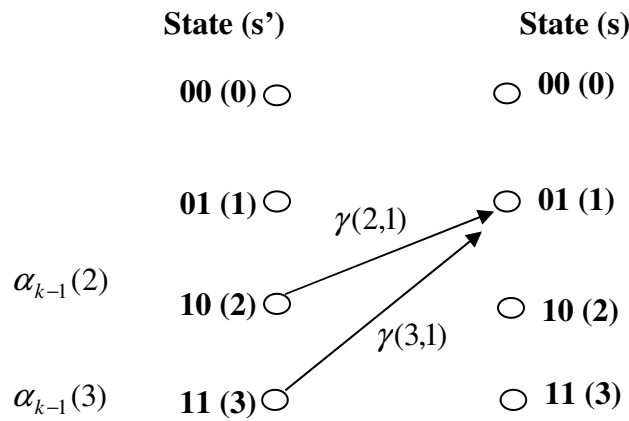


Fig. 6.10 Calculating α

From Fig. 6.10 α could be calculated as:

$$\alpha'_k(1) = \alpha_{k-1}(2) \cdot \gamma_k(2,1) + \alpha_{k-1}(3) \cdot \gamma_k(3,1) \quad (6.24)$$

This is calculated recursively assuming initial condition $\alpha_0(s) = 1; s = 0$. α'_k actually represents the un-normalized probability. To normalize it, it is divided by summation of the α' calculated for all the states, as stated in equation 6.25.

$$\alpha_k(s) = \frac{\alpha'_k(s)}{\sum_s \alpha'_k(s)} \quad (6.25)$$

The backward pass probability can be calculated as:

$$\beta_{k-1}(s') = \sum_s \beta_k(s) \cdot \gamma_k(s', s) \quad (6.26)$$

β can also be directly calculated for the trellis as follows:

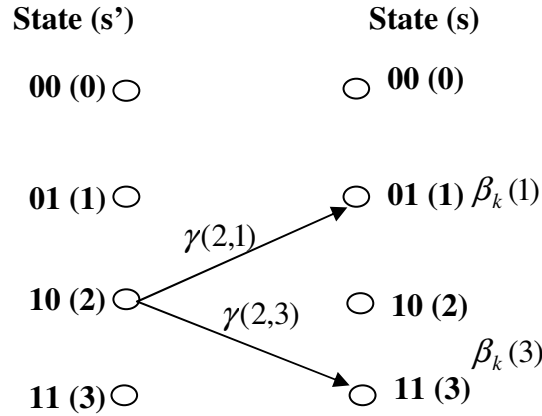


Fig. 6.11 Calculating β

From fig. 6.11, β will be calculated as:

$$\beta'_{k-1}(2) = \beta_k(1) \cdot \gamma_k(2,1) + \beta_k(3) \cdot \gamma_k(2,3) \quad (6.27)$$

β can be calculated recursively assuming initial conditions $\beta_N(s) = 1; s = 0$. To normalize β' we use the following equation:

$$\beta_{k-1}(s') = \frac{\beta'_{k-1}(s')}{\sum_{s'} \beta'_{k-1}(s')} \quad (6.28)$$

BCJR or MAP algorithm involves a high number of multiplications, to reduce the complexity, multiplications are replaced by additions and the modified versions are log-MAP and max-log-MAP algorithms.

The *log-MAP* and *Max-log-MAP* algorithms use a logarithmic domain to convert multiplications into additions by using the Jacobian algorithm, given by:

$$\ln(e^a + e^b) = \max(a, b) + \ln(1 + e^{-|a-b|}) \quad (6.29)$$

The term $\ln(1 + e^{-|a-b|})$ is actually a correcting term. In log-MAP algorithm, the correction term is included, however in max-log-MAP it is omitted. However, due to this the performance of Max-log-MAP is a bit poorer than log-MAP. However, this correcting term could be put in a look-up table containing just a few values, so there is no need to calculate it.

again and again in log-MAP, thus contributes more in decreasing the computational complexity. Let probability $P_k(s) = \ln \alpha_k(s)$; $Q_k(s) = \ln \beta_k(s)$ and $R_k(s', s) = \ln \gamma_k(s', s)$

$$\begin{aligned} P_k(s) &= \ln \left[\sum_{s'} \alpha_{k-1}(s') \gamma_k(s', s) \right] = \ln \left[\sum_{s'} e^{[P_{k-1}(s') + R_k(s', s)]} \right] \\ &= \max_{s'} [P_{k-1}(s') + R_k(s', s)] \end{aligned} \quad (6.30)$$

In this calculation, out of the two possible transitions from s' to s , the one which is generating higher value is considered.

$$\text{Similarly:} \quad Q_{k-1}(s') = \max_s [Q_k(s) + R_k(s', s)] \quad (6.31)$$

Now posteriori LLR can be calculated as:

$$\begin{aligned} \Lambda(d_k | y) &= \ln \frac{\sum_1 P(s', s, y)}{\sum_0 P(s', s, y)} = \ln \frac{\sum_1 e^{[P_{k-1}(s') + R_k(s', s) + Q_k(s)]}}{\sum_0 e^{[P_{k-1}(s') + R_k(s', s) + Q_k(s)]}} \\ &= \max_1 [P_{k-1}(s') + R_k(s', s) + Q_k(s)] - \max_0 [P_{k-1}(s') + R_k(s', s) + Q_k(s)] \end{aligned} \quad (6.32)$$

Where max value would depend on eq. 6.19 based on log-MAP or max-log-MAP algorithms.

6.3 Simulation Results

The simulations for bit error rate comparisons are done in MATLAB for various mapping schemes. Bit error rates are simulated for AWGN and various fading channels namely Rayleigh, Rician and Nakagami ($m=3$).

6.3.1 Performance Analysis for RS-CC Coded OFDM System

The parameter used for performance comparison is bit error rate (BER) and mapping schemes used are BPSK, QPSK, 16 and 64 QAM. OFDM symbols are generated using IEEE 802.11a parameter as given in table 1.1. The simulation generates almost 1000 symbols. The simulations are symbolic representation of the fact that by using channel codes the BER can be improved in fading channels. Fig. 6.12 compares BER performance of RS-CC coded and un-coded OFDM system for various mapping schemes in additive white Gaussian channel (AWGN), results clearly suggest that coded OFDM systems are much better than their un-coded counterparts.

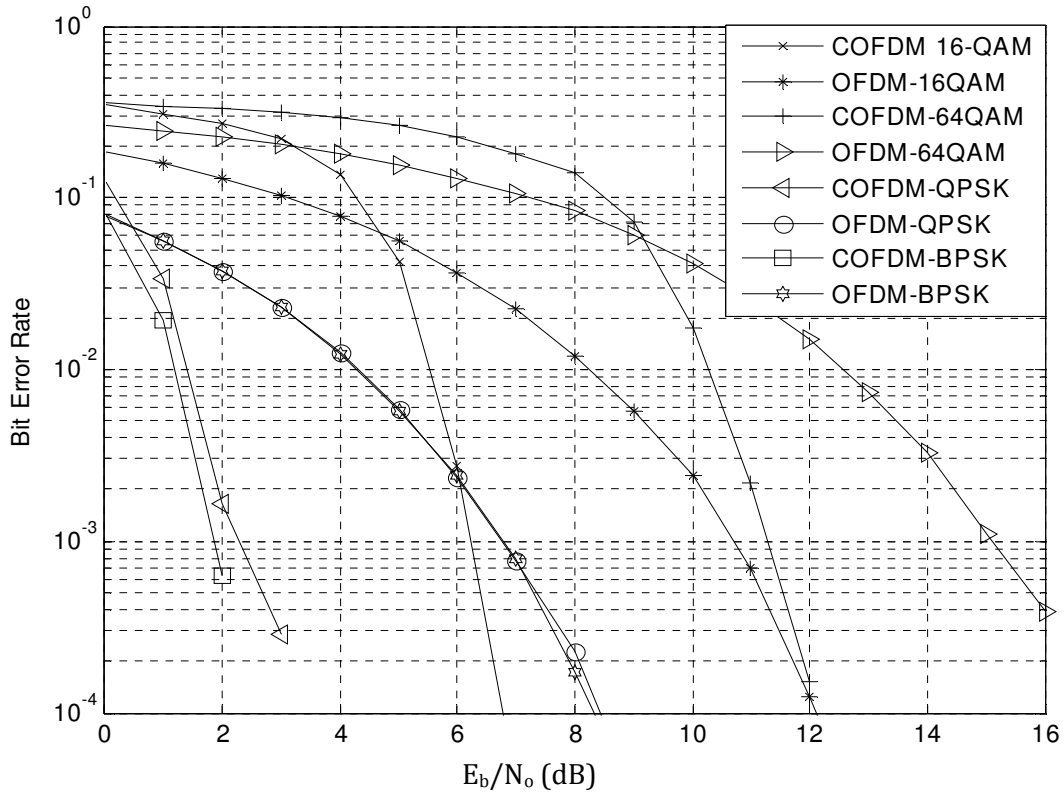


Fig.6.12 BER comparison of un-coded and RS-CC coded-OFDM system

The BER values for selected few bit energy to noise power ratio (E_b/N_0) in dB, are shown in Table 6.3, show that 64-QAM gives better performance only above 10 dB. The BER performance improves for higher value of E_b/N_0 . For higher order mapping scheme, the constellation becomes crowded thus affecting BER adversely. BER 0 results from the fact that at higher BER there is complete recovery of the signal in given conditions

Table 6.3 E_b/N_0 Vs BER values for RS-CC coded and un-coded OFDM

E_b/N_0 (dB)	BER (RS-1/2 CC coded OFDM)				BER (Un-coded OFDM)			
	BPSK	QPSK	16-QAM	64-QAM	BPSK	QPSK	16-QAM	64-QAM
0	0.1024	0.1153	0.3466	0.3602	0.1763	0.1796	0.3489	0.3641
1	0.0196	0.0323	0.3141	0.3482	0.0568	0.0556	0.3168	0.3468
2	0.001	0.0044	0.2725	0.3353	0.0367	0.0377	0.2308	0.3264
3	0*	0	0.2225	0.3168	0.0239	0.0233	0.1022	0.3039
4	0	0	0.1452	0.2930	0.0121	0.0129	0.1784	0.1795
5	0	0	0.0388	0.2590	0.0054	0.0063	0.0562	0.1564
6	0	0	0.0032	0.2226	0.0022	0.0024	0.0375	0.1320
7	0	0	0	0.1824	0.0007	0.0008	0.0229	0.1045
8	0	0	0	0.1361	0.0002	0.0002	0.0121	0.0814
9	0	0	0	0.0726	0.0000	0.0000	0.0058	0.0703
10	0	0	0	0.0167	0	0	0.0025	0.0418

* BER '0' implies that simulation did not generate any significant value

Fig. 6.13 compares the BER performance of RS-1/2 CC and RS 2/3 CC coded OFDM for various mapping schemes in Rayleigh channel with 10 taps. Due to intense fading consideration, BER curves moves to higher E_b/N_0 values. BER Vs E_b/N_0 values are tabulated in table 6.4.

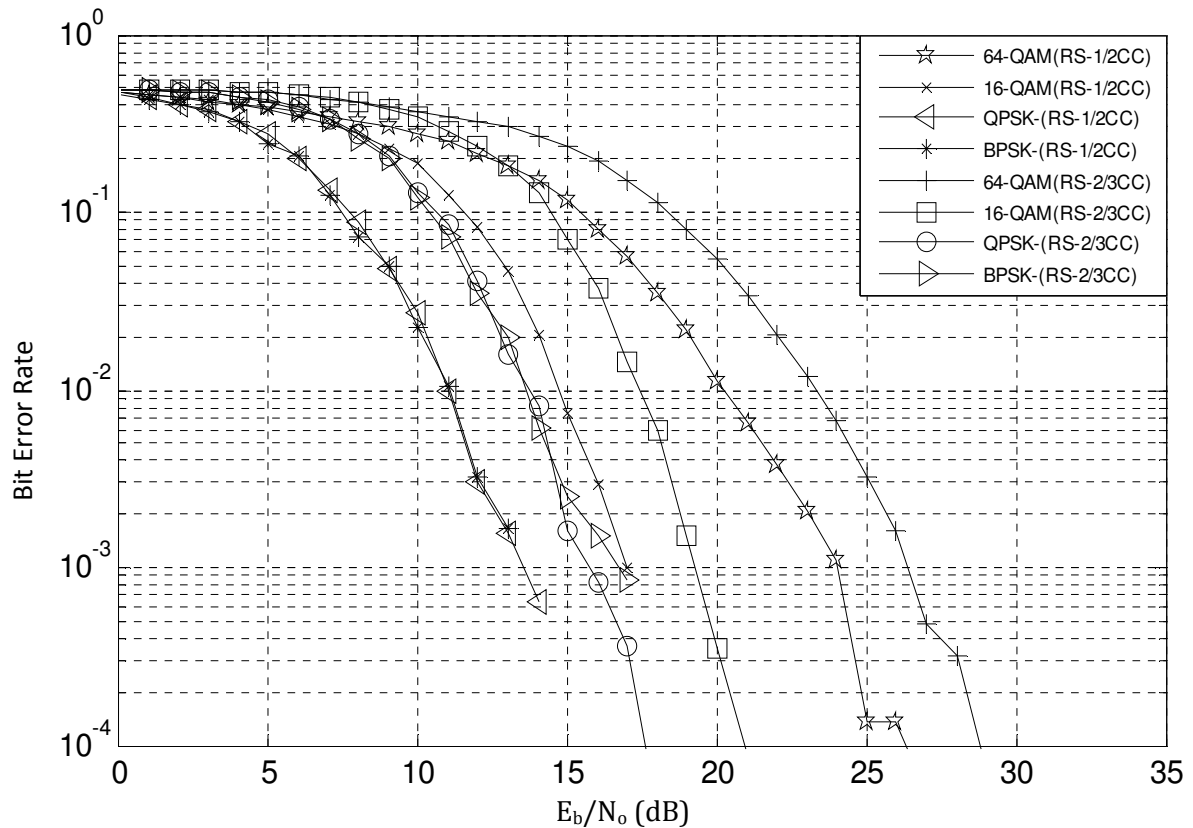


Fig. 6.13 BER comparison of RS -1/2 & 2/3 CC coded OFDM in Rayleigh channel

Table 6.4 E_b/N_0 Vs BER values for RS-CC coded OFDM in Rayleigh channel

E_b/N_0 (dB)	BER (RS-1/2 CC coded OFDM)				BER (RS-2/3 CC coded OFDM)			
	BPSK	QPSK	16-QAM	64-QAM	BPSK	QPSK	16-QAM	64-QAM
0	0.4581	0.4637	0.4795	0.4723	0.4931	0.4987	0.4983	0.4958
1	0.4331	0.4412	0.4703	0.4573	0.4921	0.4897	0.4973	0.4928
2	0.4009	0.4127	0.4525	0.4435	0.4845	0.4830	0.4932	0.4901
3	0.3595	0.3770	0.4362	0.234	0.4706	0.4739	0.4869	0.4852
4	0.3033	0.3207	0.4093	0.4053	0.4521	0.4327	0.4771	0.4760
5	0.2408	0.2586	0.3768	0.3801	0.3759	0.3923	0.4728	0.4672
6	0.1920	0.1924	0.3460	0.3670	0.3248	0.3441	0.4557	0.4527
7	0.1305	0.1313	0.3003	0.3446	0.2756	0.2715	0.4379	0.4363
8	0.0816	0.0860	0.2699	0.3199	0.2008	0.2048	0.4127	0.4182
9	0.0482	0.0448	0.2193	0.2998	0.1183	0.1387	0.3814	0.3946
10	0.0209	0.0229	0.1742	0.2792	0.0736	0.0931	0.2922	0.3739
11	0.0092	0.0100	0.1279	0.2535	0.0379	0.0464	0.2361	0.3523
12	0.0027	0.0030	0.0699	0.2214	0.0136	0.0190	0.1720	0.3230
13	0.0010	0.0010	0.0462	0.1873	0.0076	0.0089	0.1222	0.2973
14	0.0002	0.0003	0.0187	0.1480	0.0022	0.0029	0.0699	0.2662
15	0	0.0001	0.0081	0.1183	0.0014	0.0007	0.0378	0.2298

Table 6.4 shows that RS-1/2 CC code system is better than its counterpart RS-2/3 CC since the hamming weights of the codes generated are on higher side in 1/2 CC codes than 2/3 CC, resulting in higher free hamming distance for the code words. For a E_b/N_0 of 14 dB, BER for RS-1/2 CC systems are 0.0002, 0.0003, 0.0187, 0.1480 with BPSK, QPSK, 16-QAM and 64-QAM mapping schemes which are lower than BER 0.0022, .0029, 0.0699, 0.2662 for same mapping schemes in RS-2/3 CC coded OFDM systems. For most of the E_b/N_0 values, BPSK and QPSK performance are almost same. Both the scheme offers better BER than 16-QAM and 64-QAM.

Fig. 6.14 compares the BER performance of RS-1/2 CC and RS-2/3 CC coded OFDM system for various mapping schemes in Rician channel. Due to presence of LOS signal component the effect of fading on BER is less as compared to Rayleigh channel.

BER values for few selected E_b/N_0 are shown in Table 6.5. Performance of all the mapping schemes has improved as compared to Rayleigh channel. For E_b/N_0 of 9 dB, the values of BER in Rayleigh channels are 0.0482, 0.0448, 0.2193, 0.2998 against BER of 0.0002, 0.0010, 0.0433, 0.1862 for Rician channel with BPSK, QPSK, 16-QAM and 64-QAM mapping schemes.

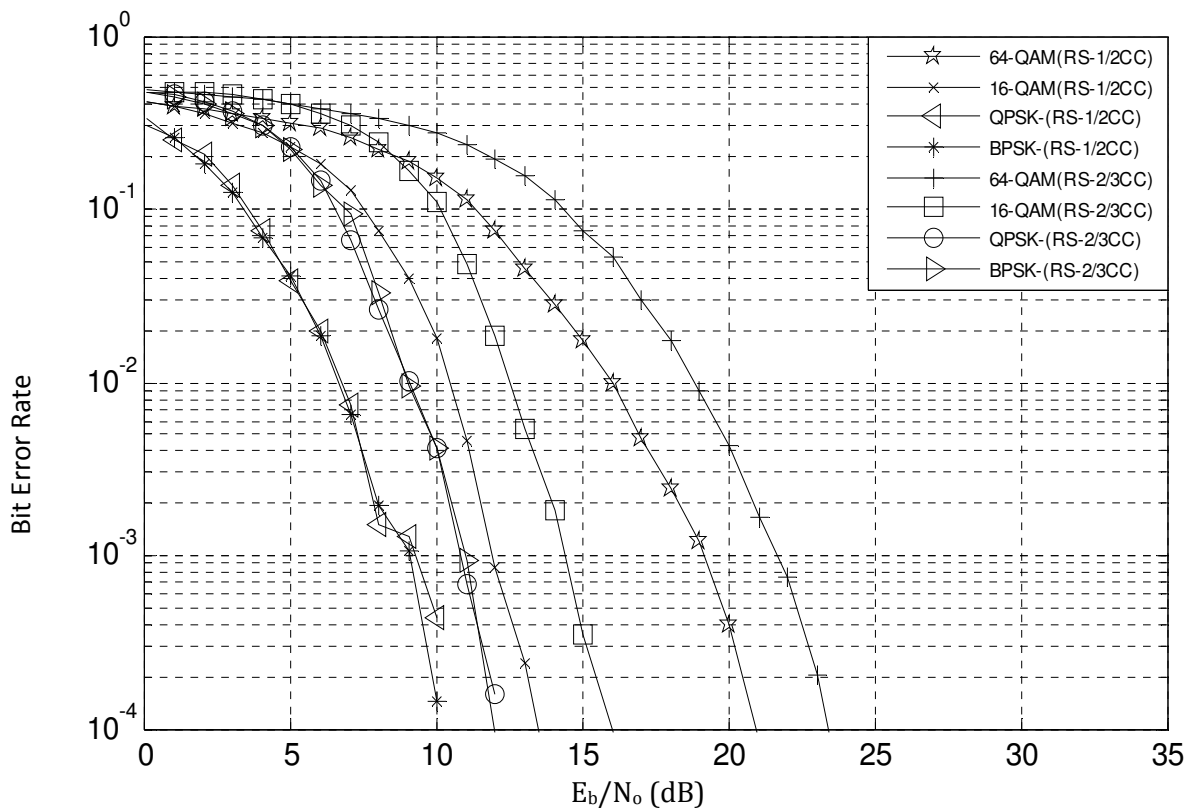


Fig. 6.14 BER comparison of RS -1/2 & 2/3 CC coded OFDM in Rician channel

Table 6.5 E_b/N_0 Vs BER values for RS-CC coded OFDM in Rician channel

E_b/N_0 (dB)	BER (RS-1/2 CC coded OFDM)				BER (RS-2/3 CC coded OFDM)			
	BPSK	QPSK	16-QAM	64-QAM	BPSK	QPSK	16-QAM	64-QAM
0	0.3187	0.3348	0.4294	0.4134	0.4754	0.4718	0.4913	0.4845
1	0.2623	0.2759	0.3967	0.3950	0.4542	0.4464	0.4822	0.4730
2	0.1821	0.2085	0.3626	0.3738	0.4064	0.4113	0.4662	0.4619
3	0.1219	0.1332	0.3206	0.3571	0.3545	0.3678	0.4562	0.4435
4	0.0778	0.0919	0.2757	0.3317	0.2688	0.3206	0.4361	0.4269
5	0.0266	0.0479	0.2349	0.3140	0.2043	0.2259	0.4025	0.4031
6	0.0170	0.0216	0.1775	0.2884	0.1114	0.1422	0.3550	0.3889
7	0.0052	0.0089	0.1278	0.2553	0.0587	0.0744	0.3082	0.3618
8	0.0018	0.0020	0.0791	0.2218	0.0236	0.0281	0.2497	0.3321
9	0.0002	0.0010	0.0433	0.1862	0.0088	0.0128	0.1725	0.3031
10	0	0.0001	0.0170	0.1464	0.0029	0.0027	0.1021	0.2695
11	0	0	0.0063	0.1104	0.0004	0.0005	0.0494	0.2306
12	0	0	0.0020	0.0772	0.0003	0.0003	0.0235	0.1940
13	0	0	0.0005	0.0495	0	0.0001	0.0060	0.1539
14	0	0	0.0002	0.0311	0	0	0.0013	0.1101
15	0	0	0	0.0149	0	0	0.0001	0.0798

Fig. 6.15 compares the BER performance of RS-1/2 CC and RS 2/3 CC codes for various mapping schemes in Nakagami ($m=3$) channel. Nakagami distribution fits more to practical data as compared to all other distribution, $m=3$ is chosen for simulation, since for $m=1$ Nakagami channel behaves same as Rayleigh channel and for $1 < m < 2$ it behaves as Rician channel. For $m=3$ the effect of fading will be less as compared to Rayleigh and Rician.

In Table 6.6, BER values for E_b/N_0 are tabulated of RS-1/2 CC and RS-2/3 CC coded OFDM system for various mapping schemes. Comparing tables 6.4-6.6, the BER values clearly indicate that system performs better in Nakagami ($m=3$) as compared to Rician channel and Rayleigh channel for a given value of E_b/N_0 .

E.g. at E_b/N_0 of 8 dB, BER values For Rayleigh are 0.0816, 0.0860, 0.2699, 0.3199 whereas, for Rician BER values are 0.0018, 0.0020, 0.0791, 0.2218 and for Nakagami BER values are 0.0008, 0.0019, 0.0376, 0.2216 using BPSK, QPSK, 16-QAM and 64-QAM mapping schemes. The values for Rician and Nakagami channels are quite close as the simulations are done for $m=3$, which have response quite closer to Rician distribution.

As far as the E_b/N_0 values are concerned they are similar to standard values determined by ultra wide band (UWB) channel modeling committee IEEE P802.15 by Intel inc. [150] thus the fading model we have used here comply with the standard multipath channel model.

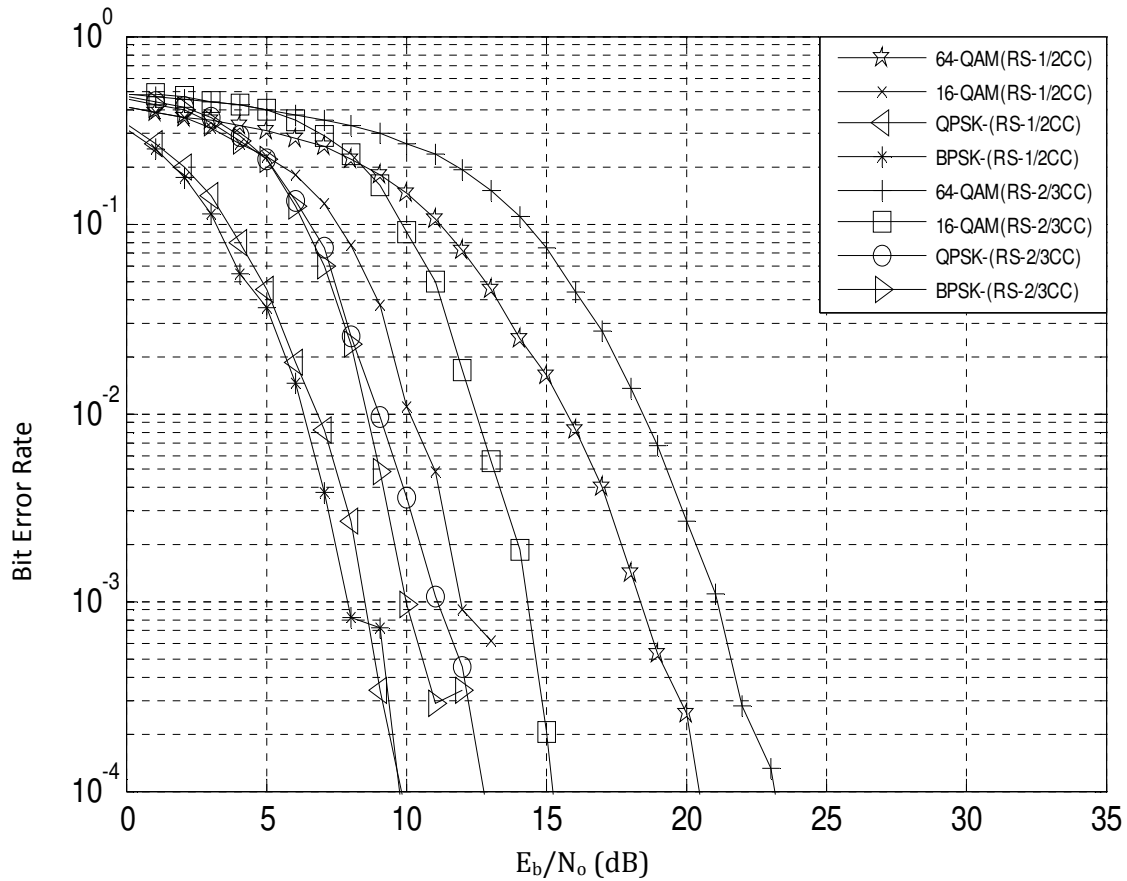


Fig. 6.15 BER comparison of RS -1/2 & 2/3 CC coded OFDM in Nakagami channel

Table 6.6 E_b/N_0 Vs BER values for RS-CC coded OFDM in Nakagami channel

E_b/N_0 (dB)	BER (RS-1/2 CC coded OFDM)				BER (RS-2/3 CC coded OFDM)			
	BPSK	QPSK	16-QAM	64-QAM	BPSK	QPSK	16-QAM	64-QAM
0	0.3157	0.3368	0.4205	0.4110	0.4635	0.4738	0.4903	0.4847
1	0.2530	0.2696	0.3953	0.3934	0.4374	0.4510	0.4818	0.4754
2	0.1756	0.2029	0.3674	0.3730	0.3989	0.4174	0.4700	0.4628
3	0.1135	0.1412	0.3207	0.3530	0.3462	0.3709	0.4519	0.4463
4	0.0549	0.0813	0.2657	0.3358	0.2786	0.2974	0.4356	0.4276
5	0.0367	0.0457	0.2304	0.3123	0.2220	0.2222	0.3995	0.4064
6	0.0142	0.0183	0.1810	0.2850	0.1237	0.1352	0.3597	0.3835
7	0.0038	0.0082	0.1301	0.2585	0.0598	0.0740	0.2976	0.3577
8	0.0008	0.0019	0.0376	0.2216	0.0232	0.0256	0.2382	0.3315
9	0.0007	0.0003	0.0109	0.1842	0.0049	0.0096	0.1611	0.3040
10	0	0.0001	0.0049	0.1468	0.0010	0.0035	0.0921	0.2664
11	0	0	0.0009	0.1077	0.0003	0.0011	0.0171	0.2366
12	0	0	0	0.0732	0.0003	0.0005	0.0056	0.1944
13	0	0	0	0.0251	0	0.0001	0.0019	0.1524
14	0	0	0	0.0158	0	0	0	0.1083
15	0	0	0	0.0082	0	0	0	0.0749

Fig. 6.16 compares the BER performance of RS- 2/3 CC coded OFDM system in AWGN, Rayleigh, Rician and Nakagami channel for 16 QAM. The BER curve clearly indicates the degradation due to multipath phenomenon in fading channels. Absence of fading is visible in BER of RS-CC OFDM system in AWGN channels.

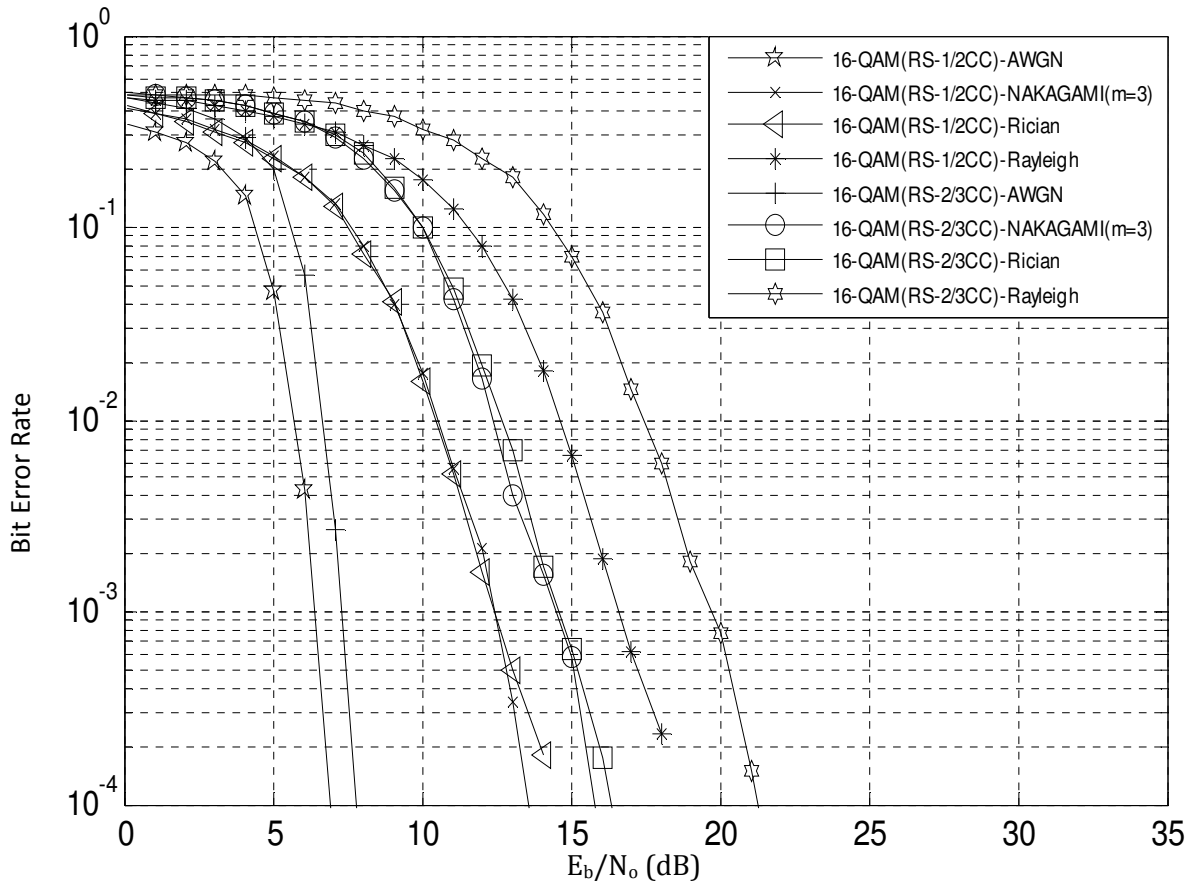


Fig. 6.16 BER comparison of RS –CC coded OFDM in various channels

The simulation results shown in previous section leads to following conclusion based on their BER performances.

Based on mapping scheme used

$$BER_{BPSK} < BER_{QPSK} < BER_{16-QAM} < BER_{64-QAM}$$

Based on fading

$$BER_{AWGN} < BER_{Nakagami-m} < BER_{Rician} < BER_{Rayleigh}$$

Based on Coding

$$BER_{RS-1/2CC} < BER_{RS-2/3CC}$$

6.3.2 Performance Analysis for Turbo Coded OFDM System

The parameters used for performance comparison is bit error rate. Mapping schemes used for OFDM are BPSK, QPSK, 16 and 64 QAM. Fig. 6.17 shows the BER curves for various mapping schemes in Rayleigh channel. Due to severe fading, low values of BER are observed at relatively higher E_b/N_0 values. These E_b/N_0 and BER values are tabulated in Table 6.7.

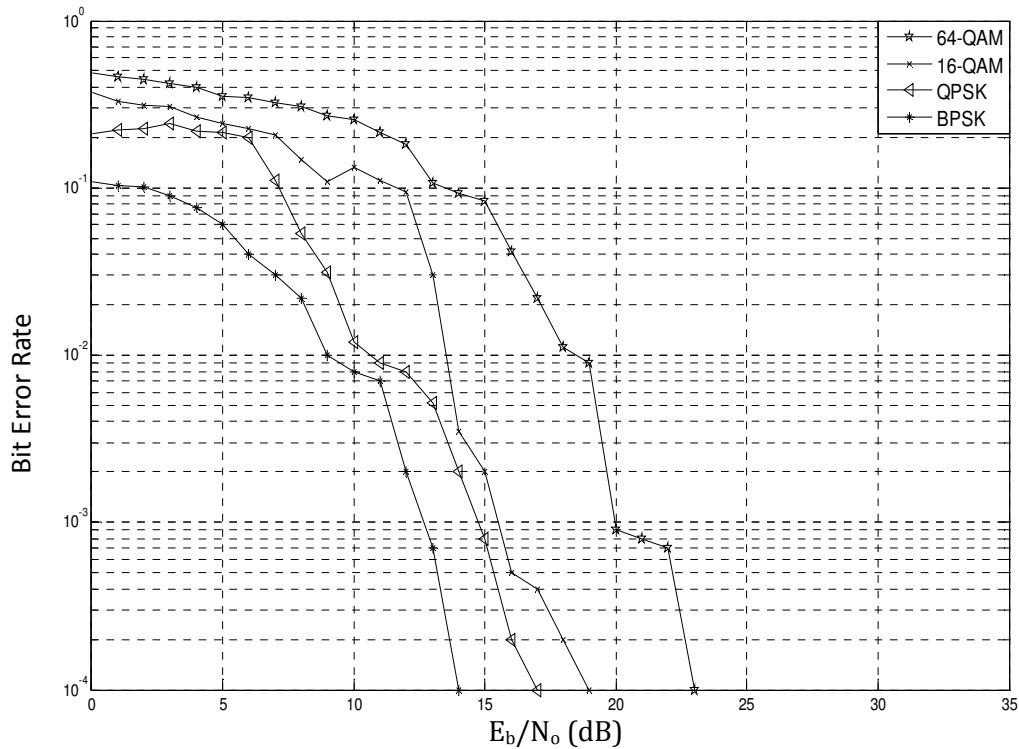


Fig.6.17 BER comparison of turbo coded OFDM in Rayleigh channel

If we compare BER values of Table 6.7 with 6.4 i.e performance of RS-1/2 CC with Turbo codes in the Rayleigh channels, we can derive the inference that turbo system performs better e.g. for E_b/N_0 6 dB the BER values for RS-1/2 CC coded OFDM system are 0.1920, 0.1924, 0.3460, 0.3670 whereas, for turbo coded OFDM system BER values are 0.0001, 0.0050, 0.1047, 0.2911 with BPSK, QPSK, 16-QAM and 64-QAM.

Figs. 6.18-6.19 show BER performance of turbo coded OFDM in Rician and Nakagami ($m=3$) fading channels. The BER curves are better as compared to Rayleigh fading due to less severe fading. The corresponding E_b/N_0 Vs BER values are given in Table 6.8. The values clearly show that system undergoes less severe fading in Rician and Nakagami channels. When we compare BER values for turbo coded OFDM with RS-CC coded OFDM system using tables 6.4-6.8, it suggests superiority of the turbo coded OFDM system,

Table 6.7 E_b/N_0 Vs BER values for Turbo –coded OFDM in Rayleigh channel

E_b/N_0 (dB)	BER for Turbo coded OFDM in Rayleigh channel			
	BPSK	QPSK	16-QAM	64-QAM
0	0.1087	0.0120	0.3720	0.4818
1	0.1023	0.2234	0.3279	0.4585
2	0.1009	0.2268	0.3103	0.4417
3	0.0899	0.2430	0.3047	0.4186
4	0.0760	0.2180	0.2667	0.3964
5	0.0600	0.2126	0.2418	0.3512
6	0.0400	0.2000	0.2275	0.3434
7	0.0220	0.0530	0.2060	0.3231
8	0.0100	0.0312	0.1471	0.3043
9	0.0070	0.0090	0.1080	0.2695
10	0.0020	0.0080	0.1330	0.2575
11	0.0007	0.0052	0.1102	0.2125
12	0	0.0020	0.0950	0.1830
13	0	0.0008	0.0302	0.1069
14	0	0.0002	0.0035	0.0933
15	0	0.0001	0.0020	0.0833

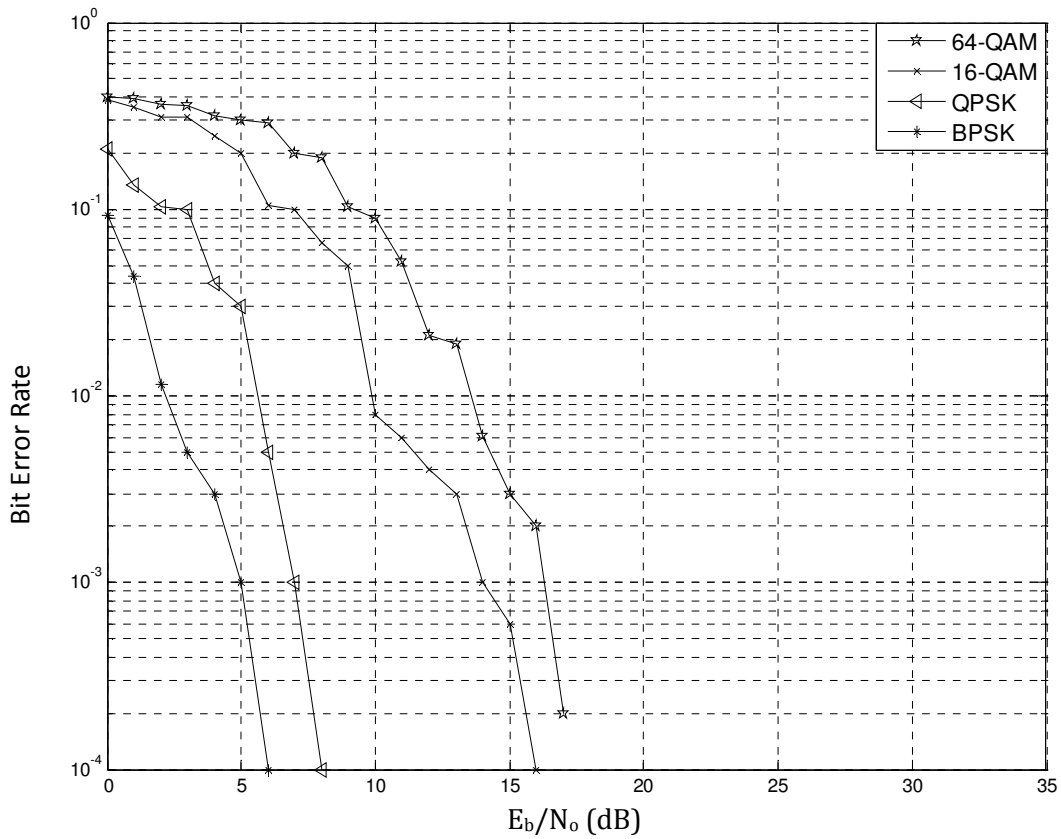


Fig. 6.18 BER comparison of turbo coded OFDM in Rician channel

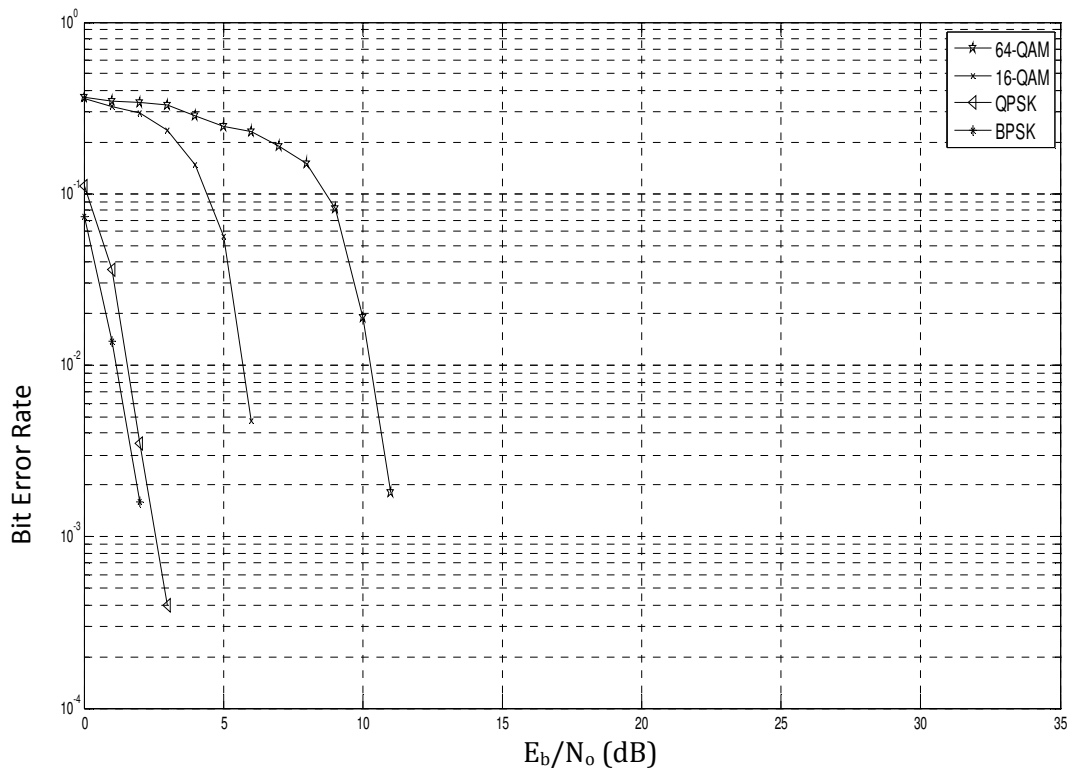


Fig. 6.19 BER comparison of turbo coded OFDM in Nakagami channel

Table 6.8 E_b/N_0 Vs BER values for Turbo –coded OFDM in Nakagami and Rician channels

Bit error rate (BER)								
E_b/N_0 (dB)	Turbo coded OFDM in Nakagami channel				Turbo coded OFDM in Rician channel			
	BPSK	QPSK	16-QAM	64-QAM	BPSK	QPSK	16-QAM	64-QAM
0	0.0732	0.1100	0.3572	0.3672	0.0932	0.2100	0.3857	0.3980
1	0.0137	0.0359	0.3198	0.3490	0.0437	0.1359	0.3498	0.3894
2	0.0016	0.0035	0.2939	0.3380	0.0116	0.1035	0.3139	0.3685
3	0	0.0004	0.2328	0.3286	0.0050	0.0994	0.3108	0.3588
4	0	0	0.1477	0.2844	0.0030	0.0400	0.2477	0.3145
5	0	0	0.0561	0.2488	0.0010	0.0300	0.2001	0.2989
6	0	0	0.0047	0.2303	0.0001	0.0050	0.1047	0.2911
7	0	0	0	0.1890	0	0.0010	0.0990	0.1999
8	0	0	0	0.1487	0	0.0001	0.0660	0.1889
9	0	0	0	0.0821	0	0	0.0500	0.1025
10	0	0	0	0.0190	0	0	0.0080	0.0895
11	0	0	0	0.0018	0	0	0.0060	0.0520
12	0	0	0	0	0	0	0.0040	0.0210
13	0	0	0	0	0	0	0.0030	0.0191
14	0	0	0	0	0	0	0.0010	0.0061
15	0	0	0	0	0	0	0.0006	0.0030
16	0	0	0	0				

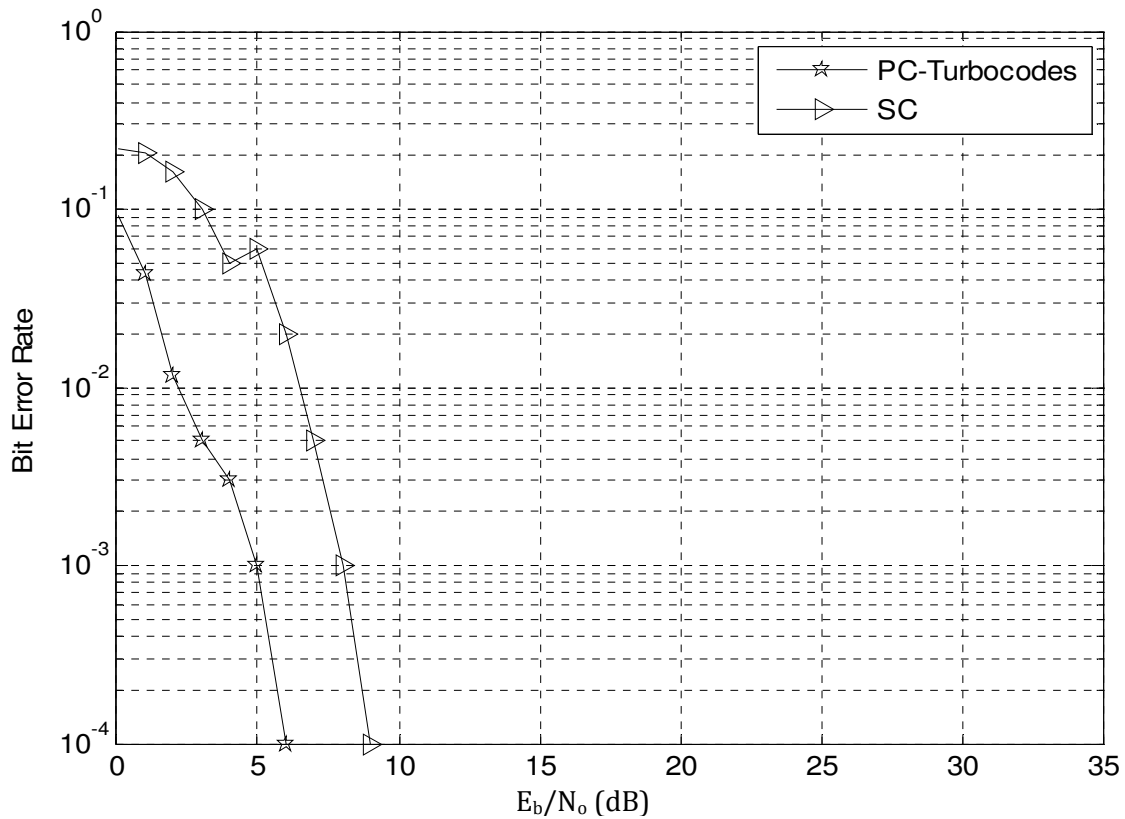


Fig. 6.20 BER comparison of serial and parallel concatenation code for PSK

Fig. 6.20 compares the performance of serial and parallel concatenation codes, showing that parallel concatenation performs much better than their serial counterpart.

All above simulation leads to following conclusions:

Based on mapping scheme used

$$BER_{BPSK} < BER_{QPSK} < BER_{16-QAM} < BER_{64-QAM}$$

Based on fading

$$BER_{AWGN} < BER_{Nakagami-m} < BER_{Rician} < BER_{Rayleigh}$$

Based on Coding

$$BER_{PC-Turbo} < BER_{SC-RS-CC}$$

Findings:

Lower bit error rate can facilitate the higher data rates over wireless multipath channels. Multipath fading severely affects the BER performance of the OFDM system. The BER

performance of the OFDM systems in fading channels can be improved using channel coding schemes.

Concatenations codes perform much better than their standalone counterparts. Reed-Solomon codes are best candidates for burst error correction but they are unable to process soft information while deciding upon received bit, however convolution codes process soft information very efficiently. We have used RS-CC together as serial concatenation and turbo codes for parallel concatenation. BER performances are evaluated in various fading environments, results indicate that turbo-coded OFDM system performs much better than their counterpart RS-CC systems in same channel conditions.

However, implementation of channel coding schemes increase hardware complexity at transmitter as well as at receiver. Since both RS-CC and turbo coded OFDM system use MAP based receivers which are complex to implement.

MODIFIED SLM, PTS AND DHT PRECODED OFDM SYSTEM FOR PAPR REDUCTION

This chapter proposes PAPR reduction in OFDM system using modified selective mapping, partial transmit sequence and discrete Hartley transform (DHT) precoding schemes.

Selective mapping and partial transmit sequence technique have been already discussed in the previous chapters. Discrete Hartley transform [151-160] is a type of precoding technique which could be used for PAPR reduction in OFDM, following section discusses the DHT precoded OFDM system.

Pre-coding is one of the techniques where the data constellations is pre-distorted prior to IFFT operation in such a way that resultant signal produce low PAPR. Data vector is multiplied by suitable transform matrix at the transmitter and at the receiver inverse action takes place as shown in Figs. 7.1-7.2.

Let P is a precoder matrix of order $N \times N$, prior to IFFT the data vector X is passed through precoder and gets modified:

$$X' = P \cdot X \tag{7.1}$$

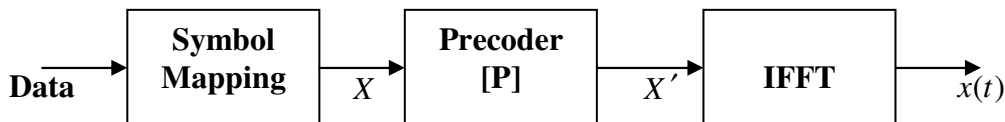


Fig. 7.1 Precoded OFDM transmitter

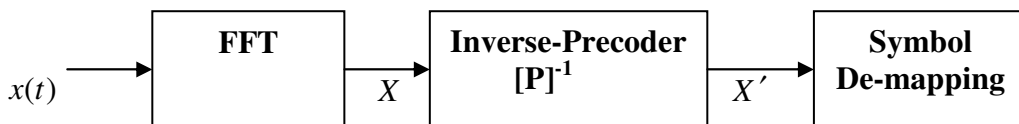


Fig. 7.2 Precoded OFDM receiver

The OFDM signal can be written as

$$x(t) = IFFT[X']$$

$$x(t) = \sum_{k=0}^{N-1} P \cdot X(k) \cdot e^{j.2\pi \cdot \frac{k}{T} \cdot t} \quad (7.2)$$

7.1 Discrete Hartley Transform Precoded OFDM System

DHT was first explored by R. N. Bracewell [151-152, 154] as a competent replacement for DFT's. DHT avoids complexity of DFT by avoiding complex numbers, it uses only real values. So there is no need of separately processing real and imaginary parts for arithmetic operations like determining power. Inverse discrete Hartley transform is similar to direct one, so same operation can perform both direct and inverse transform unlike DFT. DHT offers much lower computations as compared to DFT. Inspired from DHT in [156], authors proposed a DHT based multicarrier modulation scheme. DFT can be calculated by using simple addition [153], given in equation 7.3 and 7.4.

$$H[x(n)] = \text{Re}\{DFT[x(n)]\} - \text{Im}\{DFT[x(n)]\} \quad (7.3)$$

$$\text{Re}\{DFT[x(n)]\} = \frac{1}{2} \{DHT[x(N-n)] + DHT[x(n)]\}$$

$$\text{Im}\{DFT[x(n)]\} = \frac{1}{2} \{DHT[x(N-n)] - DHT[x(n)]\} \quad (7.4)$$

Where H represents DHT.

The N -point DHT of a real sequence is defined by:

$$S_k = \frac{1}{\sqrt{N}} \sum_{n=0}^{N-1} s_n H_k^{kn}, k = 0, 1, 2, \dots, N-1$$

Where $H_N^k = \sin(2\pi k / N) + \cos(2\pi k / N)$

If $s = [s_{N-1}, s_{N-2}, \dots, s_0]^T$ is the transform input vector and $S = [S_{N-1}, S_{N-2}, \dots, S_0]^T$ be the transform output vector. Then DHT of the s will be:

$$S = Hs$$

Where H is:

$$H = \frac{1}{\sqrt{N}} \begin{vmatrix} H_N^{(N-1)^2} & H_N^{(N-1)(N-2)} & \dots & 1 \\ H_N^{(N-1)/(N-2)} & H_N^{(N-2)^2} & \dots & 1 \\ \dots & \dots & \dots & \dots \\ 1 & 1 & 1 & 1 \end{vmatrix}$$

In past few years, authors [158-160] have investigated possible use of DHT precoded OFDM system. DHT precoded OFDM system is shown in Fig. 7.3.

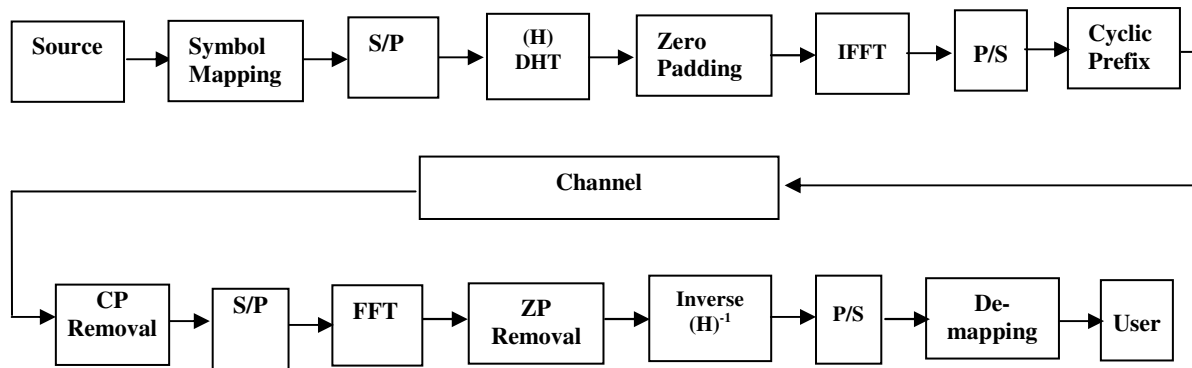


Fig. 7.3 DHT precoded -OFDM system

7.2 Modified SLM, PTS and DHT Precoded OFDM System

A modification is proposed for SLM, PTS and DHT precoded system, where post clipping and filtering is suggested. Clipping allows further suppression in the PAPR values, whereas filtering allows suppression of side lobes so that out of band power could be restrained within a limit and use of channel coding schemes such as RS-CC and turbo codes can help out in degradation in BER due to in band distortion caused by clipping. Uses of channel coding scheme and corresponding MATLAB simulations are already discussed in the previous chapter. This chapter deals with PAPR reduction performance of the proposed scheme. The block diagram of a typical clipping-filtering scheme is shown in Fig 7.4.

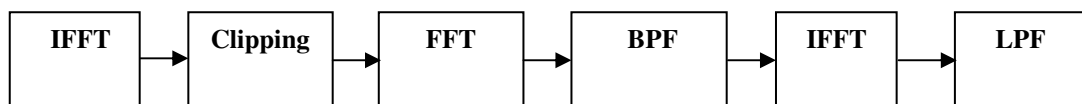


Fig 7.4 Clipping filtering scheme

The signal generated after IFFT operation is passed through a clipper circuit performing time domain clipping, the clipped signal is converted in to frequency domain back using FFT operation and then after it, a band pass filter is used to remove out of band side lobes in the power spectrum of signal.

7.3 PAPR Performance Evaluation of the Modified SLM, PTS and DHT Precoded System

The simulations are done using MATLAB 7.0. PTS technique uses block sizes $V= 2, 4, 8$ and

phase weights $W = \{1, -1\}$, SLM employs $M=16$. Number of subcarriers employed are $N=256$ and oversampling factor of 8 is used. For mapping, 16-QAM and 64-QAM schemes are employed. Clipping ratio is set at $CR = 1.4$. For filtering, a finite impulse response band pass filter (FIR BPF) filter with eqiripple response is used, with $BW= 1$ MHz, stop Band attenuation ranging from 35 to 40 dB and frequency vector varying from 1.3 to 2.5 MHz. For coding purpose, RS-CC and Turbo codes are used, which are already discussed in previous chapter.

Fig. 7.5 compares the CCDF of SLM, DHT precoded COFDM systems with modified SLM and modified DHT precoded systems.

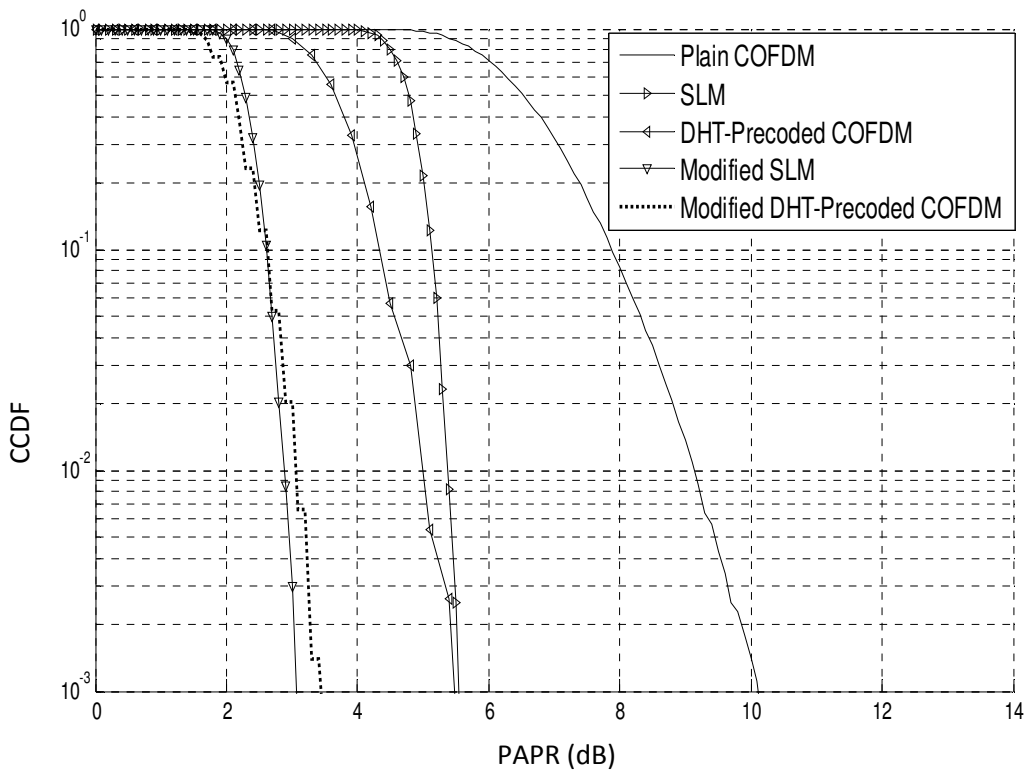


Fig. 7.5 PAPR comparison of DHT-precoded, SLM and their modified versions using 16-QAM

The PAPR performance of the SLM and DHT precoded system get improve in their modified versions. The PAPR values for DHT precoded OFDM system is improved by a margin of almost 2.3 dB and similar improvement is observed in SLM at a $CCDF$ of 10^{-2} . Both the schemes perform much better than the COFDM system without any PAPR reduction scheme being employed. Fig. 7.6 compares the PAPR performance of conventional PTS with modified PTS scheme using 16-QAM mapping scheme.

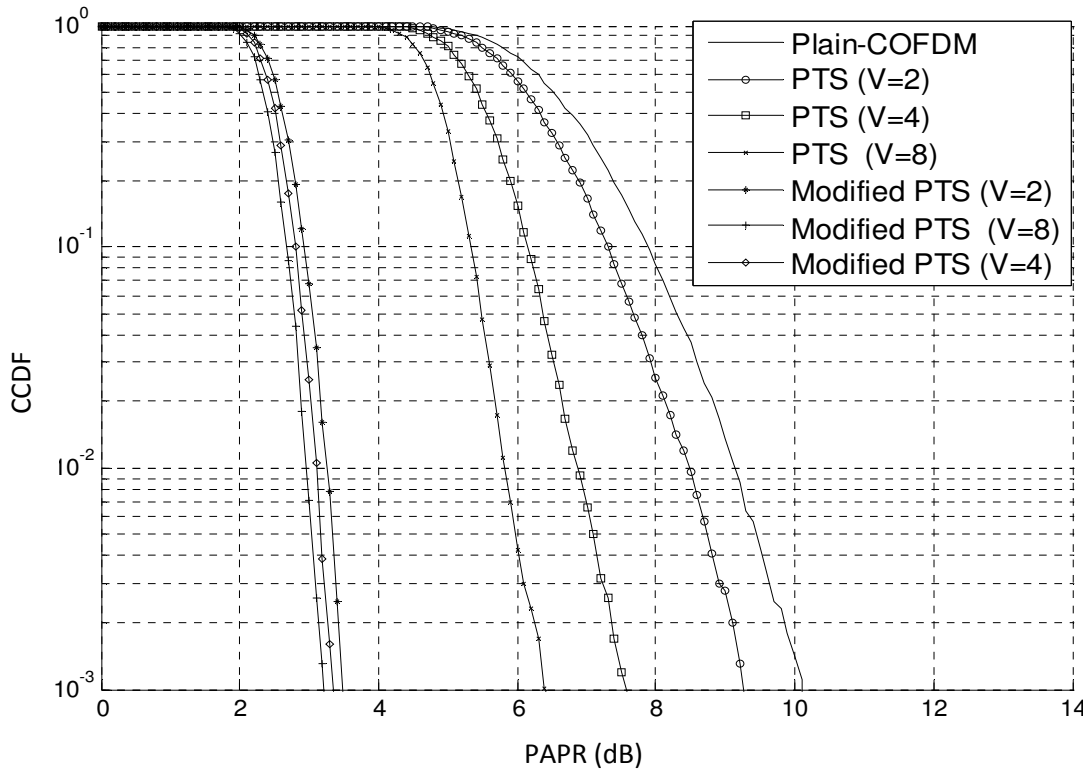


Fig. 7.6 PAPR comparison of PTS and its modified versions using 16-QAM for $V=2, 4, 6$

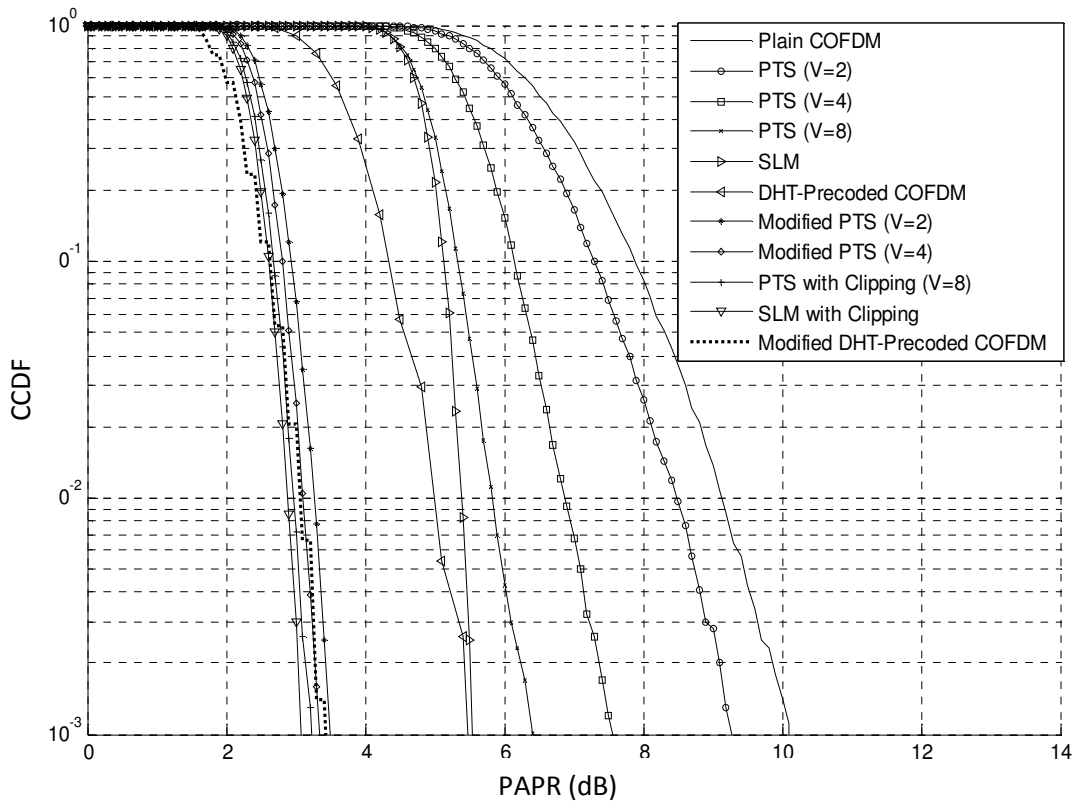


Fig. 7.7 CCDF curves for SLM, PTS, DHT precoded and their modified version for 16-QAM

The PAPR performance of the PTS scheme is improved after using modified scheme, there is an improvement of almost 5 to 6 dB in PAPR reduction performance at a $CCDF$ of 10^{-2} . For higher sub-blocking, the PAPR performance is much better.

Fig 7.7 shows the CCDF of SLM, PTS, DHT precoded schemes and their modified versions for 16-QAM mapping. From the comparison, it is quite clear that the PAPR reduction performance is quite close in case of SLM and DHT precoded system whereas performance of PTS scheme lags behind from both the schemes.

Figs. 7.8-7.10 compare PAPR performance similar to Fig. 7.5-7.7 but for 64-QAM mapping schemes, the performances are quite similar to obtained in case of 16-QAM mapping scheme.

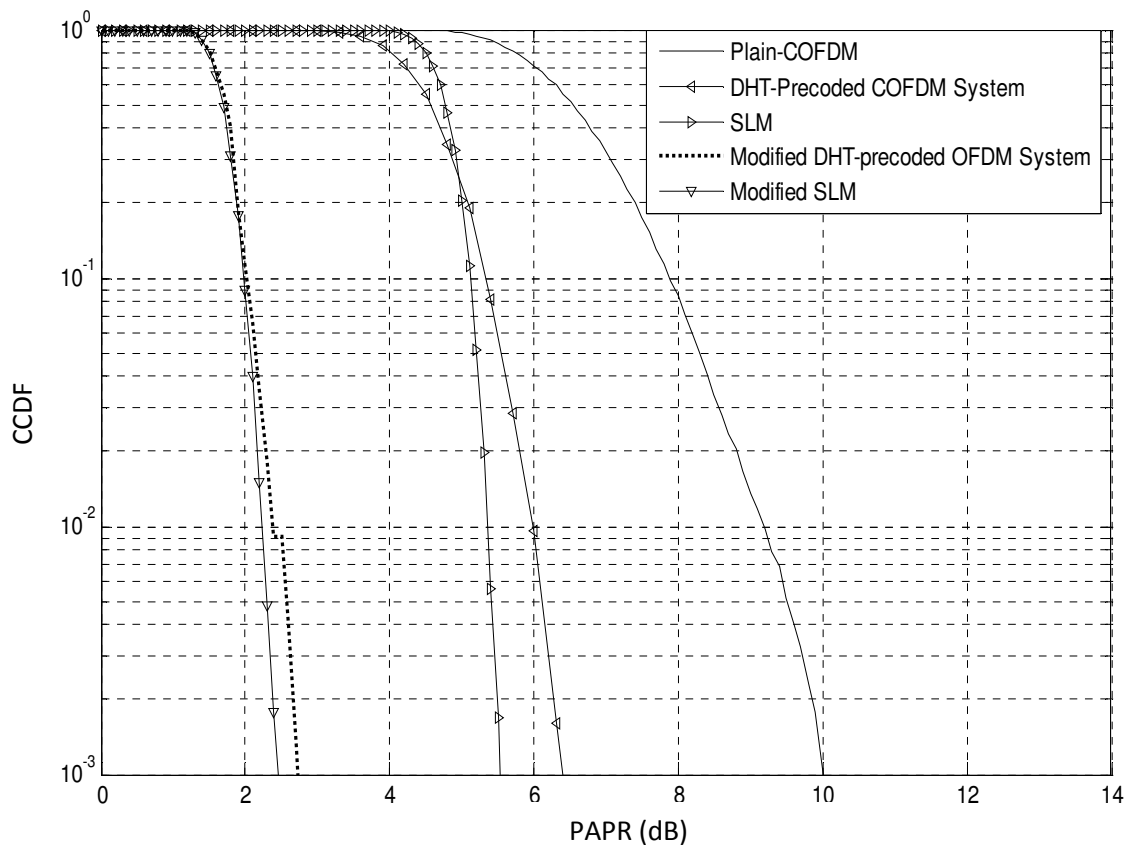


Fig. 7.8 PAPR comparison of DHT-precoded, SLM and their modified versions using 64-QAM

Fig. 7.8 compares the PAPR reduction performance of DHT precoded, SLM with their modified version for 64-QAM mapping schemes. The performance improvement is quite similar to the pervious simulations, the improvement is almost in the range of 2.5 to 3.5 dB in modified versions of DHT and SLM.

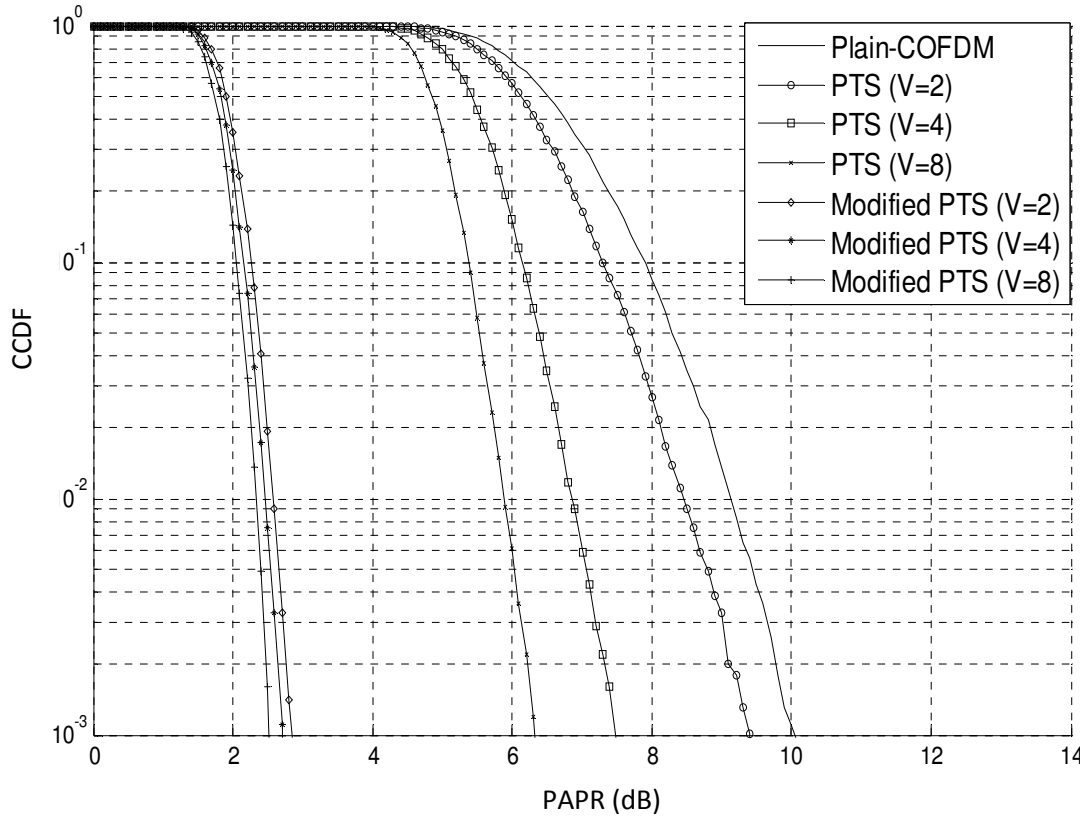


Fig. 7.9 PAPR comparison of PTS and its modified versions using 64-QAM for $V=2, 4, 6$

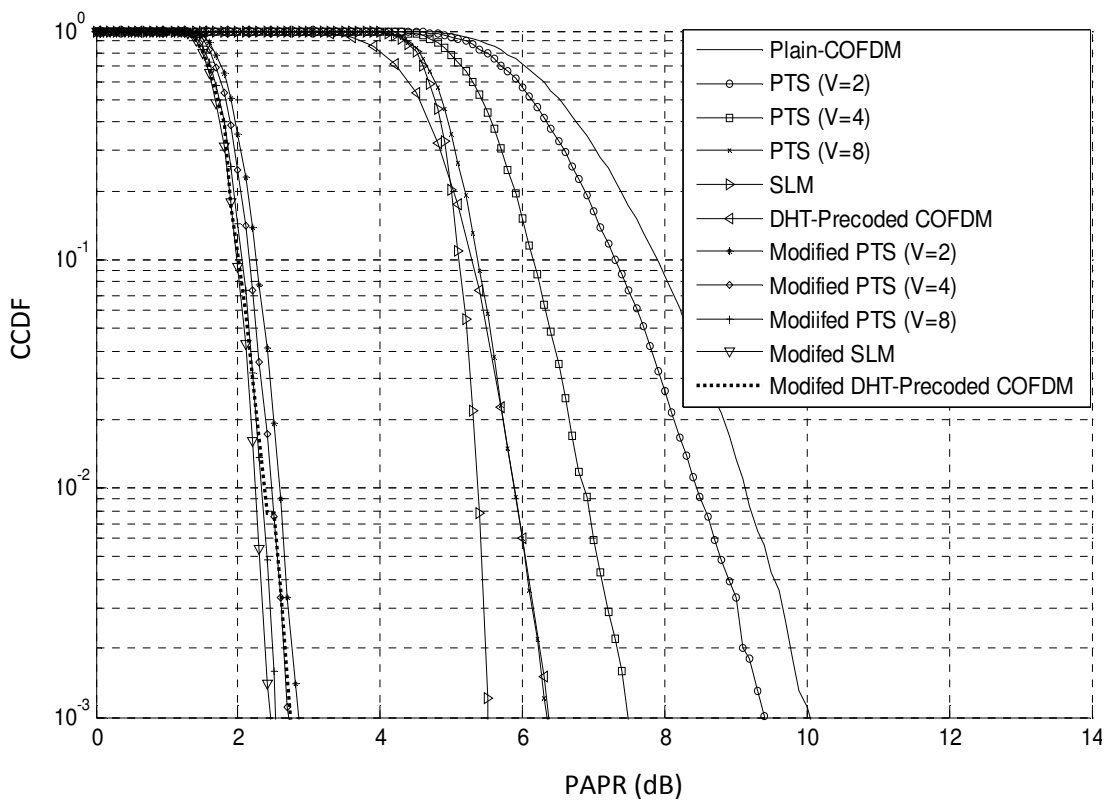


Fig. 7.10 CCDF curves for SLM, PTS, DHT precoded and their modified version for 64-QAM

Fig. 7.9 compares the PAPR performances of plain COFDM system with PTS and modified versions for $V=2, 4, 5, 6$ using 64-QAM mapping scheme. Whereas Fig. 7.10 compares PAPR of all the scheme and their modified versions.

The PAPR performance for a CCDF of 10^{-1} is tabulated in the table 7.1 as shown below, the values are in dB:

Table 7.1 PAPR in (dB) for SLM, PTS and DHT precoded schemes

SCHEME	16-QAM	64-QAM
Plain- COFDM	7.9	8.6
DHT Precoded	5.2	5.6
SLM	5.1	5.3
PTS (V=2)	7.3	7.9
PTS (V=4)	6.2	6.5
PTS (V=8)	5.4	5.7
Modified DHT	2	2.2
Modified SLM	2	2.2
Modified PTS (V=2)	2.3	2.4
Modified PTS (V=4)	2.2	2.3
Modified PTS (V=8)	2	2.2

Findings:

Clipping can be used to reduce PAPR to any desired level but this result in distortion, however filtering can be used to reduce distortion.

Post clipping and filtering improve PAPR performance of SLM, PTS and DHT precoded OFDM system significantly. The result indicates that SLM based and DHT precoded OFDM system performs better than PTS schema based OFDM system.

However, PTS is more in uses due to relatively lower computations complexity as compared to its counterparts. Uses of channel codes can reduce degradation of BER as shown in the simulations in the previous chapter. However, clipping is usually avoided for PAPR reduction as it causes in and out-of-band distortion, however in our proposed scheme use of filtering help out in curbing the distortion. Scheme could be useful in scenarios where higher PAPR reduction is of more concern at decent BER performance.

CONCLUSION AND FUTURE WORK

8.1 Conclusion

In order to achieve high speed communication over wireless channels, various applications such as WLAN, WMAN, HDSL, ADSL, LTE, WiMax etc. uses OFDM owing to its high spectral efficiency, immunity to ISI and fading. However, OFDM suffers from some major drawbacks such as high value of peak to average power ratio, poor BER in severe fading environment and interference due to carrier frequency offset.

The work embodied in the thesis targets the problem of high PAPR and poor BER in fading environments. High PAPR creates in-band and out-of-band distortion due to nonlinear characteristics of HPA. Large dynamic range of OFDM also increases the complexity and cost of the HPA, ADC and DAC circuits. To reduce PAPR in OFDM several techniques are available which are reviewed extensively in this thesis. Out of all these techniques, selective mapping and partial transmit sequence are most widely accepted distortionless techniques. SLM offers slightly better PAPR reduction as compared to PTS. But PTS is adapted more generously by the researches and engineers owing to its low computational complexity as compared to SLM.

Even after being a popular choice for PAPR reduction PTS suffers from few drawbacks, these are:

- ❖ Exhaustive searches are required to find the optimum phase factor set, which generate lowest PAPR sequence. For large number of sub-blocks and phase weights, more searches are required resulting in high computational complexity in terms of complex additions and multiplications.
- ❖ Once the optimum phase set is decided, information regarding the phase set is transmitted to receiver in form of side information, for the correct detection of OFDM symbol.

In the thesis, we have proposed a low complexity PTS scheme where the correlation between the candidate PTS is exploited. Candidates are generated with the help of one another. Our proposed scheme offers a computational complexity reduction ratio of 98.4% for a block size of just $V=8$, similar CCRR other competitive schemes offers at block size of

$V=16$. Our proposed scheme can definitely be fruitful in implementing PTS at low complexity in various applications. This is achieved without reduction in number of subcarriers and PAPR reduction is similar to as achieved in conventional PTS scheme.

Transmitting side information for correct detection of OFDM signal at the receiver puts additional burden on bandwidth and thus reduces bandwidth efficiency of the system. Various schemes proposed in literature are reviewed in the thesis and their limitations are highlighted. We have proposed an octagonal mapping scheme for avoiding side information where eight phase weights $\left\{1, \frac{1}{\sqrt{2}}(1+j), j, \frac{1}{\sqrt{2}}(-1+j), -1, \frac{1}{\sqrt{2}}(-1-j), -j, \frac{1}{\sqrt{2}}(1-j)\right\}$ are used in place of conventional 2 or 4 phase weights. Constellation is divided in groups and a simple look up table at the receiver could easily detect the transmitted symbol based on the group of detected symbol. Proposed scheme do not require any side information at no additional complexity.

BER performance of the OFDM system in fading channels can be improved using channel coding schemes. We have analyzed the performance of OFDM system using serial concatenated and parallel concatenated codes, since they perform better than the stand alone codes. For serial concatenation, we have analyzed Reed Solomon codes with 1/2 and 2/3 convolution codes (RS-CC). For parallel concatenation, Turbo codes with code rate of 1/3 are used. BER performance of coded OFDM system is compared in the Rayleigh, Rician and Nakagami channels for BPSK, QPSK, 16-QAM and 64-QAM mapping scheme. Simulation results suggest that in the presence of the channel codes, the BER performance of the OFDM system improves largely in fading environment.

In this thesis, a post clipping and filtering method is also proposed for PAPR reduction in SLM, PTS and DHT precoded system. The scheme improves the PAPR reduction by a significant margin of 2-3 dB at a CCDF of 10^{-1} . To avoid adverse effect clipping on BER performance, use of channel coding scheme such as RS-CC and turbo codes is proposed. Scheme provides a significant PAPR reduction at decent BER performance. In a nut shell, the thesis conclusion can be summarized as:

- ❖ A low complexity PTS is proposed which offers reduction in computational complexity by almost 98% at block size of $V=8$, without any reduction in subcarriers.

- ❖ PTS scheme without side information is suggested which employs eight phase weights. Scheme achieves PAPR reduction same as achieved in conventional PTS. This improves the bandwidth efficiency of the system.
- ❖ Post clipping and filtering scheme is suggested for SLM, PTS and DHT precoding OFDM systems, for improving PAPR reduction performance. BER performance could be improved using RS-CC and turbo codes in fading environments.

8.1 Future Work

PTS is still a favourite research area among the researchers. Still a lot of work is going on to address various issues related to PTS. Artificially intelligence (AI) techniques are currently being excessively explored for reducing the number of searches in PTS scheme which can further reduce the computational complexity.

AI scheme such as genetic algorithm (GA), harmony algorithm (HA), opposition based learning (OBL) with GA and HA, parallel tabu search etc and their modifications are already implemented. Particle swarm optimization has already given astounding results in PAPR reduction. Invasive weed and biogeography-based optimization techniques are still being explored for PAPR reduction.

So there is still a huge work space for researcher to work around the PAPR problem and improving PTS in terms of computational complexity and making it side information free.

Apart from this currently work is also going on generalized frequency division multiplexing (GFDM) technique which offers lower PAPR than OFDM and uses traditional filter bank multi-branch multicarrier concept. GFDM is extensively being investigated for achieving data rates higher than 4-G systems i.e a step towards 5th generation (5G).

REFERENCES

- [1] Chang R. W., “*Synthesis of band-limited orthogonal signals for multichannel data transmission*”, Bell Syst. Tech. Journal, vol. 45, pp. 1775–1797, Dec. 1966.
- [2] Saltzberg B., “*Performance of an Efficient Parallel Data Transmission System*”, IEEE Transactions on Communication Technology, vol.15, no.6, pp. 805-811, Dec. 1967
- [3] Salz J., Weinstein S. B., “*Fourier transform communication system*”, Computers and Communication Conference, Pine Mountain, Gn., Oct. 1969.
- [4] Weinstein S., Ebert P., “*Data Transmission by Frequency-Division Multiplexing Using the Discrete Fourier Transform*”, IEEE Transactions on Communication Technology, vol.19, no.5, pp.628-634, Oct. 1971.
- [5] Cimini L.J., “*Analysis and Simulation of a Digital Mobile Channel Using Orthogonal Frequency Division Multiplexing*”, IEEE Transactions on Communications, vol.33, no.7, pp.665-675, Jul 1985.
- [6] Haitham .J.T., Salleh M.F.M., “*Multi-carrier rransmission Techniques for Wireless Communication Systems: A Survey*”, WSEAS Trans. On Commun., Vol. 8, Issue 5, pp.457-472, 2009.
- [7] Hwang T., Yang C.,Wu G., Li S., Li G.Y., “*OFDM and Its Wireless Applications: A Survey*”, IEEE Transactions on Vehicular Technology, vol.58, no.4, pp.1673-1694, May 2009.
- [8] Richard V. N., Prasad R., “*OFDM for Wireless Communications*”, Boston: Artech House, 2000.
- [9] Soo C.Y., Kim J., Yang W. Y., Kang C. G., “*MIMO OFDM Wireless communication with MATLAB*”, IEEE Press, pp.111-151 & 209-241, 2010.
- [10] Jha U.S., Prasad R., “*OFDM Towards Fixed and Mobile Broadband Wireless Access*”, Artech House (Universal Personal Communications), pp. 29-81,2007.
- [11] Prasad, R., “*OFDM for Wireless Communications Systems*”, Artech House (Universal Personal Communications), pp.149-180,2004
- [12] Schulze H., L'uders C., “*Theory and Applications of OFDM and CDMA*”, John Wiley & Sons Ltd, pp.145-263, 2005

- [13] IEEE 802.11 detailed documentation [Online]. Available at: <http://standards.ieee.org/getieee802> ,Last accessed on 18/08/2012
- [14] Van Nee R., de Wild A., “*Reducing the peak-to-average power ratio of OFDM,*” *Vehicular Technology Conference*”, 48th IEEE VTC 98, vol.3, pp.2072-2076 ,18-21 May 1998
- [15] Han S.H., Lee J. H., “*An overview of peak-to-average power ratio reduction techniques for multicarrier transmission*”, IEEE Transaction on Wireless Communications, vol. 12, no.2, pp. 56–65, 2005.
- [16] Wulich D., “*Definition of efficient PAPR in OFDM,*” IEEE Communications Letters, vol.9, no.9, pp.832-834, Sep 2005.
- [17] Rahmatallah Y., Mohan S., “*Peak-To-Average Power Ratio Reduction in OFDM Systems: A Survey And Taxonomy,*” IEEE Communications Surveys & Tutorials, vol.15, no.4, pp.1567-1592, Fourth Quarter 2013.
- [18] O'Neill R., Lopes L. B., “*Envelope Variations and Spectral Splatter in Clipped Multicarrier Signals*”, in proceedings of IEEE conference PIMRC, Toronto, Canada, pp. 71–75, Sept. 1995.
- [19] Li X., Cimini L.J. Jr., “*Effects of clipping and filtering on the performance of OFDM,*” IEEE Communications Letters, vol. 2, no. 5, pp. 131-133, May 1998.
- [20] Armstrong J., “*Peak-to-average power reduction for OFDM by repeated clipping and frequency domain filtering*”, Electronics Letters, vol.38, no.5, pp-246-247, 2002.
- [21] Deng S.K., Lin M.C., “*OFDM PAPR reduction using clipping with distortion control,*” in proceedings of IEEE International Conference on Communications, vol.4, pp.2563-2567, 16-20 May 2005.
- [22] Wang L., Tellambura C., “*Clipping-Noise Guided Sign-Selection for PAR Reduction in OFDM Systems*”, IEEE Transactions on Signal Processing, vol.56, no.11, pp.5644-5653, Nov. 2008.
- [23] Hyun-Bae J., Jong-Seon N., Dong-Joon S., “*A New PAPR Reduction Scheme Using Efficient Peak Cancellation for OFDM Systems*”, IEEE Transactions on Broadcasting, , vol.58, no.4, pp.619-628, 2012.

- [24] Liang L., Wang J., Song J., “*Adaptive algorithm for OFDM PAPR reduction using clipping-noise guided sign-selection,*” in proceedings of IEEE Symposium on International Broadband Multimedia Systems and Broadcasting (BMSB), pp.1-3, 5-7 June 2013 .
- [25] Chen H., Haimovish M., “*Iterative Estimation and Cancellation of Clipping Noise for OFDM Signals,*” IEEE Communication Letters, vol. 7, no. 7, pp. 305–07, July 2003.
- [26] Wang Xi., Tjhung T.T., Ng C.S., “*Reduction of peak-to-average power ratio of OFDM system using a companding technique,*” IEEE Transactions on Broadcasting, vol.45, no.3, pp.303-307, Sep 1999.
- [27] Huang X., Lu Ji., Zheng J., “*Reduction in PAPR of OFDM system using a revised companding,*” in the proceedings of 8th International Conference on Communication Systems, vol.1, pp.62-66 ,25-28 Nov. 2002.
- [28] Ojima M., Hattori T., “*PAPR Reduction Method Using Clipping and Peak-Windowing in CI/OFDM System,*” in proceedings of IEEE 66th Vehicular Technology Conference, pp.1356-1360, Sept. 30 2007-Oct. 3 2007.
- [29] Cha Su., Park M., Lee Su., Bang K-J., Hong D., “*A new PAPR reduction technique for OFDM systems using advanced peak windowing method,*” IEEE Transactions on Consumer Electronics, vol.54, no.2, pp.405-410, May 2008.
- [30] Chen Gu., Ansari R., Yao Y., “*Improved Peak Windowing for PAPR Reduction in OFDM,*” in proceedings of IEEE 69th Vehicular Technology Conference, pp.1-5, 26-29 April 2009.
- [31] Jones A.E., Wilkinson T.A., Barton S.K., “*Block coding scheme for reduction of peak to mean envelope power ratio of multicarrier transmission schemes,*” Electronics Letters , vol.30, no.25, pp.2098-2099, 8 Dec 1994.
- [32] Wilkinson T.A., Jones A.E., “*Minimisation of the peak to mean envelope power ratio of multicarrier transmission schemes by block coding*”, in proceedings of IEEE 45th Vehicular Technology Conference, vol.2, pp.825-829 ,25-28 Jul 1995.
- [33] Jones A.E., Wilkinson T.A., “*Combined coding for error control and increased robustness to system nonlinearities in OFDM*”, in proceedings of IEEE 46th Vehicular Technology Conference, vol.2, pp.904-908 , 28 Apr-1 May 1996 .

- [34] Tarokh V., Hamid J., “*On the computation and reduction of the peak-to-average power ratio in multicarrier communications,*” IEEE Transactions on Communications, vol.48, no.1, pp.37-44, Jan 2000.
- [35] Golay, Marcel J E, “*Complementary series,*” IRE Transactions on Information Theory, vol.7, no.2, pp.82-87, April 1961.
- [36] Davis J.A., Jedwab J., “*Peak-to-mean power control and error correction for OFDM transmission using Golay sequences and Reed-Muller codes,*” Electronics Letters, vol.33, no.4, pp.267-268, 13 Feb 1997.
- [37] Davis J.A., Jedwab J., “*Peak-to-Mean Power Control in OFDM, Golay Complementary Sequences, and Reed–Muller Codes,*” IEEE Trans. Info. Theory, vol. 45, no. 7, pp. 2397–17, Nov. 1999.
- [38] Patterson K., “*Generalized Reed-Muller Codes and Power Control in OFDM Modulation,*” IEEE Trans. Info. Theory, vol. 46, no. 1, pp. 104–120, Jan. 2000.
- [39] Chong C.V., Tarokh V., “*A Simple Encodable/Decodable OFDM QPSK Code with Low Peak-to-Mean Envelope Power Ratio,*” IEEE Trans. Info. Theory, vol. 47, no. 7, pp. 3025–3029, Nov. 2001.
- [40] Taha Z., Liu X., “*Low PMEPR code based on STAR-16-QAM constellation for OFDM,*” IEEE Communication Letters, vol. 11, no. 9, pp. 747–749, September 2007.
- [41] Liu X., Wu H., “*Novel asterisk 16QAM constellation for COFDM,*” IEEE Communication Letters, vol. 14, no. 7, pp. 596–598, July 2010.
- [42] Huang S., Wu H., Chang S., Liu X., “*Novel sequence design for low-PMEPR and high-code-rate OFDM systems,*” IEEE Transaction on Communications, vol. 58, no. 2, pp. 405–410, Feb. 2010.
- [43] Sabbaghian M., Kwak Y., Tarokh V., “*New codes from dual BCH codes with applications in low PAPR OFDM,*” IEEE Transaction on Communications ,vol. 10, no. 12, pp. 3990–3994, Dec. 2011.
- [44] Lin M-C., Chen K-C., Li S-L., “*Turbo coded OFDM system with peak power reduction,*” 58th IEEE Vehicular Technology Conference, vol.4, pp.2282-2286, vol.4, 6-9 Oct. 2003.

- [45] Tsai Y.C., Ueng Y.L., “*A Tail-Biting Turbo Coded OFDM System for PAPR and BER Reduction*,” in proceedings of IEEE 66th Vehicular Technology Conference, pp.1067-1071, Sept. 30 2007-Oct. 3 2007.
- [46] Gallager R.G., “*Low-density parity-check codes*,” IRE Transactions on Information Theory, vol.8, no.1, pp.21-28, Jan. 1962.
- [47] Horstein M., “*Review of 'Low-Density Parity-Check Codes' (Gallager, R. G.; 1963)*,” IEEE Transactions on Information Theory, vol.10, no.2, pp.172-172, Apr. 1964.
- [48] Daoud O., Alani O., “*Reducing the PAPR by utilisation of the LDPC code*”, IET Communications, vol. 3, no.4, pp. 520 – 529, Apr. 2009.
- [49] Lu B., Yue G., Wang X., “*Performance analysis and design optimization of LDPC-coded MIMO OFDM systems*,” IEEE Transactions on Signal Processing, vol.52, no.2, pp.348-361, Feb. 2004.
- [50] Bauml R.W., Fischer R. F.H., Huber J.B., “*Reducing the peak-to-average power ratio of multicarrier modulation by selected mapping*,” Electronics Letters, vol.32, no.22, pp.2056-2057, 24 Oct. 1996.
- [51] Breiling M., Muller-Weinfurtner S.H., Huber, J.B., “*SLM peak-power reduction without explicit side information*,” IEEE Communications Letters, vol.5, no.6, pp.239-241, June 2001.
- [52] Jayalath A. D S., Tellambura, C., “*A blind SLM receiver for PAR-reduced OFDM*,” in proceedings of IEEE 56th Vehicular Technology Conference, vol.1, pp.219-222 2002.
- [53] Jayalath A. D S., Tellambura, C., “*SLM and PTS peak-power reduction of OFDM signals without side information*,” IEEE Transaction on Wireless Communications, vol. 4, no. 5, pp. 2006–2013, Sept. 2005.
- [54] Baxley R.J., Zhao C., Zhou G.T., “*Magnitude-Scaled Selected Mapping: A Crest Factor Reduction Scheme for OFDM Without Side-Information Transmission*,” in proceedings of IEEE International Conference on Acoustics, Speech and Signal ,vol.3, pp.III-373-III-376, 15-20 Apr. 2007.

- [55] Joo H.S., Heo S.J., Jeon H.B., No J.S., Shin D.J., "A *New Blind SLM Scheme with Low Complexity of OFDM Signals*," in proceedings of IEEE 70th Vehicular Technology Conference , pp.1-5, 20-23 Sept. 2009.
- [56] Joo H.S., No J.S., Shin D.J., "A *blind SLM PAPR reduction scheme using cyclic shift in STBC MIMO-OFDM system*," in proceedings of International Conference on Information and Communication Technology Convergence ,pp.272-273, 17-19 Nov. 2010.
- [57] Joo H.S., Heo S.J., Jeon H.B., No J.S., Shin D.J., "A *New Blind SLM Scheme With Low Decoding Complexity for OFDM Systems*," IEEE Transactions on Broadcasting, vol.58, no.4, pp.669-676, Dec. 2012.
- [58] Jiang T., Chunxing Ni., Guan L., "A *Novel Phase Offset SLM Scheme for PAPR Reduction in Alamouti MIMO-OFDM Systems Without Side Information*," IEEE Signal Processing Letters, vol.20, no.4, pp.383-386, Apr. 2013.
- [59] Ji J., Ren G., "A *New Modified SLM Scheme for Wireless OFDM Systems Without Side Information*," IEEE Signal Processing Letters, vol.20, no.11, pp.1090-1093, Nov. 2013.
- [60] Lim D.W., No J.S., Lim C.W., Chung H., "A *new SLM OFDM scheme with low complexity for PAPR reduction*," IEEE Signal Processing Letters, vol.12, no.2, pp.93-96, Feb. 2005.
- [61] Heo S.J., Noh H.S., No J.S., Shin D.J., "A *Modified SLM Scheme With Low Complexity for PAPR Reduction of OFDM Systems*," IEEE Transactions on Broadcasting, vol.53, no.4, pp.804-808, Dec. 2007.
- [62] Wang S.H., Li C.P., "A *Low-Complexity PAPR Reduction Scheme for SFBC MIMO-OFDM Systems*," IEEE Signal Processing Letters, , vol.16, no.11, pp.941-944, Nov. 2009.
- [63] Wang J.S., Lee J.H., Park J.C., Song I., Kim Y.H., "Combining of *Cyclically Delayed Signals: A Low-Complexity Scheme for PAPR Reduction in OFDM Systems*," IEEE Transactions on Broadcasting, vol.56, no.4, pp.577-583, Dec. 2010.
- [64] Jeon H.B., No J.S., Shin D.J., "A *Low-Complexity SLM Scheme Using Additive Mapping Sequences for PAPR Reduction of OFDM Signals*," IEEE Transactions on Broadcasting, vol.57, no.4, pp.866-875, Dec. 2011.

- [65] Kim K.H, Jeon H.B., No J.S., Shin D.J., “*Low-complexity selected mapping scheme using cyclic-shifted inverse fast Fourier transform for peak-to-average power ratio reduction in orthogonal frequency division multiplexing systems,*” IET Communications, vol.7, no.8, pp.774-782, May 2013.
- [66] Adegbite S.A., McMeekin S.G., Stewart B.G., “*Low-complexity data decoding using binary phase detection in SLM-OFDM systems,*” Electronics Letters , vol.50, no.7, pp.560-562, March 2014.
- [67] Muller S.H., Huber J.B., “*OFDM with reduced peak-to-average power ratio by optimum combination of partial transmit sequences,*” Electronics Letters , vol.33, no.5, pp.368-369, Feb 1997.
- [68] Muller S.H., Huber J.B., “*A novel peak power reduction scheme for OFDM,*” in proceedings of 8th IEEE International Symposium on Personal, Indoor and Mobile Radio Communications, vol.3, pp.1090-1094, 1-4 Sep 1997.
- [69] Baxley R.J., Zhou G.T., “*Comparison of Selected Mapping and Partial Transmit Sequence for Crest Factor Reduction in OFDM,*” in proceedings of IEEE Military Communications Conference, pp.1,4, 23-25 Oct. 2006.
- [70] Hassan Y., El-Tarhuni M., “*A comparison of SLM and PTS peak-to-average power ratio reduction schemes for OFDM systems,*” in proceedings of the 4th International Conference on Modeling, Simulation and Applied Optimization, pp.1-4, Apr. 2011.
- [71] Wu D.X., “*Selected mapping and partial transmit sequence schemes to reduce PAPR in OFDM systems,*” in proceedings of International Conference on Image Analysis and Signal Processing , pp.1-5, 2011 .
- [72] Janjic M., Neskovic N., “*A comparative analysis of techniques for PAPR reduction of OFDM signals,*” 21st Telecommunications Forum (TELFOR), pp.256-259, 26-28 Nov. 2013.
- [73] Eetvelt P.V., Wade G., Tomlinson M., “*Peak to Average Power Reduction for OFDM Schemes by Selective Scrambling,*” Elect. Letters, vol. 32, no. 21, pp. 1963–64, Oct. 1996.
- [74] Hill G. R., Faulkner M., Singh J., “*Reducing the Peak-to-Average Power Ratio in OFDM by Cyclically Shifting Partial Transmit Sequences,*” Elect. Letters, vol. 36, no. 6, pp. 560–561, Mar. 2000.

- [75] Jayalath A.D.S., Tellambura C., “*Reducing the peak to-average power ratio of orthogonal frequency division multiplexing signal through bit or symbol interleaving,*” IEE Electronic Letters, vol. 36,no. 13, pp. 1161–1163, June 2000.
- [76] Jayalath A.D.S., Tellambura C., “*Reducing the peak to-average power ratio of an OFDM signal by interleaving,*” in Proceedings of International Symposium on Wireless Personal Multimedia Communications, pp.698–703, Bangkok, Thailand, 2000.
- [77] Jayalath A.D.S., Tellambura C., “*The use of interleaving to reduce the peak to-average power ratio of an OFDM signal,*” in Proc. IEEE Global Communications Conference , pp.82–86, San Francisco, California, USA, 2000.
- [78] Jayalath A.D.S., Tellambura C., “*Peak to-average power ratio reduction of an OFDM signal using data permutation with embedded side information,*” in Proceedings of IEEE International Symposium on Circuits and Systems, no. 4, pp. 562–565, Sydney, Australia, 2001.
- [79] Tellado J., Cioffi J. M., “*Peak power reduction for multicarrier transmission,*” in Proceedings of IEEE Global Communications Conference Sydney, Australia, November 1998.
- [80] Wattanasuwakull T., Benjapolakul W., “*PAPR reduction for OFDM transmission by using a method of tone reservation and tone injection,*” in Proceedings of 5th International Conference on Information, Communications and Signal Processing, pp. 273– 277, Bangkok, Thailand, December 2005,
- [81] Yang G., Yang Z., “*PAPR reduction in the OFDM system employing tone reservation based on FFT/IFFT,*” in Proceedings of 3rd IEEE/IFIP International Conference in Central Asia on Internet, pp.1-4, 26-28 Sept. 2007.
- [82] Hussain S., Louet Y., “*Tone Reservation's Complexity Reduction Using Fast Calculation of Maximal IDFT Element,*” International Wireless Communications and Mobile Computing Conference, pp.2000-204, 6-8 Aug. 2008.
- [83] Choi J.J., Yang S.C., Shin Y., “*A PRSC selection scheme based on PN code for OFDM PAPR reduction,*” Proceedings of International Symposium on Intelligent Signal Processing and Communication Systems, pp.222-225, 18-19 Nov. 2004.

- [84] Wang L., Tellambura C., “*Analysis of Clipping Noise and Tone-Reservation Algorithms for Peak Reduction in OFDM Systems,*” IEEE Transactions on Vehicular Technology, vol.57, no.3, pp.1675-1694, May 2008.
- [85] Li H., Jiang T., Zhou Y., “*An Improved Tone Reservation Scheme With Fast Convergence for PAPR Reduction in OFDM Systems,*” IEEE Transactions on Broadcasting, vol.57, no.4, pp.902-906, Dec. 2011.
- [86] Chen J.C., Li C.P., “*Tone Reservation Using Near-Optimal Peak Reduction Tone Set Selection Algorithm for PAPR Reduction in OFDM Systems,*” IEEE Signal Processing Letters, vol.17, no.11, pp.933-936, Nov. 2010.
- [87] Rubinstein R. Y., Kroese D. P., “*The Cross-Entropy Method: A Unified Approach to Combinatorial Optimization, Monte-Carlo Simulation, and Machine Learnin,*” New York: Springer-Verlag, July 2004.
- [88] Wang Y., Chen W., Tellambura C., “*Genetic Algorithm Based Nearly Optimal Peak Reduction Tone Set Selection for Adaptive Amplitude Clipping PAPR Reduction,*” IEEE Transactions on Broadcasting, vol.58, no.3, pp.462-471, Sept. 2012.
- [89] Jiang T., Ni Ch., Chang X., Qi Q., “*Curve Fitting Based Tone Reservation Method with Low Complexity for PAPR Reduction in OFDM Systems,*” IEEE Communications Letters , vol.18, no.5, pp.805-808, May 2014.
- [90] Han S.H., Cioffi J.M., Lee J.H., “*Tone injection with hexagonal constellation for peak-to-average power ratio reduction in OFDM,*” IEEE Communications Letters, vol.10, no.9, pp.646-648, Sept. 2006.
- [91] Chen J.C., Wen C.K., “*PAPR Reduction of OFDM Signals Using Cross-Entropy-Based Tone Injection Schemes,*” IEEE Signal Processing Letters, vol.17, no.8, pp.727-730, Aug. 2010.
- [92] Hou J., Tellambura C., Ge J., “*Clipping noise-based tone injection for PAPR reduction in OFDM systems,*” in Proceedings of IEEE International Conference on Communications , pp.5759-5763, 9-13 June 2013.
- [93] Jacklin N., Ding Z., “*A Linear Programming Based Tone Injection Algorithm for PAPR Reduction of OFDM and Linearly Precoded Systems,*” IEEE Transactions on Circuits and Systems, vol.60, no.7, pp.1937-1945, July 2013.

- [94] Jones D., “*Peak power reduction in OFDM and DMT via active channel modification,*” in Proceedings of 33rd Asilomar Conference on Signals, Systems, and Computers, vol. 2, pp. 1076–1079, 1999.
- [95] Krongold B.S., Jones D.L., “*PAR reduction in OFDM via active constellation extension,*” IEEE Transactions on Broadcasting, vol.49, no.3, pp.258-268, Sept. 2003.
- [96] Kou Y., Lu W., Antoniou A., “*New peak-to-average power-ratio reduction algorithms for multicarrier communications,*” IEEE Transaction on Circuits System, vol. 51, no. 9, pp. 1790–1800, Sept.2004.
- [97] Kang B.M., Ryu H.G., Ryu S.B, “*A PAPR Reduction Method using New ACE (Active Constellation Extension) with Higher Level Constellation,*” in Proceedings of IEEE International Conference on Signal Processing and Communications, pp.724-727, 24-27 Nov. 2007.
- [98] Saul A., “*Generalized active constellation extension for peak reduction in OFDM systems,*” IEEE International Conference on Communications, vol.3, pp.1974-79, May 2005.
- [99] Sezginer S., Sari H., “*Metric-Based Symbol Pre-distortion Techniques for Peak Power Reduction in OFDM Systems,*” IEEE Transactions on Wireless Communications, vol.6, no.7, pp.2622-2629, July 2007
- [100] Bae K., Andrews J.G., Powers E.J., “*Adaptive active constellation extension algorithm for peak-to-average ratio reduction in OFDM,*” IEEE Communications Letters, vol.14, no.1, pp.39-41, January 2010.
- [101] Cimini L. J., Sollenberger N.R., “*Peak-to-average power ratio reduction of an OFDM signal using partial transmit sequences,*” IEEE Communication Letters, vol. 4, no. 3, pp. 86–88, March 2000.
- [102] Jayalath A. D. S., Tellambura C., “*Adaptive PTS approach for reduction of peak-to-average power ratio of OFDM signal,*” Electronics Letters, vol.36, no.14, pp.1226-1228, Jul 2000.
- [103] Tellambura C., “*Improved phase factor computation for the PAR reduction of an OFDM signal using PTS,*” IEEE Communications Letters, vol.5, no.4, pp.135-137, April 2001.

- [104] Han S.H., Lee J.H., “*PAPR reduction of OFDM signals using a reduced complexity PTS technique,*” IEEE Signal Processing Letters, vol.11, no.11, pp.887-890, Nov. 2004.
- [105] Alavi, A., Tellambura, C., Fair I., “*PAPR reduction of OFDM signals using partial transmit sequence: an optimal approach using sphere decoding,*” IEEE Communications Letters, vol.9, no.11, pp.982-984, Nov. 2005.
- [106] Lim D.W., Heo S.J., No J.S., Chung H., “*A new PTS OFDM scheme with low complexity for PAPR reduction,*” IEEE Transactions on Broadcasting, vol.52, no.1, pp.77-82, March 2006.
- [107] Jiang T., Xiang W., Richardson P.C., Guo J., Zhu G., “*PAPR Reduction of OFDM Signals Using Partial Transmit Sequences With Low Computational Complexity,*” IEEE Transactions on Broadcasting, vol.53, no.3, pp.719-724, Sept. 2007.
- [108] Ghassemi A., Gulliver T.A., “*A Low Complexity IFFT-Based PTS Technique for PAPR Reduction in OFDM Systems,*” in Proceedings of 66th IEEE Vehicular Technology Conference, pp.616-619, Sept. 30 2007-Oct. 3 2007.
- [109] Xiao Y., Lei X., Wen Q., Li Sh., “*A Class of Low Complexity PTS Techniques for PAPR Reduction in OFDM Systems,*” , IEEE Signal Processing Letters, vol.14, no.10, pp.680-683, Oct. 2007.
- [110] Yajun Wang., Wen Chen., Tellambura, C., “*A PAPR Reduction Method Based on Artificial Bee Colony Algorithm for OFDM Signals,*” IEEE Transactions on Wireless Communications, vol.9, no.10, pp.2994-2999, October 2010.
- [111] Basturk B., Karaboga D., “*An artificial bee colony (ABC) algorithm for numeric function optimization,*” IEEE Swarm Intelligence Symposium, Indianapolis, Indiana, USA, 12–14 May 2006.
- [112] Karaboga D., Basturk B., “*A powerful and efficient algorithm for numeric function optimization: artificial bee colony (ABC) algorithm,*” Journal of Global Optimization, vol.39, pp-459-471, 2007.
- [113] Hou J., Ge J., Jing Li, “*Peak-to-Average Power Ratio Reduction of OFDM Signals Using PTS Scheme With Low Computational Complexity,*” IEEE Transactions on Broadcasting, vol.57, no.1, pp.143-148, March 2011

- [114] SI Yang L., Soo K. K., Li S.Q., Siu Y. M., “*PAPR Reduction Using Low Complexity PTS to Construct of OFDM Signals Without Side Information,*” IEEE Transactions on Broadcasting, vol.57, no.2, pp.284-290, June 2011
- [115] Press W. H., Teukolsky S. A., Vetterling W. T., Flannery B. P., “*Numerical Recipes in C: The Art of Scientific Computing,*” 2nd ed. Cambridge, U.K.: Cambridge Univ. Press, 1992.
- [116] Lu G., Wu P., Carlemalm-Logothetis C., “*Enhanced interleaved partitioning PTS for peak-to-average power ratio reduction in OFDM systems,*” Electronics Letters, vol. 42, no. 17, pp. 983–984, Aug. 2006.
- [117] Wang L., Liu J., “*PAPR Reduction of OFDM Signals by PTS With Grouping and Recursive Phase Weighting Methods,*” IEEE Transactions on Broadcasting, vol.57, no.2, pp.299-306, June 2011
- [118] Taspinar N., Kalinli A., Yildirim M., “*Partial Transmit Sequences for PAPR Reduction Using Parallel Tabu Search Algorithm in OFDM Systems,*” IEEE Communications Letters, vol.15, no.9, pp.974-976, September 2011.
- [119] Cho Y.J., No J.S., Shin D.J., “*A New Low-Complexity PTS Scheme Based on Successive Local Search Using Sequences,*” IEEE Communications Letters, vol.16, no.9, pp.1470-1473, September 2012
- [120] Jinqun L., Tang Y., Wang H., “*Cyclic Codes and Sequences: The Generalized Kasami Case,*” IEEE Transactions on Information Theory, vol.56, no.5, pp.2130-2142, May 2010.
- [121] Qi X., Li Y., Huang H., “*A Low Complexity PTS Scheme Based on Tree for PAPR Reduction,*” IEEE Communications Letters, , vol.16, no.9, pp.1486-1488, September 2012.
- [122] Al-Dalakta E., Al-Dweik A., Hazmi A., Tsimenidis C., Sharif B., “*PAPR Reduction Scheme using Maximum Cross Correlation,*” IEEE Communications Letters, vol.16, no.12, pp.2032-2035, Dec. 2012.
- [123] Al-Dalakta E., Al-Dweik A., Hazmi A., Tsimenidis C., Sharif B., “*Efficient BER reduction technique for nonlinear OFDM transmission using distortion prediction,*” IEEE Transaction on Vehicular Technology, vol. 61, pp. 2330–2336, June 2012.

- [124] Ye Ch., Li Z., Jiang T., Ni Ch., Qi Qi, “*PAPR Reduction of OQAM-OFDM Signals Using Segmental PTS Scheme With Low Complexity,*” IEEE Transactions on Broadcasting, vol.60, no.1, pp.141-147, March 2014.
- [125] Cimini L.J., Sollenberger N.R., “*Peak-to-average power ratio reduction of an OFDM signal using partial transmit sequences with embedded side information,*” IEEE Global Telecommunications Conference, vol.2, pp.746-750, 2000.
- [126] Jayalath A.D.S., Tellambura C., “*Side information in PAR reduced PTS-OFDM signals,*” 14th IEEE Proceedings on Personal, Indoor and Mobile Radio Communications, vol.1, no.1, pp.226-230 ,7-10 Sept. 2003.
- [127] Giannopoulos T., Paliouras V., “*A Low-Complexity PTS-based PAPR Reduction Technique for OFDM Signals without Transmission of Side Information,*” IEEE Workshop on Signal Processing Systems Design and Implementation, pp.434-439, 2-4 Oct. 2006.
- [128] Nguyen T.T., Lampe L., “*On partial transmit sequences for PAR reduction in OFDM systems,*” IEEE Transactions on Wireless Communications, vol.7, no.2, pp.746-755, Feb 2008.
- [129] Giannopoulos T., Paliouras V., “*A Low-Complexity PTS-based PAPR Reduction Technique for OFDM Signals without Transmission of Side Information,*” Journal of Signal Processing Systems, vol.56, no. 2-3, pp 141-153, 2009.
- [130] Zhou Y., Jiang T., “*A Novel Multi-Points Square Mapping Combined with PTS to Reduce PAPR of OFDM Signals Without Side Information,*” IEEE Transactions on Broadcasting, vol.55, no.4, pp.831-835, Dec. 2009.
- [131] Guan L., Jiang T., Zhou Y., Cai Li, “*A novel constellation extension for reduction of peak-to-average-power radio in OFDM systems,*” IEEE International Symposium on Broadband Multimedia Systems and Broadcasting, pp.1-4, March 2010.
- [132] Guan L., Jiang T., Qu D., Zhou Y., “*Joint Channel Estimation and PTS to Reduce Peak-to-Average-Power Radio in OFDM Systems Without Side Information,*” IEEE Signal Processing Letters, vol.17, no.10, pp.883-886, Oct. 2010.
- [133] Kim H., Hong E., Ahn C., Har D., “*A Pilot Symbol Pattern Enabling Data Recovery Without Side Information in PTS-Based OFDM Systems,*” IEEE Transactions on Broadcasting, vol.57, no.2, pp.307-312, June 2011.

- [134] Ku S.H., Wang C.L., “A new side-information free PTS scheme for PAPR reduction in OFDM systems,” 8th IEEE International Conference on Wireless and Mobile Computing, Networking and Communications, pp.108-112, 8-10 Oct. 2012.
- [135] Kalaiselvan E., Elavarasan P., Nagarajan G., “PAPR reduction of OFDM signals using pseudo random PTS without side information,” in Proceedings of International Conference on Communications and Signal Processing, pp.29-33, 3-5 Apr. 2013.
- [136] Jiang T., Ni Ch., Guan L., Qi Qi, “Peak-to-average power ratio reduction in Alamouti multi-input-multi-output orthogonal frequency division multiplexing systems without side information using phase offset based-partial transmit sequence scheme,” IET Communications, vol.8, no.5, pp.564-570, March 2014.
- [137] Rappaport T.S., “Wireless communication-Principle and practice”, 2nd edition, PHI India , pp 177-212, 2002.
- [138] Joshi A., Saini D.S., “COFDM performance in various Multipath fading environment,” in Proceedings of IEEE International Conference, vol.3, pp 127-131, Singapore, Feb 2010.
- [139] Nakagami M., “The *m*-distribution, a general formula of intensity distribution of rapid fading in Statistical Methods in Radio Wave Propagation,” Oxford, U.K.: Pergamon, 1960.
- [140] Elnoubi S., Chahine S.A., Abdallah H., “BER performance of GMSK in Nakagami fading channels,” in proceedings of IEEE Twenty-First National Radio Science Conference, pp.C13- 18, March 2004.
- [141] Forney G.D., “Concatenated codes”, MIT Press, 1966
- [142] Byun,K., Jung,S., Shin D.J., Um J.S., “Performance comparison of RS-CC concatenated codes using NSC and RSC codes,” in proceedings of 2nd IEEE International Conference on Network Infrastructure and Digital Content , pp.992-994, Sept. 2010.
- [143] B. Sklar, “Digital communications- Fundamentals and Applications” ,2nd edition, PHI India , pp 437-505,2009.

- [144] Berrou C., Glavieux A., Thitimajshima P., “*Near Shannon limit error-correcting coding and decoding: Turbo codes*”, in Proceedings of International Conference on Communications, pp. 1064–1070, May 1993.
- [145] Burr G., White G.P., “*Performance of Turbo-coded OFDM*,” International Conference on Universal Personal Communications, pp.1-8, 1999
- [146] Gnanasekaran T., Aarathi V., “*Effect of Constraint Length and Code Rate on the Performance of Enhanced Turbo Codes in AWGN and Rayleigh Fading Channel*”, WSEAS Trans. On Communication, vol. 10, no. 5, pp.137-146, 2011.
- [147] Bahl L., Cocke, J., Jelinek F., Raviv, J., “*Optimal decoding of linear codes for minimizing symbol error rate,*” IEEE Transactions on Information Theory, vol.20, no.2, pp.284-287, Mar 1974.
- [148] Pietrobon S.S., “*Implementation and Performance of a Turbo/MAP Decoder,*” International Journal of Satellite Communications, vol. 16, pp. 23-46, 1998.
- [149] Silvio A. A., “*From BCJR to turbo decoding: MAP algorithms made easier,*” © Silvio A. Abrantes, April 2004
- [150] Foerster J., Li Q., “*UWB channel modelling contribution from Intel,*” EEE P802.15-02/279rO-SG3a, June 2002.
- [151] Bracewell R.N., “*Discrete Hartley transform,*” The Journal of the Optical Society of America , vol. 73, pp. 1832- 1835, Dec. 1983.
- [152] Bracewell, R.N., “*The fast Hartley transform,*” Proceedings of the IEEE , vol.72, no.8, pp.1010,1018, Aug. 1984
- [153] Sorensen H.V., Jones D.L., Burrus C.S., Heideman M., “*On computing the discrete Hartley transform,*” IEEE Transactions on Acoustics, Speech and Signal Processing, vol.33, no.5, pp.1231-1238, Oct 1985.
- [154] Bracewell R.N., “*Assessing the Hartley transform,*” IEEE Transactions on Acoustics, Speech and Signal Processing, vol.38, no.12, pp.2174-2176, Dec 1990.
- [155] de Frein C., Fagan A.D., “*Maximum Likelihood Frequency Detection for Precoded OFDM,*” Irish Signals and Systems Conference, pp.277-282, 28-30 June 2006.

- [156] Wang C.L., Chang C.H., Fan J.L., Cioffi J.M., “*Discrete Hartley Transform Based Multicarrier Modulation*,” in proceedings of IEEE International Conference on Acoustics, Speech, and Signal Processing, , vol.5, pp. 2513-2516,2000.
- [157] Sembiring Z., Malek M.F.A, Rahim H., “*Low Complexity OFDM Modulator and Demodulator Based on Discrete Hartley Transform*”, in Proceedings of Fifth Asia International Conference Modelling Symposium pp.252-256, 2011.
- [158] Baig I., Jeoti V., “PAPR analysis of DHT-precoded OFDM system for M-QAM,” International Conference on Intelligent and Advanced Systems, pp.1,4, 15-17 June 2010.
- [159] Ali I., Pollok A., Luo Li., Davis L., “*A DHT precoded OFDM system with full diversity and low PAPR*,” 23rd IEEE International Symposium on Personal Indoor and Mobile Radio Communications , 2012, pp.2383-2388, 9-12 Sept. 2012.
- [160] Ouyang X., Jin J., Jin G., Wang Z., “*Low complexity discrete Hartley transform precoded OFDM for peak power reduction*,” Electronics Letters , vol.48, no.2, pp.90-91, Jan.2012.

Author's Publications

International Journals (Indexed in SCOPUS)

1. A. Joshi, Davinder S. Saini, "Performance Analysis and PAPR Reduction of Coded OFDM System using Modified SLM, PTS and DHT Pre-coding in Fading Environments", in *WSEAS Trans. on Communication*. Vol. 12, Issue 1, pp.14-28, January 2013. (indexed in Scopus, Elsevier, Inspec/IET)
2. A. Joshi, Davinder S. Saini, "Peak-to-Average Power Ratio Reduction of OFDM signals Using Improved PTS Scheme with Low Computational Complexity", in *WSEAS Trans. on Communication*. Vol. 12, Issue 12, pp. 630-640, December 2013. (indexed in Scopus, Elsevier, Inspec/IET)
3. A. Joshi, Davinder S. Saini, "PTS using Novel constellation extension scheme for PAPR Reduction of OFDM signals without side information", in *Inderscience Journal on Information and Communication Technology*, accepted for publication (indexed in Scopus, ACM DL)

International conferences

1. A. Joshi, Davinder S. Saini, "A comparative performance analysis of OFDM using IEEE 802.11a standard with BPSK,QPSK,QAM-16 & 64," in proceedings of International conference *RTSCIT 10, Bhopal India, Feb-2010*
2. A. Joshi, Davinder S. Saini, "COFDM performance in various Multipath fading environment ", in *proceedings of IEEE International Conference (ICCAE 2010) ,vol.3, pp 127-131,Singapore, Feb 26-28, 2010. (indexed in IEEE Xplore)*
3. A. Joshi, Davinder S. Saini, "Performance Analysis of Coded OFDM for Various Modulation Schemes in 802.11a Based Digital Broadcast Applications", in *proceedings of International Conference (BAIP 2010) , Kerala,Vol-70,pp 60-64, INDIA. March 2010 (indexed in Springer LNCS-CCIS)*
4. A. Joshi, Davinder S. Saini, "Performance Analysis of coded- OFDM with ICI due to Frequency Offset", *IET UK/IEEE International conference on Advances in Recent Technologies in communication & Computing, ARTCOM-2011;Bangalore, Sept14-15,2011 (indexed in IEEE Xplore and IET DL)*
5. A. Joshi, Davinder S. Saini, " PAPR Analysis of Coded- OFDM System and Mitigating its Effect with Clipping, SLM and PTS ", in *proceedings of IEEE International Conference (ICIMU-2011), Malaysia, Nov. 14-16, 2011. (indexed in IEEE Xplore)*
6. A. Joshi, Davinder S. Saini, " Performance Analysis Of Coded-OFDM with RS-CC and Turbo codes in Various Fading Environment ", in *proceedings of IEEE International Conference (ICIMU-2011), Malaysia, Nov. 14-16, 2011. (indexed in IEEE Xplore)*
7. A. Joshi, Davinder S. Saini , "PAPR reduction in OFDM with FEC (RS-CC and Turbo coding) system using DHT pre-coding" *IEEE International symposium (IMSNA-2012), July,2012 Shenyang, China.(indexed in IEEE Xplore)*

8. A. Joshi, Davinder S. Saini, "PAPR and Performance analysis of LDPC-RS concatenated OFDM system with modified PTS", in *proceedings of Second International Conference on Emerging Research in Computing, Information, Communication and Applications*"(ERCICA-2014), Vol-1, pp-573-579, 01-02 Aug. 2014 **(Indexed in DBLP, Search and Elsevier ST)**.
9. A. Joshi, Davinder S. Saini, "Performance Analysis and PAPR Reduction of Turbo Coded OFDM using hybrid ZCT based PTS", in *proceedings of Second International Conference on Emerging Research in Computing, Information, Communication and Applications*"(ERCICA-2014), Vol-1, pp580-586, 01-02 Aug. 2014 **(Indexed in DBLP, Search and Elsevier ST)**.

(ALOK JOSHI)